DEPOSITIONAL ENVIRONMENTS OF CRETACEOUS-PALEOGENE COAL BEDS AND SURROUNDING STRATA WITHIN THE RATON BASIN OF COLORADO AND NEW MEXICO, USA

by

Ross Ingram Harrison

Bachelor of Arts in English, 2011

Texas Christian University

Fort Worth, TX

Bachelor of Science in Geology, 2016

Louisiana State University

Baton Rouge, LA

Submitted to the Graduate Faculty of

The College of Science and Engineering

Texas Christian University

In partial fulfillment of the requirements for the degree of

MASTER OF SCIENCE IN GEOLOGY

August 2018

Acknowledgements

I would first and foremost like to thank my parents and family for supporting me on this journey I began nearly five years ago. I would especially like to thank my parents for always believing in me and giving me an advantage that most in this world do not have—for that I am profoundly grateful. I would like to thank TCU Geology Department admissions and Dr. John Holbrook for seeing an ability in me to take on and complete a graduate project. I would like to thank Dr. Holbrook for his guidance on this project, and for pushing me to continually improve this manuscript. I want to thank Sean Horne for the countless hours spent working on this project, both in scientific and moral support. I am very grateful for Dr. Thomas Demchuk and his expertise, which was necessary for the completion of this project. I would like to thank Dr. Richard Denne and Bo Henk for serving on my committee. I would also like to thank Pioneer Natural Resources for the funding provided for this project as well as providing the core used in this study. I would especially like to thank Shannon Osterhout, specifically for her help working with the core, and for being available and helpful. I would also like to thank my faithful drone pilot, Cody Finally I would like to thank my fellow graduate students at TCU, my friends and professors from LSU, my friends from home, and my girlfriend Anna Thorson (who also shares a love for geology) for all of their uplifting words and actions throughout my long, roundabout, educational voyage.

Table of Contents

Table of Contents ..... **iii**

List of Figures ..... **iv**

List of Tables ..... **vii**

CHAPTER ONE: Introduction **1**

CHAPTER TWO: Data and Methods **16**

CHAPTER THREE: Results **25**

CHAPTER FOUR: Discussion **60**

CHAPTER FIVE: Conclusion **76**

References. **78**

APPENDIX

VITA

ABSTRACT

List of Figures

Figure 1 Raton Basin 2

Figure 2 (left) Map of Raton Basin, with major structural features 3

Figure 3 Stratigraphic column of the basin..... 4

Figure 4 and 5 Paleographic maps chronicling retreat of the Western Interior Seaway..... 5

Figure 6 Contact of the Cretaceous-Paleogene Raton and Cretaceous Vermejo Formation 7

Figure 7 Depositional models for the Trinidad Sandstone, Vermejo Formation, Raton Formation, and Poison Canyon Formation. 8

Figure 8 Stacking patterns and strata characteristic of a high accommodation fluvial system. 9

Figure 9 Typical facies associations and architectural relations in a low net-gross, high accommodation fluvial overbank setting..... 10

Figure 10 Controls on Peat Geometry. 11

Figure 11 Components of macerals. 12

Figure 12 Planform and cross-sectional views of a Distributive Fluvial System. 14

Figure 13 Geologic map with outcrop and core locations marked for this study as well as the Horner 2016 study. 20

Figure 14 Stratigraphic position of outcrop, core, and coal samples. 22

Figure 15 Hierarchies of architectural units 24

Figure 16 Maceral counts for each coal sample..... 27

Figure 17 Total maceral counts for all coal samples. 29

Figure 18 Proportional maceral type for each individual coal sample. 30

Figure 19 Eight photomicrographs of macerals.. 31
Figure 20 Eight photomicrographs of macerals 32
Figure 21 Eight photomicrographs of macerals. 33
Figure 22 Eight photomicrographs of pollen specimens 35
Figure 23 Lithofacies examples in outcrop and core. 39
Figure 24 Set of bars representing amalgamating channel-belts. 41
Figure 25 Channel-fill element with measured section. 42
Figure 26 Four examples of preserved vegetation 43
Figure 27 Annotated blowout wing 43
Figure 28 Examples of Lithofacies assemblages 49
Figure 29 Unannotated and annotated DOM of Trinidad Lake State Park Outcrop. 52
Figure 30 Generalized measured sections from Trinidad Lake State Park Outcrop. 53
Figure 31 Unannotated and annotated DOM of King Coal Outcrop. 55
Figure 32 Generalized measured sections from King Coal Outcrop. 56
Figure 33 Unannotated and annotated DOM of Wild Boar Outcrop. 58
Figure 34 Generalized measured sections from Wild Boar outcrop. 59
Figure 35 Proportional maceral composition of all coals. 60
Figure 36 Palynofloral assemblages identified by Farley (1990). 62
Figure 37 Geomorphological features of the Grijalva River 64
Figure 38 Time series of images from Google Earth of the Grijalva River. 65
Figure 39 Channel width equation. 66
Figure 40 Hay-Zama Lake System. 68
Figure 41 Depositional model for Upper and Lower Coal Zone of Raton Fm. 71

Figure 42 Oil and gas windows relative to vitrinite reflectance. 73

List of Tables

Table 1 Coal sample labels 17

Table 2 Names of wells cored..... 19

Table 3 Outcrops worked in this study. 21

Table 4 Proximate / ultimate analysis results 25

Table 5 Vitrinite reflectance results. 26

Table 6 Table of lithofacies 38

Table 7 Channel story thicknesses..... 45

Table 8 Summary of lithofacies assemblages. 50

CHAPTER ONE: Introduction

The Raton Basin of northeastern New Mexico and southeastern Colorado has been economically important for nearly 200 years. This is especially true for its coal deposits, with the first discovery of coal in 1841, and commercial mining since around 1870 (Pillmore, 1969). Coal Bed Methane is the dominant industry currently active in the basin, with several thousand wells currently in production after the first well was drilled in 1982. The basin contains several thousand wells, and over 1,500+ billion cubic feet of gas (BCF) in cumulative production as of 2014 (Osterhout, 2014).

Lithology within the Raton Basin is highly variable, reflecting a range of depositional environments. Previous studies of the Raton Basin include those on tectonics, lithologies, facies, depositional environments, resources, fracture networks, igneous activity, provenance, architectural analysis and lithofacies affiliation (Hills, 1888; Lee, 1917; Johnson and Wood, 1956; Wanek, 1963; Pillmore, 1969; Pillmore and Flores, 1984; Flores, 1987; Johnson and Finn, 2001; Clarke, 2004; Bush, 2016; Horner, 2016; McGregor, 2017). Researchers still lack a strong understanding of the interaction of depositional environments and the driving depositional controls within the basin. This is especially true for the coals and their associated depositional environments.

The objective of this study is to develop an understanding of the depositional environments of coal beds in the Raton Formation of the Raton Basin. This work provides a model for coal deposition, and aids in understanding the vertical and horizontal interaction between the coal and bounding fluvial lithofacies. This study also aims to determine how the deposition of these coals fits into the Distributive Fluvial System (DFS)

model. This study has economic significance in addition to scientific significance, as understanding the nature of the coal and its surrounding lithologic associations could help to aid in CBM / coal bed gas production (**Figure 1**).

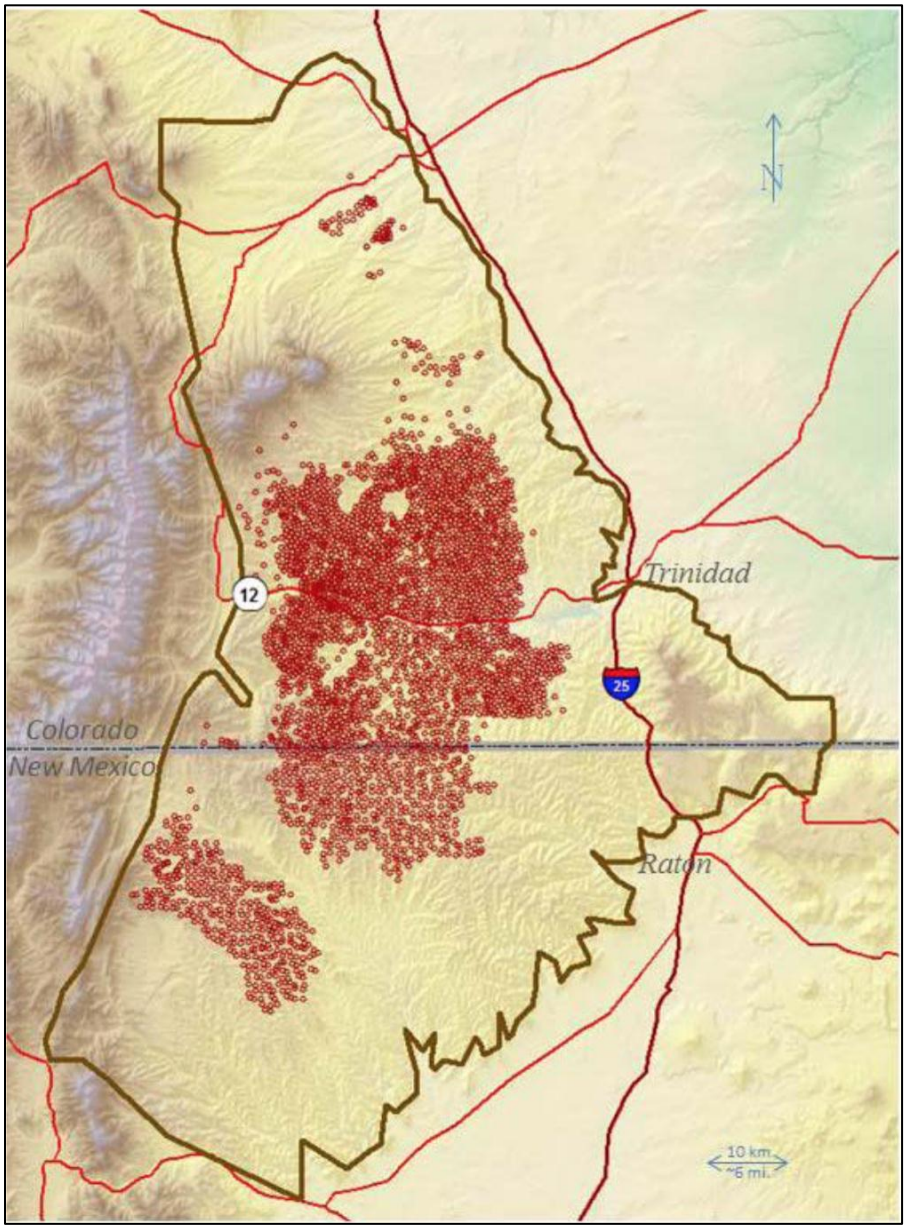

Figure 1 Raton Basin (outlined in brown), with each Coal Bed Gas (Methane) well represented by a red dot (Osterhout, 2014).

Geologic Background

Raton Basin

The Raton Basin is an approximately 2,500 square mile (6500 km^2) north-south trending, asymmetric structural foreland basin that spans northeastern New Mexico and southeastern Colorado. The basin is Laramide in origin, and is bounded by the Wet Mountains (north), the Cimarron Mountains (south), the Sangre de Cristo Mountains (west), and a series of arches (east) (**Figure 2**). The fill of the basin comprises rocks ranging from Late Cretaceous to early Paleogene, and represents a prograding sequence of marine, marginal marine, coastal, and alluvial deposits (Bush et al., 2016). Strata of the basin dips gently westward in the east (approximately 1-5°) and dips more steeply eastward in the western portion of the basin, and is even locally overturned. (Johnson and Wood, 1956; Baltz, 1965; Pillmore, 1969, 1976; Pillmore and Flores, 1987; Flores and Bader, 1999; Johnson and Finn, 2001; Clarke, 2004; Topper, 2011; Bush et al., 2016).

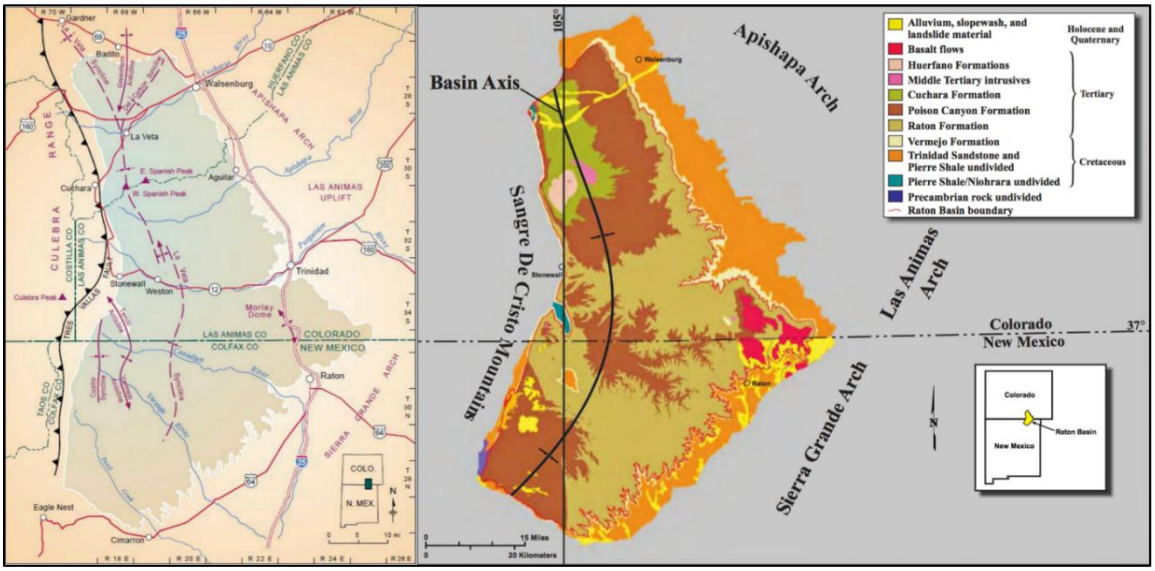

Figure 2 (left) Map of Raton Basin, with major structural features (from Topper, 2011). Map of Raton Basin (right), with major lithologic units (from Flores and Bader, 1999).

Lithology and Stratigraphy

The Raton Basin fill contains five major stratigraphic units. From oldest-to-youngest, these units are: the Upper Cretaceous Pierre Shale (Campanian to Maastrichtian), Trinidad Sandstone (Maastrichtian), Vermejo Formation (Maastrichtian), Raton Formation (Maastrichtian and Paleocene), and the Poison Canyon Formation (Maastrichtian and Paleocene) (**Figure 3**).

The Cretaceous Pierre Shale is a silty, gray-to-black non-calcareous marine shale that is up to approximately 2,500' thick, and is representative of a delta front environment (Johnson and Wood, 1956; Pillmore, 1969; Topper, 2011). The upper part of the Pierre Shale contains interbedded siltstone and sandstone beds, which increase in abundance up to the base of the Trinidad Sandstone. The contact between the Pierre Shale and the Trinidad Sandstone is uncertain, located either at the top or the base of this transition zone (Topper, 2011).

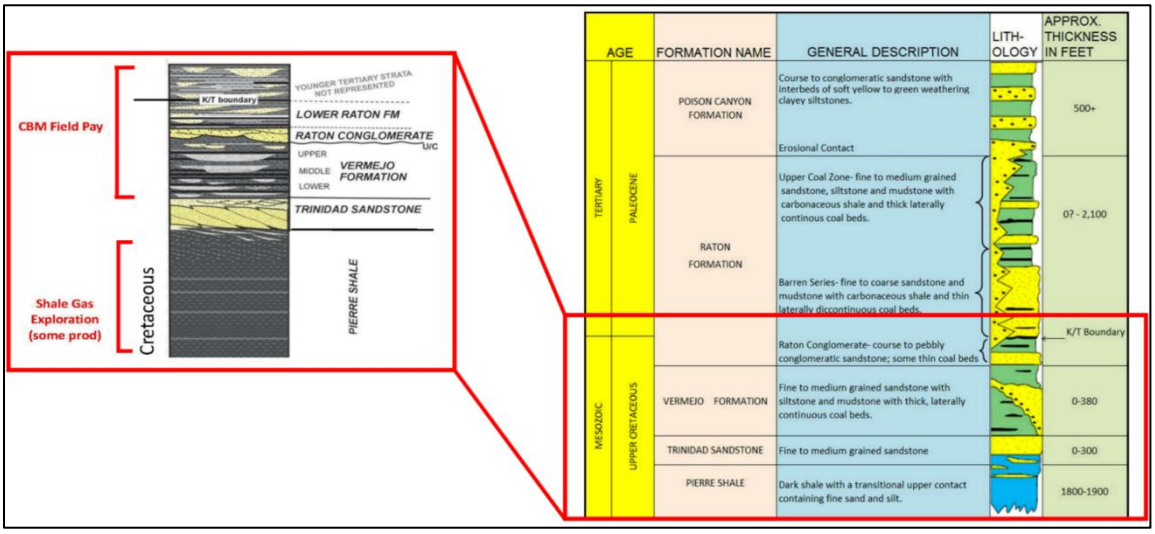

Figure 3 Stratigraphic column of the basin (right, modified from Johnson and Finn, 2001), with an inset of the column that displays stratigraphic position of CBM and Shale Gas plays, as well as a more detailed lithologic representation (left, modified from Osterhout (2014).

The Trinidad Sandstone overlies the Pierre Shale, and is a generally tabular, cliff-forming, very fine to medium-grained sandstone that weathers to large rounded blocks (Matuszczak, 1979; Pillmore and Flores, 1990). The thickness of the Trinidad Sandstone (0-300') varies depending on inclusion or exclusion of the "transition zone" with the Pierre Shale (Matuszczak, 1979; Topper, 2011). The most diagnostic feature of the Trinidad Sandstone is highly abundant *Ophiomorpha* sp. and light "buff" color (Matuszczak, 1979). The Trinidad Sandstone also contains the ichnofossil *Diplocaterion*. This unit records a prograding shallow marine coastline delta front and barrier shoreline (Pillmore and Flores, 1987; Johnson and Finn, 2001).

The Cretaceous Vermejo Formation further chronicles the retreat of the Western Interior Seaway (**Figure 4**), and conformably overlies the Trinidad Sandstone (Pillmore and Flores, 1987). The Vermejo Formation varies in thickness (0- 380'), and consists of interbedded sandstone, siltstone, mudstone, carbonaceous mud, carbonaceous shale, shale,

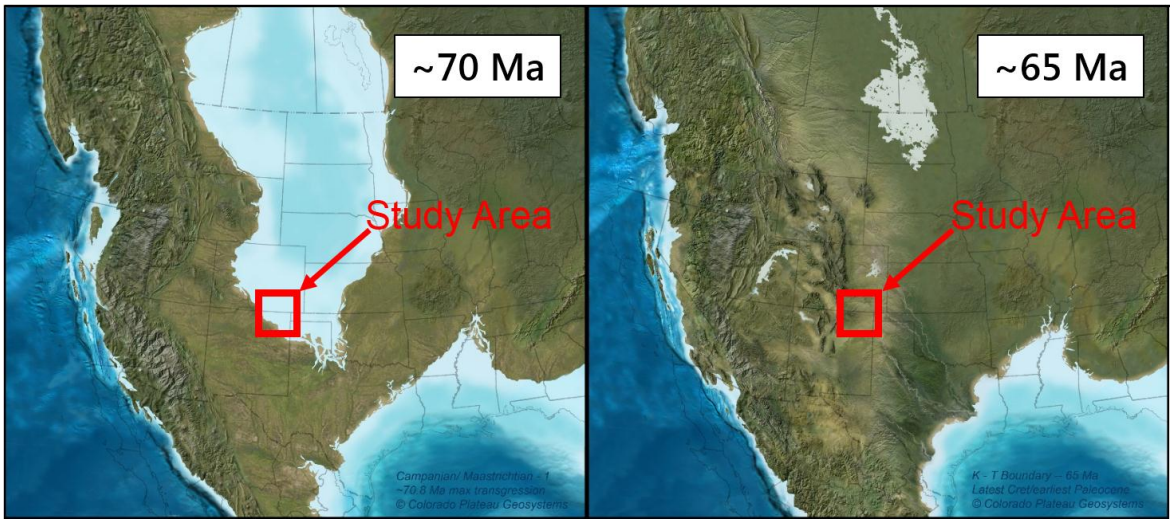

Figure 4 and 5 Paleographic maps chronicling retreat of the Western Interior Seaway from 70Ma to 65Ma (modified from Blakey, 2010).

and coal (Pillmore and Flores, 1987). Coal beds in the formation are up to 14 feet thick (Personal Comm. 2018, Roy Pillmore), and it is estimated that the Raton and Vermejo

Formations contain 1.5 – 5 billion short tons of coal combined (Wanek, 1963; Johnson and Finn, 2001). The Vermejo Formation represents the updip alluvial section of its downdip counterpart (Trinidad Sandstone). The depositional environments of the Vermejo Formation.includes fluvial, overbank, crevasse splay, lacustrine, and other low-lying environments (Strum, 1985; Flores, 1985; Flores and Pillmore, 1987; Johnson and Finn, 2001).

The Cretaceous-Paleogene Raton Formation lies unconformably on top of the Vermejo Formation, and varies in thickness from 0 - 2000' thick. The Raton Formation contains sandstone, siltstone, shale, paleosols, and coal, with a basal conglomerate (**Figure 6**) that ranges in thickness from 0 – 75' (Harbour and Dixon, 1959; Topper, 2011). Raton Formation sediments are a result of Laramide related uplift to the west of the Raton Basin (Bush et al., 2016). These lithologies represent a very complex vertical and lateral interaction of depositional environments. This study uses the three informal members coined by Pillmore and Flores (1984): 1) a lower coal zone (LCZ); 2) a non-coal-bearing "barren" unit; and 3) an upper coal zone (UCZ). The Raton Formation also contains a very well preserved and well-documented Cretaceous-Paleogene (Cretaceous-Tertiary) boundary, based on an iridium anomaly and pollen / spore extinctions (Orth et al., 1981; Pillmore and Flores, 1984; Pillmore and Fleming, 1990; Pillmore, 1999).

The Paleocene Poison Canyon Formation conformably overlies and intertongues with the Raton Formation, and varies in thickness (0-250'). Lithology of the formation consists of conglomeratic arkosic sandstone, siltstone, and mudstone, with grain size coarsening to the western part of the basin (Hills, 1888; Johnson and Wood, 1956; Flores,

Figure 6 Contact of the Cretaceous-Paleogene Raton and Cretaceous Vermejo Formations. The top half of the image is the Raton Conglomerate of the Raton Fm. Notebook for scale. Photo taken on Vermejo Park Ranch, NM.

1987; Johnson and Finn, 2001; Topper, 2001). In some parts of the basin, the bottom of the Poison Canyon Formation is equivalent in age to the bottom of the Raton Formation in other parts of the basin (Pillmore, 1969). The Poison Canyon Formation records a fluvial and upper alluvial fan environment resulting from the Laramide orogeny (Pillmore and Flores, 1990; Bush et al., 2016).

All of these units were heavily intruded during the Tertiary, in the form of dikes, sills, laccoliths, and stocks. The center of this intrusive activity is the East (12,683') and West (13,724') Spanish Peaks. East and West Spanish Peaks are different compositions. The Eastern Spanish peak is divided at 11,000' elevation into a granodiorite porphyry

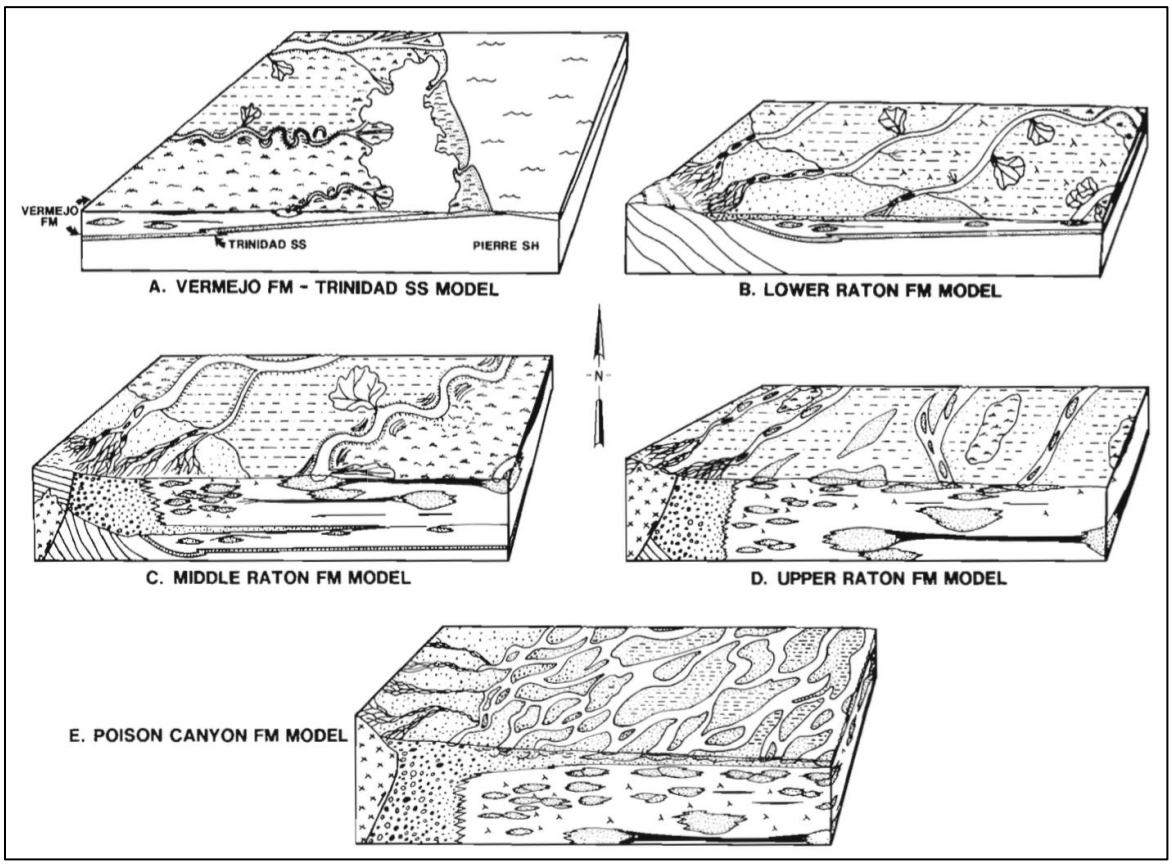

Figure 7 Depositional models for the Trinidad Sandstone, Vermejo Formation, Raton Formation, and Poison Canyon Formation (Flores, 1985).

above and a granite porphyry below, and the Western Spanish Peak is a fine-to-medium grained quartz syenite (Penn and Lindsey, 1996). Other intrusions of the region range in composition from silicic to mafic (Penn and Lindsey, 1996). These intrusions are well studied (Hills, 1888; Carter, 1956; Pillmore, 1969; Johnson and Finn, 2001), including studies into the effects on coal beds by intrusions such as elevated coal grade, widespread coking of coals, and generation of coal bed methane (Cooper, 2006).

Accommodation and Drainage

Accommodation is the volume available for deposition of sediments, and is controlled by base level (Jervey, 1988; Bohacs and Suter, 1997; Huerta et al., 2011).

Accommodation in paralic or non-marine environments is typically subaerial and controlled by either base level or subsidence; in peat-forming environments, this base level is the groundwater table (Bohacs and Suter, 1997). In inland regions, climate and tectonics are the main controls on base level (Catuneau, 2006).

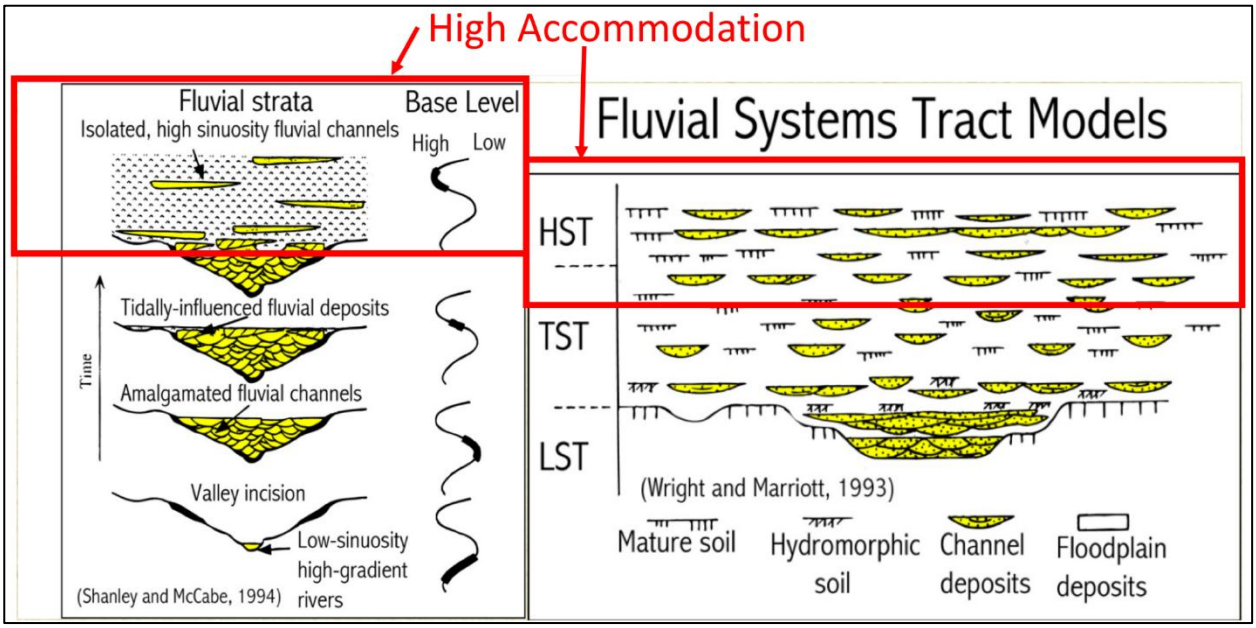

Figure 8 Stacking patterns and strata characteristic of a high accommodation fluvial system, with isolated channels surrounded by floodplain deposits (modified from Wright and Marriott, 1993; Shanley and McCabe, 1994).

The Raton and Vermejo Formations contain low net-to-gross sediments with disconnected channel belts and prevalent floodplain deposits, and are interpreted as reflecting a high accommodation setting (Clarke, 2014; Horner, 2016). Typical stacking patterns and strata characteristics within a high accommodation fluvial setting are shown in **Figure 8**. Facies associations typified in low net-gross high accommodation fluvial environments (**Figure 9**) include crevasse and terminal splay complexes / deltas, floodplain fines, lake-fill, paleosols, levees, distributary channels, and secondary and tertiary channels (Stuart et al., 2014).

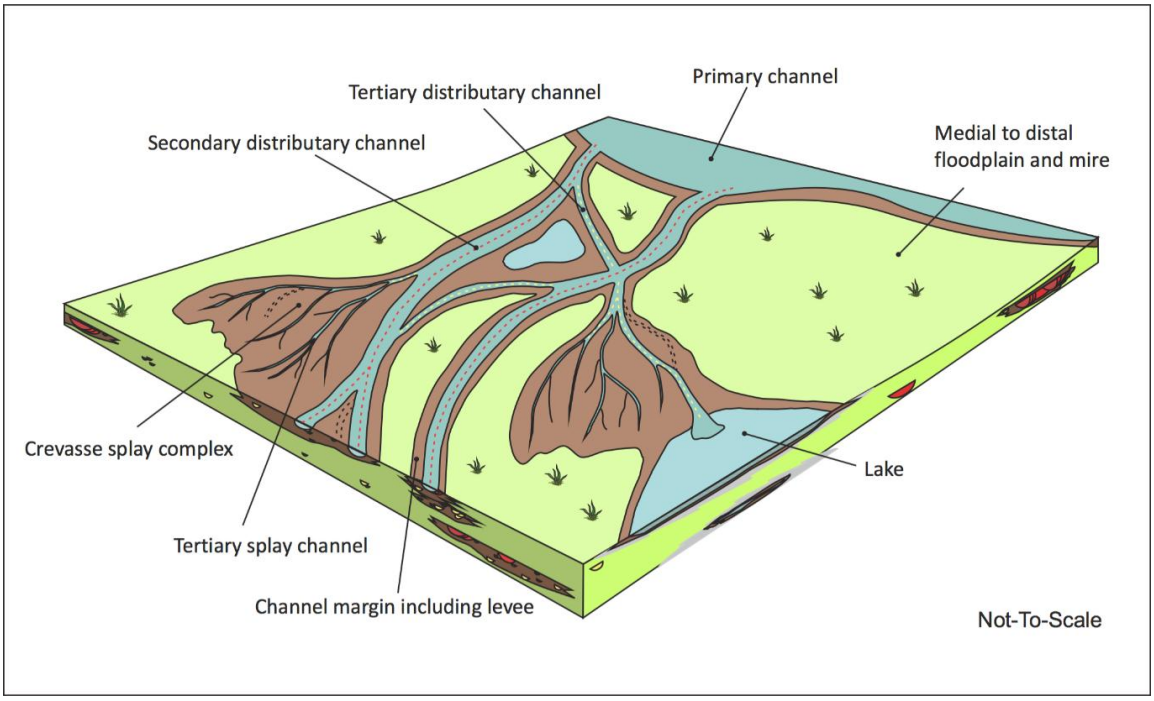

Figure 9 Typical facies associations and architectural relations in a low net-gross, high accommodation fluvial overbank setting (from Stuart et al., 2014).

Peat and Coal Production

The accumulation of significant organic matter or peatlands is dependent on: 1) primary organic activity, 2) preservation of organic matter, 3) dilution by mineral matter, and 4) subsidence (Bohacs and Suter, 1997). Spring line, or groundwater table, is the major base level control on peat formation, because vegetation that typically forms a peatland thrives in ever-wet ground, and organic preservation is at a maximum when the water table is near or at the surface (Diessel, 1992; Bohacs and Suter, 1997). Rising or high water table with little to no clastic sediment input favors peat production. Foreland basins are ideal candidates for these conditions, especially those along the Western Interior Seaway like the Raton Basin (McCabe and Parish, 1992). While clastics can aid in vegetation growth,

they are typically competing for space when filling a basin and a large input of clastic sediment can dilute or replace organics.

Peat thickness and geometry are controlled by the rate of peat production and accommodation. The ratio of Accommodation Rate / Peat Production Rate determines peat thickness and lateral extent (**Figure 10**, Bohacs and Suter, 1997). The "sweet spot," or characteristics most allowing for peat / coalbed preservation, occurs when accommodation and peat production rates are at an ideal ratio (**Figure 10**).

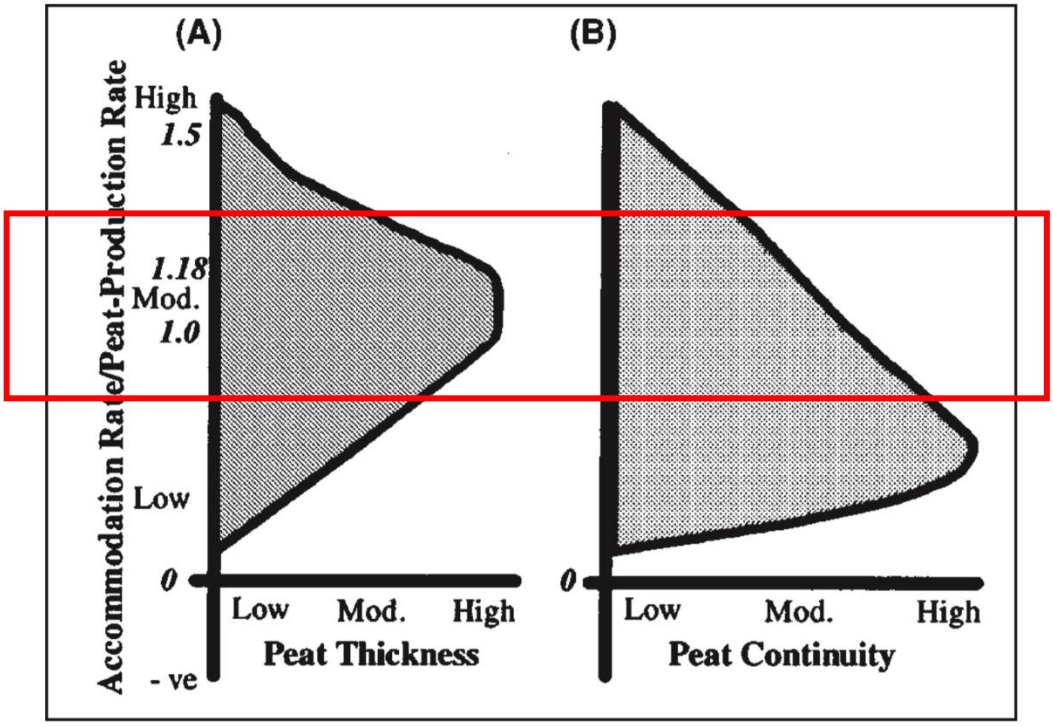

Figure 10 Controls on Peat Geometry: Accommodation Rate/Peat Production Rate (from Bohacs and Suter, 1997), with "sweet spot" outlined.

Organic Composition of Coals and Peat

Organic petrography examines the components and materials that make up coal and other organic-rich rocks. It concentrates on the kerogen or dispersed organic matter (DOM)

found in rocks, the rank of coals, and the ratio of organic components in coals in the form of macerals (Personal Comm. 2018, Dr. Thomas Demchuk). Macerals consist of three major groups: liptinite, inertinite, and huminite / vitrinite (**Figure 11**, Suarez-Ruiz, 2012). The liptinite group comprises resistant lipoid parts of plants, such as spores, cuticles, waxy secretions, oils, resins, and algal material (Tissot and Welte, 1984; Taylor et al., 1998). The inertinite maceral group originates from plant material that is highly altered or degraded during pre-deposition or the peat stage (Tayler et al., 1998; ICCP, 2001) Vitrinite / huminite groups originate from lignin, cellulose, and tannins of woody plants (Suarez-Ruiz, 2012). The environment in which a coal or peat swamp formed can be determined based on maceral types and their proportionality.

Liptinite Group	Inertinite Group	Huminite Group		Vitrinite Group	
Sporinite	Fusinite	Telohuminite	Textinite	Telovitrinite	Telinite
Cutinite	Semifusinite		Ulminite		Collotelinite
Resinite	Funginite	Detrohuminite	Attrinite	Detrovitrinite	Vitrodetrinite
Alginite	Secretinite		Densinite		Collodetrinite
Suberinite	Macrinite	Gelohuminite	Corpohuminite	Gelovitrinite	Corpogelinite
Chlorophyllinite	Micrinite		Gelinite		Gelinite
Fluorinite	Inertoditrinite				
Bituminite					
Exudatinite					
Liptodetrinite					

Figure 11 Components of macerals, with the major groups highlighted in the top row (from Suarez-Ruiz, 2012).

Distributive Fluvial Systems (DFS)

Horner (2016) determined that deposits of the Raton Formation fit well into the context of the Distributive Fluvial System model. A Distributive Fluvial System is a geomorphic and depositional model for fluvial sediments in basins and is "a deposit of a fluvial system which in planform displays a radial, distributive channel pattern" (Hartley et al., 2010). In general, a DFS initiates at a point where a confined river channel becomes unconfined (termed the apex), and comprises a: 1) proximal, 2) medial, and 3) distal zone. Several characteristics are prevalent among large-scale distributive fluvial systems in the world, including a downstream radiation of channels with a decrease in channel size down-DFS, a general decrease in grain size down-DFS with increased floodplain preservation toward the distal portions, and a lack of channel confinement (**Figure 12**). These systems exist in all climate and basin types (Hartley et al., 2010). The distal portion of the DFS contains poorly drained floodplain deposits such as marshes, lakes, and back-swamps, frequently avulsing and bifurcating channels, and terminal splay complexes, which are all found in the Raton Formation (Nichols and Fisher, 2007; Weissmann et al., 2013; Horner, 2016; McGregor, 2017).

Characteristics of the distal deposits of a DFS align with those typical of the Raton Formation of the Raton Basin. Distal DFS deposits contain plentiful floodplain facies, a low abundance of channel-fill deposits, sediment flows that occur outside of the channel, and mud-filled channel deposits (Graham, 1983; Nichols and Fisher, 2007; McGregor, 2017). All of these deposits have been previously identified within the Raton Formation, and compared to the distal portion of the DFS (Alrefaei, 2016; Horner, 2016; McGregor, 2017).

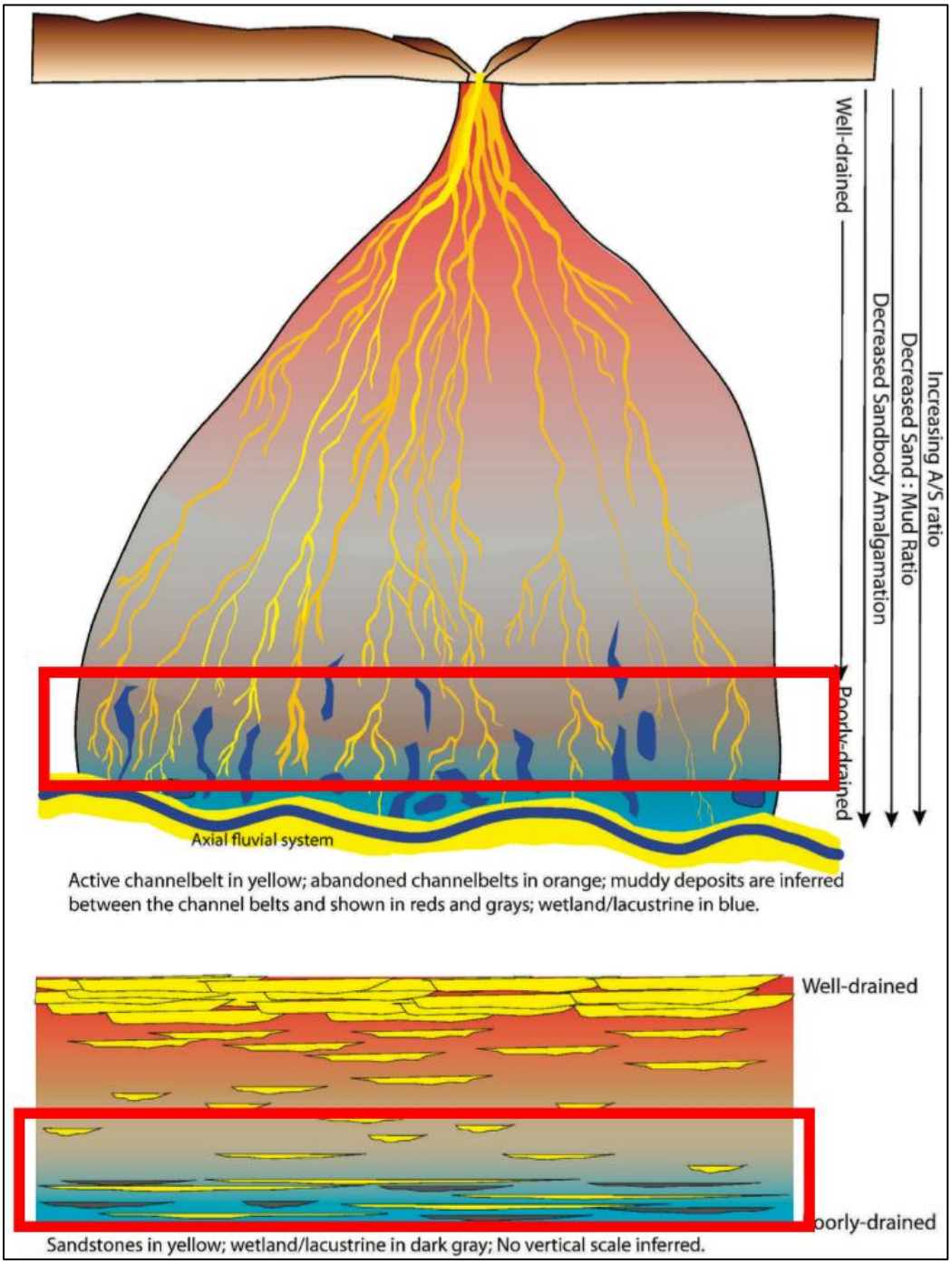

Figure 12 Planform and cross-sectional views of a Distributive Fluvial System, with characteristics annotating them, and Distal Portions highlighted by a red box (Weissmann et al., 2013).

Previous Coal Depositional Models

The coal units of the Raton Formation have traditionally been described in literature as discrete, discontinuous beds that typically do not continue for more than one thousand feet before truncation by a fluvial channel or depositionally pinching out (Flores and Bader, 1999; Clarke and Turner, 2002; Topper, 2011). However, recent work has found that individual coals can be mapped for multiple-to-tens of miles (Osterhout, 2014; Personal Comm. 2018, Roy Pillmore; Personal Comm. 2018, Sean Horne). Depositional models for Raton coals range from organic-rich marshes parallel to the Cretaceous coastline (Jurich and Adams, 1984; Carlton, 2006) to raised, interfluve peat swamps (Flores, 1985). The model proposed by Flores (**Figure 7**) is the most popular and describes coal deposition in the abandoned alluvial back-swamp floodplain of a meandering river. In the model, this floodplain is in the distal part of the flood basin, is poorly drained, experienced rapid subsidence, and is situated away from any detrital influx. The water table is proposed to have risen due to expelling of water trapped in pore spaces. Depositional loading is proposed to have forced water out of pore space, increasing the groundwater table level and aiding in peat preservation (Flores, 1985). The thickest coals are accounted for by a presence of raised or "domed" woody peat swamps, which allows for resistance to compaction, similar to the woody thick coals of the Powder River Basin (Flores, 1985).

CHAPTER TWO: Data and Methods

Overview

This study defines the coal-forming environment of the Raton Formation depositional system by incorporating and analyzing data from these rocks at the meso to micro-scale. The study included organic petrography, chemical analysis, vitrinite reflectance, palynology of coals, core analysis, and outcrop analysis.

Organic Petrography and Palynology Data

Seven total coal samples were collected from four outcrop locations (King Coal, Wild Boar, Trinidad Lake State Park, and Bosque del Oso) for proximate / ultimate chemical analysis, organic petrography, palynology, and vitrinite reflectance analysis (**Tables 1**). One representative sample (>1kg), containing the entire vertical extent of each coal bed, was taken from the most prominent coal seams at each outcrop. In two samples, 1A BDO and 2C King Coal, combined results suggest that these samples are more similar to carbonaceous shales than coals.

Organic Petrography and Palynology Methods

Coal samples were shipped to Dr. Thomas Demchuk, Adjunct Professor at Louisiana State University and geologist at RPS Group Inc., who packaged and sent a portion of each sample to Dr. Cortland Eble at the Kentucky Geological Survey for proximate / ultimate chemical analysis, a process which analyzes the chemical and organic constituents of coals. Dr. Demchuk also had samples prepared for organic petrography, palynology, and vitrinite reflectance analysis, then performed these analyses and produced

representative photomicrographs. RPS Group Inc., prepared the samples for organic petrography and palynology.

Each sample underwent a 300 maceral count, a minimum of 50 random vitrinite reflectance measurements, and a qualitative analysis of palynology slides. A lack of spore abundance, general degradation of spores, and abundance of opaque kerogen made identification very difficult and negated the possibility of quantifying spore abundance.

Coal Label	**Outcrop Origin**	**Latitude (N)**	**Longitude (W)**	**Details**
1A	Bosque del Oso	37,09,02.39	104,55,15.70	Taken from major base coal of BDO
2A	King Coal	37,07,29.99	104,42,55.03	Taken from top of major coal in KC
2B	King Coal	37,07,29.99	104,42,55.03	Taken from middle of major coal in KC
2C	King Coal	37,07,29.99	104,42,55.03	Taken from base of major coal in KC
3A	Wild Boar	37,08,03.11	104,41,51.62	Taken from left of coal attic
3B	Wild Boar	37,08,03.11	104,41,51.62	Taken from coal near river
4A	Trinidad Lake State Park	37,07,49.40	104,38,17.40	Taken from major lateral coal at base of TLSP

Table 1 Coal sample labels, outcrop from which sample was collected, location of each sample, and details about each sample.

Core Data

Pioneer Natural Resources loaned fourteen cores from the Raton Basin to TCU, and these were stored in the TCU Energy Institute Core Lab Facility for the duration of this project. Pioneer Natural Resources and Evergreen Resources originally cored these wells

to investigate generative potential for coal intervals and reservoir potential of sandstone intervals (Horner, 2016).

This study analyzed four cores (**Figure 14**) in the upper or lower coal zone (UCZ and LCZ) with high relative coal abundance. Coal abundance for the cores was determined using gamma ray and density logs. Pioneer Natural Resources provided the stratigraphic position of the cored intervals, which are here confirmed. The cores selected for this study were State of Colorado AS #21-36 TR, Zamora #22-14V, Maverick #12-29 TR, and Dover #21-1TR. **Table 2** contains the locations of the selected cores, as well as the four cores interpreted from the Horner (2016) study. These cores were used as a basis for lithofacies interpretation in this study.

Core Methods

Core description (totaling 949 feet) is on inch-basis and includes lithology, primary and secondary sedimentary structures, organic content, and bioturbation. Core descriptions were entered adjacent to gamma ray (GR; API) and density (RHOB; g/cc) logs, to display log response to lithologic features using Easy-Core software, courtesy of EasyCopy (**Table 2**). These core descriptions are available in **Appendix Items 6-9**.

Well Name	Base Poison Canyon (-ft)	Upper Raton Coal (-ft)	Top of Barren Series (-ft)	Top of Vermejo Fm. (-ft)	Cored Interval (top-bottom) (-ft)	Fm. Interval
ZAMORA 22-14V	397.38	868.17	1278.51	1851.48	708 to 883	UCZ
DOVER 21-1TR	414.38	889.82	1354.43	1583.98	855 to 1067	LCZ
MAVERICK 12-29 TR	NO INFO	362.87	781.01	1232.45	980 to 1189	UCZ
STATE OF COLORADO AS 21-36 TR	350.64	917.29	1378.31	1824.92	505 to 804	UCZ
Cheetah 14-2	740.2	1158.18	1666.9	1936.3	1810 to 1320	LCZ
Zamora 22-14V	397.39	868.17	1278.51	1851.48	1118 to 1320	UCZ / Top Barren
King Kong 41-26	1185.02	1523.65	2072.5	2596.67	1798 to 1918	UCZ
King Kong 41-26	1185.02	1523.65	2072.5	2596.67	2070 to 2250	Barren
Old Yeller 31-32	877.78	1438.71	1946.07	2486.13	1380 to 1795	UCZ

Table 2 Names of wells cored, depths of formation tops from Pioneer Natural Resources, the cored intervals described, and the corresponding formation intervals for each well. Grayed boxes indicate cores from Horner, 2016. UCZ = Upper Coal Zone, LCZ = Lower Coal Zone).

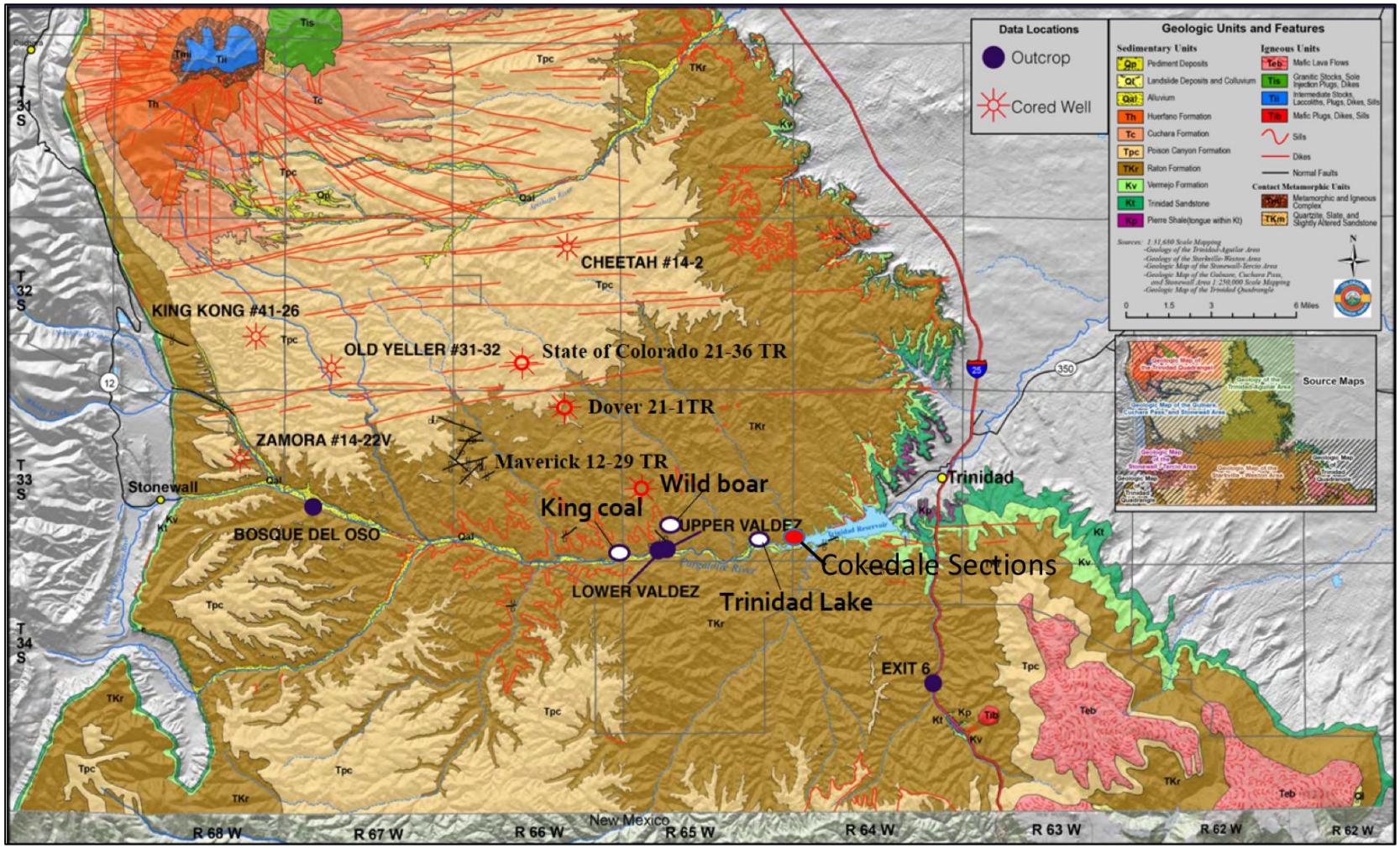

Figure 13 Geologic map with outcrop and core locations marked for this study as well as the Horner 2016 study. White circles and white gas wells denote locations for this study, while purple circles and red gas wells denote location (modified from Topper et al., 2011).

Outcrop Data

The Cretaceous-Paleogene strata of the Raton Formation crops out throughout the Raton Basin in both southern Colorado and northern New Mexico. Road cuts in Colorado along Colorado HWY 12 have high vertical and lateral extent and are the optimal for this study. They are also proximal to previously studied and analyzed outcrops.

The three outcrops along Colorado State HWY 12 that were studied (**Table 3**) contain significant coal deposits. Stratigraphic position of these outcrops is determined via relative location and elevation compared to a confirmed Cretaceous-Paleogene boundary (Pillmore, 1999) (**Figure 14**). These outcrops are the King Coal, Wild Boar, and Trinidad Lake State Park. King Coal (KC) is located just east of Segundo, CO. Wild Boar (WB) is located just north of Valdez, CO, north of HWY-12, and adjacent to Pioneer Natural Resources water disposal well Wild Boar 21-32. Trinidad Lake State Park is on the north side of HWY 12, approximately 1.5 miles west of the Cokedale exit and across from Madrid Bridge.

Outcrop	Latitude (N)	Longitude (W)	Elevation (ft)	Formation Interval
Bosque del Oso	37,09,02.39	104,55,15.70	7253 +/- 12	Upper Coal Zone
King Coal	37,07,29.99	104,42,55.03	6512 +/- 9	Upper Coal Zone
Wild Boar	37,08,03.11	104,41,51.62	6525 +/- 9	Upper Coal Zone
Trinidad Lake State Park	37,07,49.40	104,38,17.40	6305 +/- 9	Lower Coal Zone

Table 3 Outcrops worked in this study, their locations, elevations, and interval of Raton Fm. that contains them.

Horner (2016) studied four road cut outcrops, three of which were determined to be in the upper coal zone (UCZ), and one in the lower coal zone (LCZ) of the Raton

Formation. They are the Upper Valdez (UV), Lower Valdez (LV), Bosque del Oso (BDO), and Exit 6 (E6) outcrops--Exit 6 is the lone LCZ outcrop of the study. For this study, the Upper and Lower Valdez outcrops are considered to be located in the Barren series.

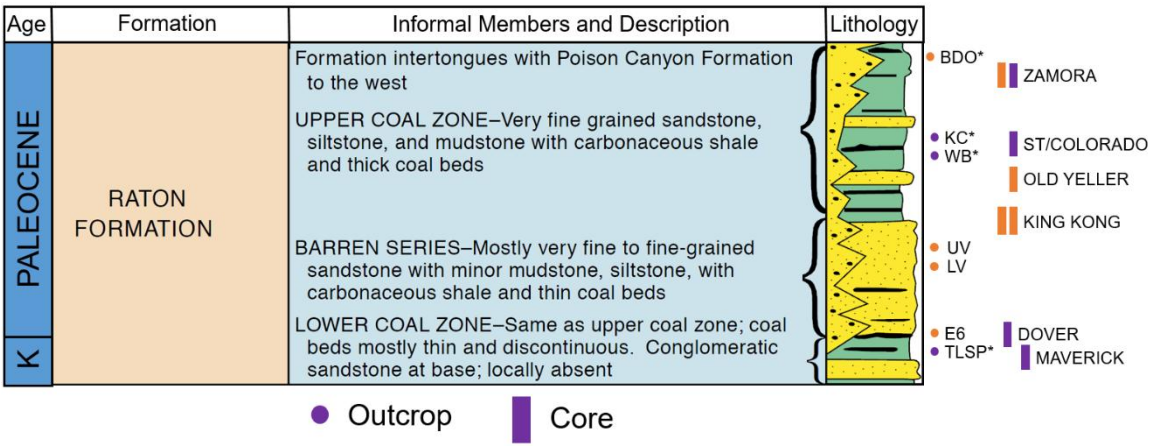

Figure 14 Stratigraphic position of outcrop, core, and coal samples. Asterisks at end of outcrops indicate coal samples were taken from this outcrop. Multiple "core" bars indicate more than one core interval studied for that well. Purple indicates data from this study, and orange indicates data from Horner (2016).

Four outcrops were imaged using a DJI Phantom 4 Pro+ drone, providing thousands of high-resolution geo-referenced photographs along the length of the outcrops. Resulting photos were then filtered for any features that would deter from model building (e.g., cars, poor sunlight, animals, etc.), entered into Agisoft PhotoScan Professional, masked, and used to build a 3-Dimensional Digital Outcrop Model. The resulting 3-D DOM was then flattened, transformed into an orthomosaic photographic panorama, and used for architecture and general outcrop analysis. Tavani et al. (2014) describes similar methods and general usage of DOMs. Sections were measured at each outcrop to constrain lithofacies along the extent of the outcrops.

Lithofacies mapping was performed on the three outcrops by applying lithofacies identified in core to outcrops, and then analyzing geometric relationships from the outcorps. Lithofacies analysis was performed by first identifying lithofacies, lithofacies

assemblages, and bounding surfaces in from cores in outcrop. These were then field mapped and drawn onto the DOMs in Adobe Illustrator CC 2018. Some targeted architecture analysis was done within the channel-belt assemblage, and valley-fill superassemblage. Identification and interpretation of bounding surfaces was based on Miall (1985-; 1988-; 1996) and Holbrook (2001), relying heavily on the principles of cross-cutting relationships and superposition and specifically based on the principles outlined by Holbrook (2001), and abridged by Horner (2016):

1) Each surface is considered to be laterally continuous and unique until truncated or indiscernible.
2) Surfaces may truncate one another, but they may not cross one another.
3) Surfaces may be diachronous but all points along a surface must be older than the materials or surfaces it locally binds and must be younger than the material or surfaces it locally cuts.
4) Surfaces can only be truncated by surfaces of equal or higher order.

The purpose of lithofacies mapping was to determine the vertical and lateral relationships between lithofacies and lithofacies assemblages, with the focus on coals and surrounding components. Lithofacies mapping coupled with targeted architectural analysis places coals within the context of their contemporary deposits and within a more integrated depositional system.

Grp	Time scale of process (a)	Examples of processes	Instan-taneous sedimentation rate (m/ka)	Fluvial, deltaic depositional units	Rank and characteristics of bounding surfaces
1	10^{-6}	Burst-sweep cycle		Lamina	0th-order, lamination surface
2	10^{-5} -10^{-4}	Bedform migration	10^{5}	Ripple (microform)	1st-order, set bounding surface
3	10^{-3}	Bedform migration	10^{5}	Diurnal dune increment, reactivation surface	1st-order, set bounding surface
4	10^{-2} -10^{-1}	Bedform migration	10^{4}	Dune (mesoform)	2nd-order, coset bounding surface
5	10^{0} -10^{1}	Seasonal events, 10-year flood	10^{2-3}	Macroform growth increment	3rd-order, dipping 5–20° in direction of accretion
6	10^{2} -10^{3}	100-year flood, channel and bar migration	10^{2-3}	Macroform, e.g., point bar, levee, splay immature paleosol	4th-order, convex-up macroform top, minor channel scour, flat surface bounding floodplain elements
7	10^{3} -10^{4}	Long-term geomorphic processes, e.g. channel avulsion	10^{0}–10^{1}	Channel, delta lobe, mature paleosol	5th-order, flat to concave-up channel base
8	10^{4} -10^{5}	5th-order (Milankovitch) cycles, response to fault pulse	10^{-1}	Channel belt, alluvial fan, minor sequence	6th-order, flat, regionally extensive, or base of incised valley
9	10^{5} -10^{6}	4th-order (Milankovitch) cycles, response to fault pulse	10^{-1}–10^{-2}	Major dep. system, fan tract, sequence	7th-order, sequence boundary; flat, regionally extensive, or base of incised valley
10	10^{6} -10^{7}	3rd-order cycles. Tectonic and eustatic processes	10^{-1}–10^{-2}	Basin-fill complex	8th-order, regional disconformity

Figure 15 Hierarchies of architectural units (Miall, 1996).

CHAPTER THREE: Results

Coal Characterization

Coal Chemical Analysis

Proximate / ultimate analysis revealed that the six true coals that were sampled shared similar characteristics (**Table 4**). Proximate results reveal that inherent moisture ranged from 1.55-5.62%, sulfur content was low (<1%), and ash content ranged from 5.28-61.12%. Five out of seven samples are low ash coals (≤10%). Dry ash-free coals yielded relatively high dry ash-free (daf) fixed-carbon values that ranged from 46.68-69.43%. Discounting sample BDO the range reduces to 64.74-69.43% FC (daf).

Sample	Carbon (%, dry)	Carbon (%, daf)	Sulfur (%)	Moisture (%)	Ash (%, dry)	VM (%, dry)	VM (%, daf)	FC (%, dry)	FC (%, daf)
Coal 2A	80.16	87.43	0.64	2.43	8.32	29.95	32.67	61.73	67.33
Coal 2B	81.38	87.99	0.56	1.63	7.51	29.91	32.34	62.57	67.65
Coal 2C	63.74	85.19	0.46	1.42	25.18	26.38	35.26	48.44	64.74
Coal 3A	80.38	86.56	0.55	4.19	7.14	28.38	30.57	64.48	69.43
Coal 3B	82.61	87.21	0.61	3.29	5.28	31.68	33.44	63.04	66.56
Coal 4A	77.33	86.86	0.67	1.55	10.97	27.84	31.27	61.20	68.74
BDO	26.99	69.42	0.25	5.62	61.12	20.73	53.32	18.15	46.68

Table 4 Proximate / ultimate analysis results. "dry" indicates coal samples have been air-dried. "daf" means dry-ash-free coal. "VM" = Volatile Matter. "FC" stands for Fixed Carbon.

Vitrinite Reflectance (R_o) / Coal Maturity

A minimum of 55, and up to 67, random R_o measurements was performed for each coal sample. Measurements showed a range of 0.73 to 0.99 % for mean randomly measured R_o, and calculated max R_o ranged from 0.77 to 1.05 %. Standard deviation for randomly measured Ro ranged from 0.029 to 0.5. All coals were ranked as high-volatile bituminous A or B coals (**Table 5**).

Sample Name	**R_o % (random)**	**R_o % (max: calculated)**	**Coal Rank**	**Standard Deviation**	**No. of Data Points**
1A Bosque del OSO	0.73	0.77	High-volatile Bituminous A/B	0.500	55
2A King Coal Top	0.99	1.05	High-volatile Bituminous A	0.031	56
2B King Coal Middle	0.98	1.04	High-volatile Bituminous A	0.041	61
2C King Coal Bottom	0.99	1.05	High-volatile Bituminous A	0.029	61
3A Wild Boar Top	0.97	1.03	High-volatile Bituminous A	0.039	67
3B Wild Boar Bottom	0.97	1.02	High-volatile Bituminous A	0.032	62
4A Trinidad Lake	0.99	1.05	High-volatile Bituminous A	0.037	60

Table 5 Vitrinite reflectance results.

Organic Petrography and Composition

Vitrinite exceeded all other maceral types in total counts, followed by inertinite, liptinite, general mineral matter, and solid bitumen (**Figure 16**). Maceral proportions varied between samples (**Figures 16-21**). 1A Bosque del Oso contained significantly more liptinite and mineral matter than other coal samples, as well as less vitrinite. 2A King Coal was dominated by vitrinite (90.33%)—making it the most vitrinite-rich coal of the seven

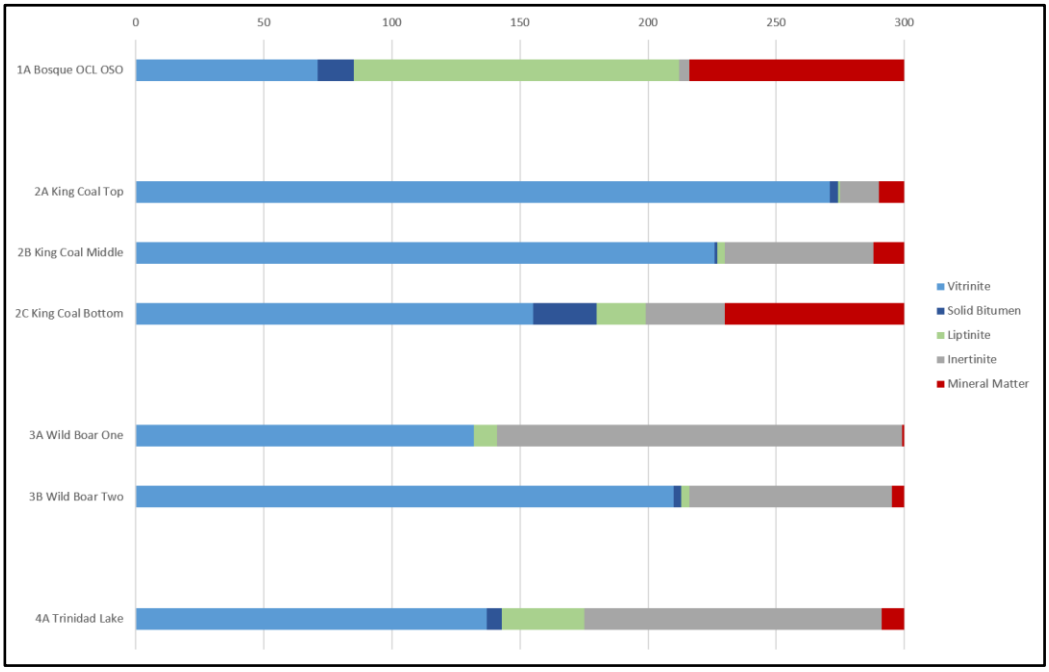

Figure 16 Maceral counts for each coal sample.

samples. 2B King Coal was dominated by vitrinite, followed by inertinite and mineral matter. 2C King Coal was dominated by vitrinite, followed by mineral matter, inertinite, and solid bitumen—2C KC contained the most solid bitumen of any coal sample. 3B Wild Boar was dominated by vitrinite, followed by inertinite, and minor amounts of liptinite, mineral matter, and solid bitumen. 4A Trinidad Lake State Park sample is dominated by vitrinite, followed by inertinite, liptinite, mineral matter, and lastly solid bitumen. Maceral proportionality reflects the components of the peat that formed a coal, and identifying

which macerals dominate samples is central to identifying the depositional environment of a peatland (Stach, 1981; Taylor et al., 1998; Sykorova et al., 2005; Suarez-Ruiz, 2012).

All maceral groups were identified in coal samples, as well as specific sub-categories for each group (**Figures 16-20**). Vitrinite group macerals identified include: Tellinite, Collotelinite, Bitroderinite, Collodetrinite, and Corpogelinite. Liptinite group macerals identified include: Terrestrial Sporonite, Lptrodetrinite, Amorphinite, Exsudatinite, and Cutinite. Inertinite group macerals identified include: Fusinite, Semifusinite, Secretinite, Inertodetrinite, Micrinite, and Macrinite. Mineral matter idientified includes: Clay, Quartz, Massive Pyrite, and Small Framboidal Pyrite.

Coal samples included a prominent amount of the vitrinite maceral group, often in groundmass (**Figures 19-21**). This is indicative of a woody environment, and best represents the organic petrography data as a whole (**Figure 19**). In addition to vitrinite, some samples (3A WB, 3B WB, and 4A TLSP) contained more inertinite (**Figures 20**), indicative of peats which underwent some form of degradation during deposition. 1A BDO differs from the rest of the samples, as it is liptinite-dominated, containing the waxy derivatives of plants and spores. All coal samples also contained solid bitumen (product of hydrocarbon generation (**Figure 21**)), with 1A BDO and 2C KC containing more than double of any other sample.

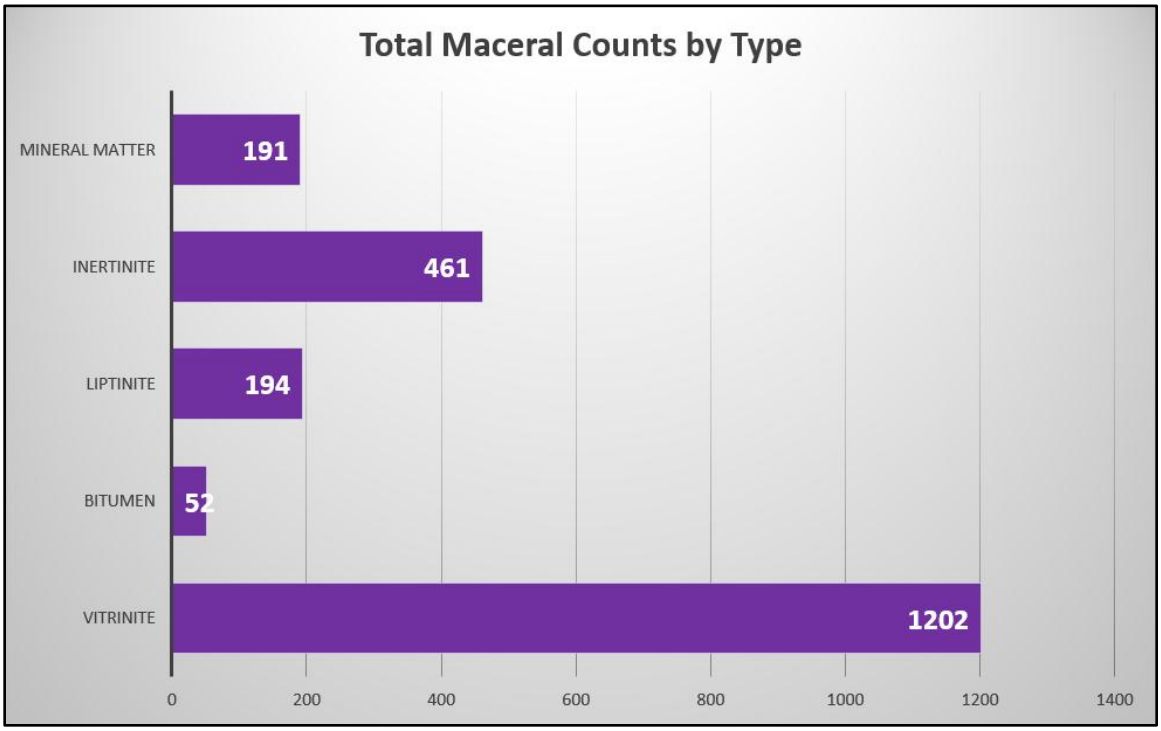

Figure 17 Total maceral counts for all coal samples.

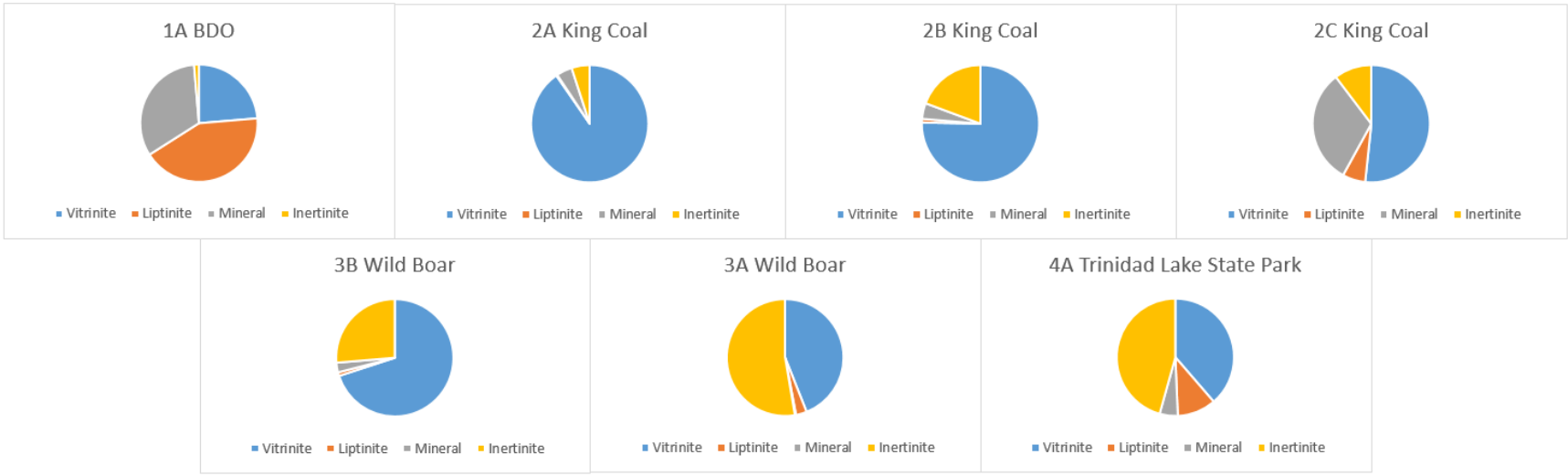

Figure 18 Proportional maceral type for each individual coal sample, represented as a pie chart.

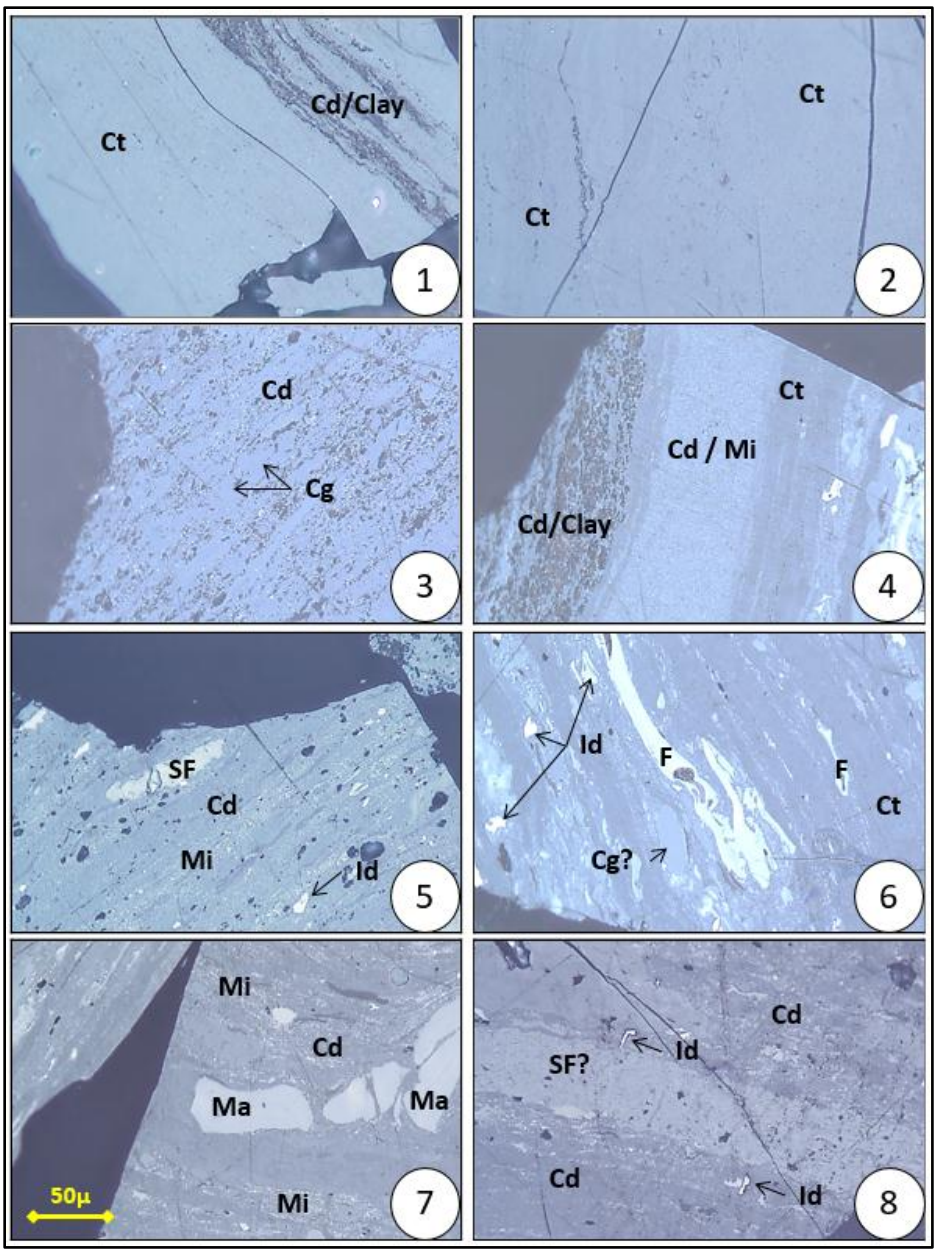

Figure 19 Eight photomicrographs taken in reflected white polarized light. Magnification for all photos is 500x. Scale bar (#7) pertains to all photos. ***[1]*** *Collotelenite (Ct), homogeneous vitrinite groundmass; and Collodetrinite (Cd), mottled vitrinite groundmass, with clay (from 1A BDO).* ***[2]*** *(Ct), homogenous vitrinite groundmass (from 1A BDO).* ***[3]*** *(Cd), mottled vitrinitic groundmass; and Corpogelinite (Cg), homogenous cell fillings (from 2A KC).* ***[4]*** *(Ct), homogenous vitrinite groundmass; (Cd) and Micrinite (Mi), mottled vitrinite groundmass with small rounded grains of inertinite; and (Cd), mottled vitrinite groundmass, with clay (from 2B KC).* ***[5]*** *(Cd) with (Mi), mottled vitrinitic groundmass with small rounded grains of inertinite; Inertodetrinite (Id), small discrete inertinite particles of varying shape; and Semifusinite (SF), inertinite of intermediate reflectance with visible cellular structure (from 2C KC).* ***[6]*** *(Ct), homogenous vitrinite groundmass; possible (Cg), homogenous cell fillings; Fusinite (F), highly reflecting inertinite with visible cell structure; and (Id), small discrete inertinite particles of varying shape (from 3A WB).* ***[7]*** *(Cd) with Macrinite (Ma) and (Mi), mottled vitrinitic groundmass with amorphous structureless inertinite bodies, and small rounded grains of inertinite (3B WB).* ***[8]*** *(Cd), mottled vitrinitic groundmass; with (SF), inertinite of intermediate reflectance with visible cell structure; and (Id), small discrete inertinite particles of varying shape (from 4A TLSP).*

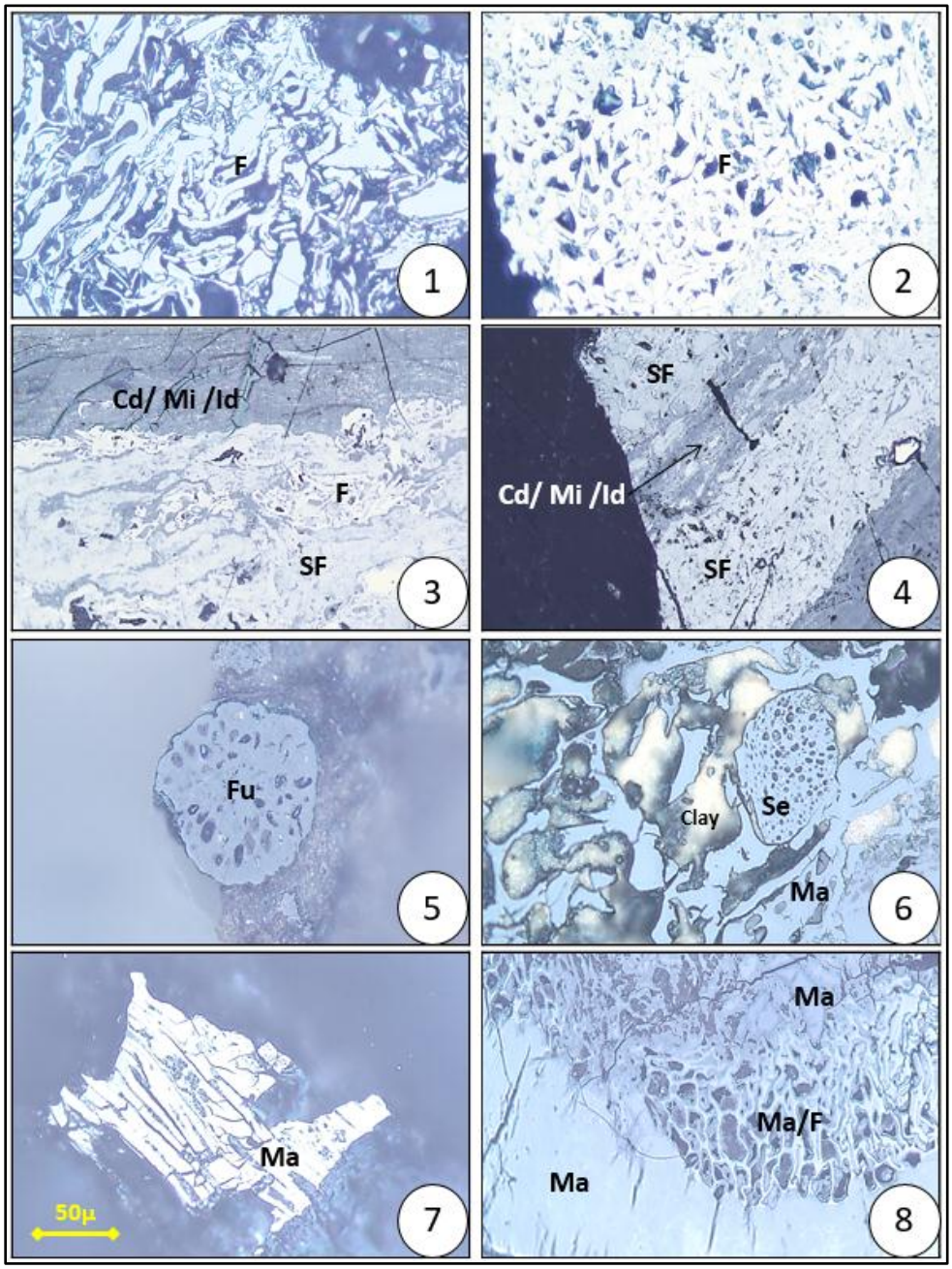

Figure 20 Eight photomicrographs taken in reflected white polarized light. Magnification for all photos is 500x. Scale bar (#7) pertains to all photos. ***[1]*** *Fusinite (F), highly reflecting inertinite with visible cell structure (from 2A KC).* ***[2]*** *(F), highly reflecting inertinite with visible cell structure (from 3A WB).* ***[3]*** *(F), highly reflecting inertinite with visible cell structure; Semifusinite (SF), inertinite of intermediate reflectance with visible cell structure; and Collodetrinite (Cd) with Micrinite (Mi) and Inertodetrinite (Id), mottled vitrinitic groundmass, small rounded grains of inertinite, and small discrete inertinite particles of varying shape (from 3B WB).* ***[4]*** *(SF), inertinite of intermediate reflectance with visible cell structure; and (Cd) with (Mi) and (Id), mottle vitrinite groundmass, small rounded grains of inertinite, and small discrete inertinite particles of varying shape (from 4A TLSP)* ***[5]*** *Funginite (Fu), highly reflecting fungal spore sclerotia (from 1A BDO).* ***[6]*** *Secretinite (Se), round inertinite bodies without plant structure thought to be the oxidation product of resins or humic gels; Macrinite (Ma), amorphous structureless inertinite bodies, and clay (from 2A KC).* ***[7]*** *Macrinite (Ma), amorphous structureless inertinite bodies (2B KC).* ***[8]*** *(Ma), amorphous structureless inertinite bodies; and possible (F), highly reflecting inertinite with visible cell structure (from 3A WB).*

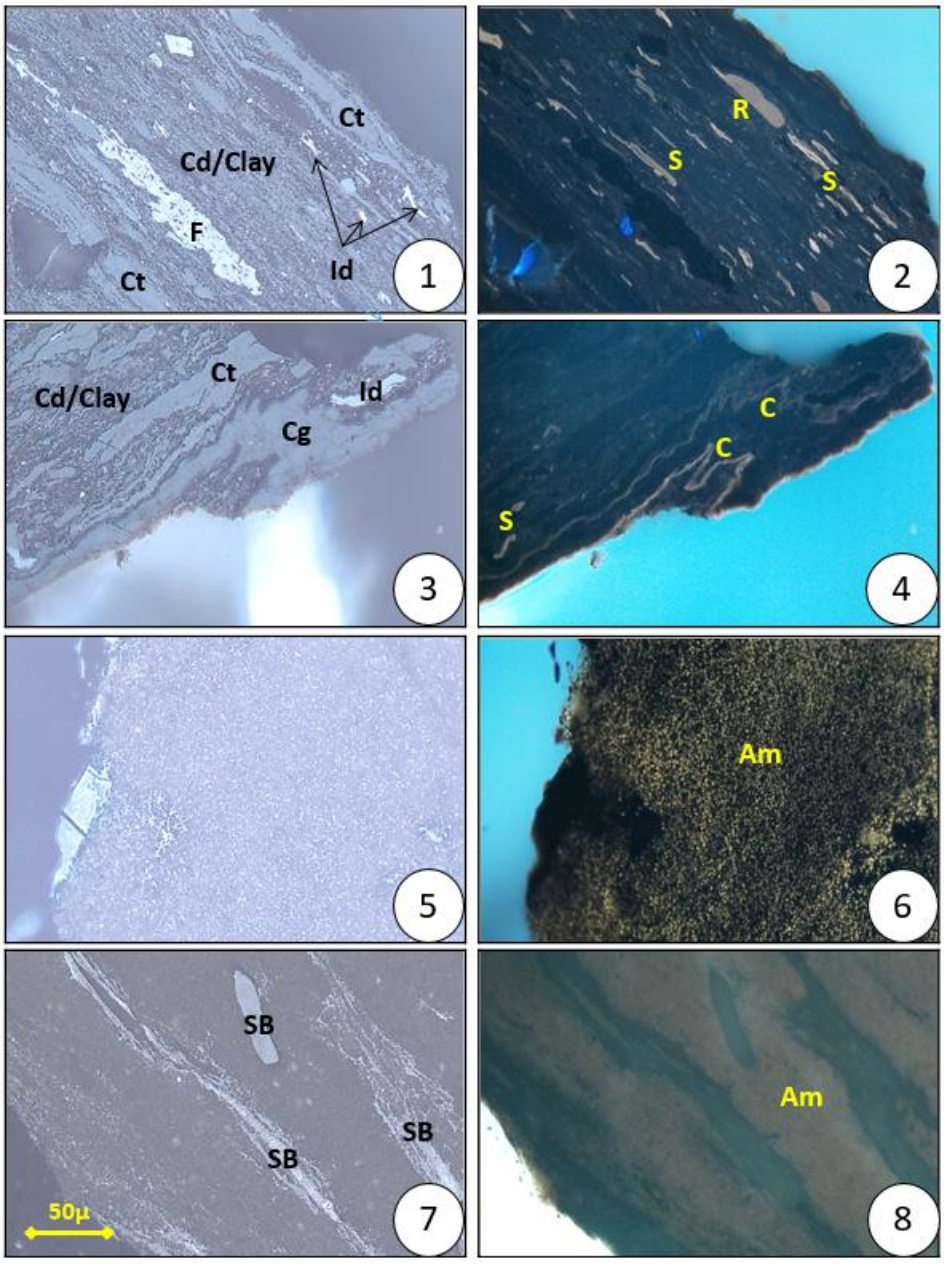

Figure 21 Eight photomicrographs, with the photos on the left taken in reflected white polarized light, and the right being a matching photo taken in UV-light. Magnification for all photos is 500x. Scale (#7) on bottom left pertains to all photos. ***[1]*** *Collotelinite (Ct), homogenous vitrinite groundmass; Fusinite (F), highly reflecting inertinite with visible cell structure; Inertodetrinite (Id), small discrete inertinite particles of varying shape; and Collodetrinite (Cd), mottled vitrinitic groundmass, with clay.* ***[2]*** *Resinite (R) derived from plant resins; and Sporinite (S) derived from the waxy coatings of pollen and spores (from 1A BDO).* ***[3]*** *(Ct), homogenous vitrinite groundmass; Corpogelinite (Cg), homogenous cell fillings;(Id), small discrete inertinite particles of varying shape;Collodetrinite (Cd), mottled vitrinitic groundmass, with clay.* ***[4]*** *Cutinite (C), derived from the waxy outer coating of leaves, roots and stems; and (S), derived from the waxy coatings of pollen and spores (from 1A BDO).* ***[5]*** *Clay, with possible dispersed Solid Bitumen, an early product of hydrocarbon generation.* ***[6]*** *Possibly Amorphinite (Am), amorphous and discrete fluorescing bodies, of unknown origin, perhaps bacterial or amorphous kerogen/algae (from 2A KC).* ***[7]*** *Solid Bitumen (SM),), likely wurtzilite, an early product of hydrocarbon generation.* ***[8]*** *Possibly Amorphinite (Am), low fluorescent clay, fluorescing organic matter of unknown origin, likely amorphous kerogen/algae (from 4A TLSP).*

Palynology

Coal samples were individually analyzed for palynofloral assemblages. Sample 1A Bosque del Oso was the only sample that yielded identifiable spores—; it contained a sparse assemblage, dominated by structured plant material, such as cuticles and other structured plant debris. All other coal samples lacked identifiable palynomorphs, being entirely dominated by opaque vitrinite / kerogen.

The palynofloral assemblage in sample 1A Bosque del Oso (**Figure 22**) was dominated by the tree fern spore *Laevigatosporites* sp., with lesser amounts of *Gleicheniidites* sp., non-descript lacustrine algae, and rare non-descript fern spores, bisaccate pollen, angiosperm pollen, and one fungal spore. All of the identifiable pollen occur in places that are at least seasonally wet, with lacustrine algae indicating presence of true standing water for some period. The angiosperm pollen (walnut family) stands out from the rest of the identified palynomoprhs, and could have easily been windblown. Due to the low abundances, quantitative abundance counts were not possible. It is worth noting that the only sample with identifiable spores (1A BDO), is the sample with the highest amount of liptinite (preserved waxy leaf components), least inertinite, and a high amount of solid bitumen.

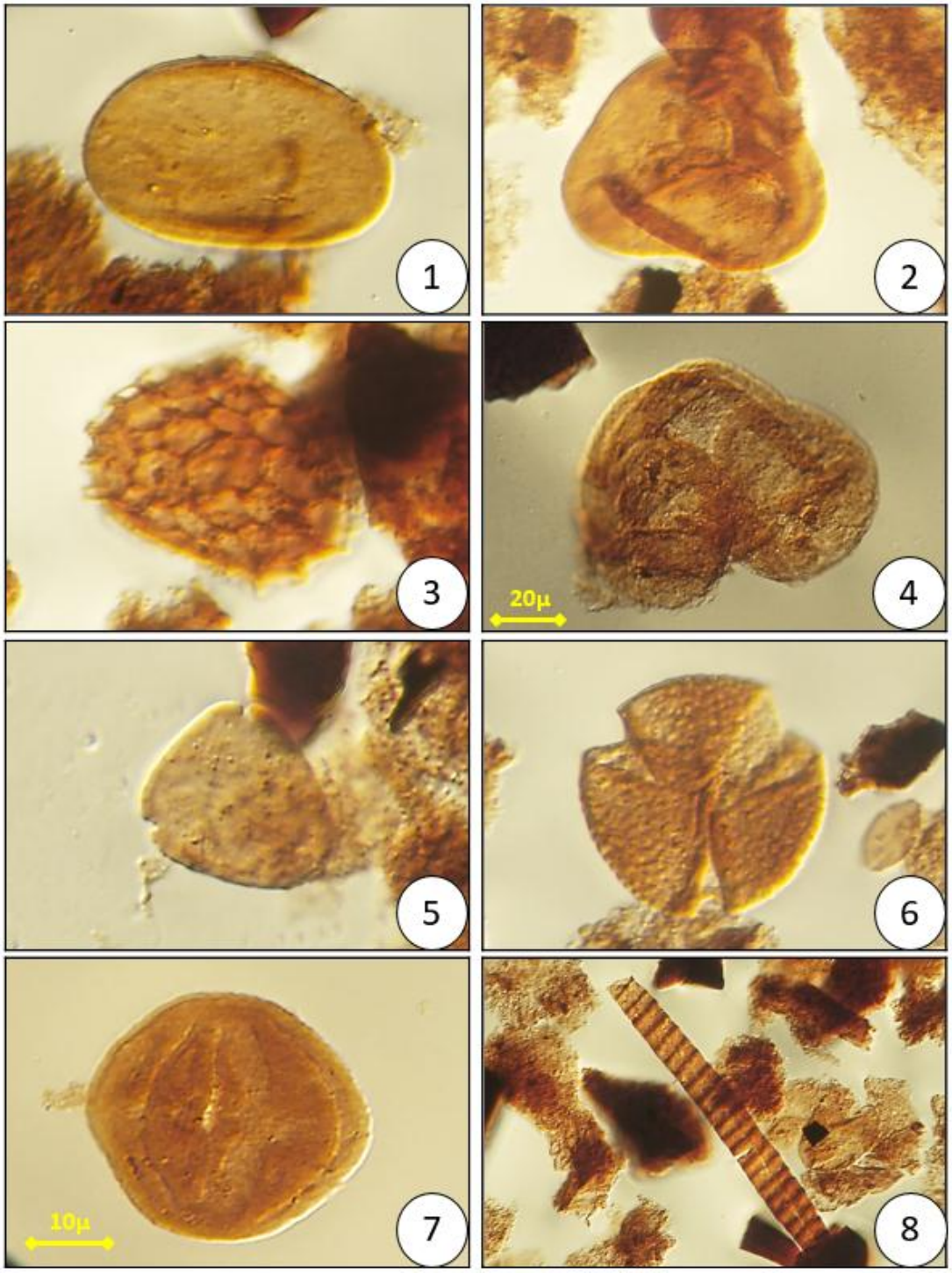

Figure 22 Eight photomicrographs of specimens from the 1A Bosque del Oso sample, taken in transmitted white polarized light. Magnification for all photos is 640x, except for photo 4 which is 400x. ***[1]*** *Laevigatosporites sp. (Monolete fern spore).* ***[2]*** *Gleicheniidites sp. (Trilete fern spore).* ***[3]*** *Reticuloidisporites sp. (Trilete fern spore, reticulate ornamentation).* ***[4]*** *Bisaccate pollen (Gymnosperm pollen, possible Pinaceae)* ***[5]*** *Momipites sp. (Triporate pollen grain, Angiosperm, Juglandaceous affinity, Walnut family).* ***[6]*** *Tricolpites sp. (Tricolpate pollen grain, foveolate sculpture, unknown botanical affinity).* ***[7]*** *Tricolporites sp. (Tricolporate pollen grain, psilate to finely scabrate sculpture, unknown botanical affinity).* ***[8]*** *Fungal spore (Fungal hyphae: filamentous structure of a fungus, oomycete, or actinobacterium.*

Core and Outcrop

Cretaceous-Paleogene Raton Formation strata contain thirteen distinct lithofacies (**Table 6, Figure 23**) in both core and outcrop. Lithofacies are grouped into three Lithofacies Assemblages and Architectural Elements are further defined for sandstone-rich lithofacies (**Table 8**).

Grain Size	Lithofacies (Code)	Lithology	Characteristics	Fossils, Special Features	Interpretation
C	Conglomerate (Cg)	Pebble-sized, poorly sorted conglomerate, reddish brown	No major observable features, massive, poorly sorted conglomerate	None observed	Braided streams and alluvial fan deposits, upper flow regime, represents Raton Conglomerate
S	Trough cross-laminated sandstone (St)	Fine to coarse-grained quartzose sandstone , white (fresh) to dark tan / yellow (weathered)	Sets range in thickness from 0.1-2m, commonly at base of multiple sandstone sets	Commonly in scour at base, frequent mud rip-ups and local preserved organics (sticks)	Migration of dunes, high energy flow
S	Planar cross-laminated sandstone (Spx)	Fine to coarse-grained quartzose sandstone , white (fresh) to dark tan / yellow (weathered)	Sets range in thickness from 0.1 to 3.5m and tend to fine up. Scours within / between sets identifiable. Contains both low and high angle cross-laminations	Commonly in scour at base, some preserved organics (sticks)	Dunes and bars in low flow regime
S	Planar-laminated sandstone (Sp)	Very fine to coarse-grained quartzose sandstone, white (fresh) to dark tan / yellow (weathered)	1mm-1cm horizontal laminations, with lamination sets ranging from 1-75cm. Contain isolated ripple laminations	Abundant preserved organics at base (leaves, stick impressions)	Upper flow regime plane bed
S	Ripple-laminated sandstone (Sr)	Very fine to medium-grained quartzose sandstone, white (fresh) to tan (weathered)	1-3 cm ripple laminations, ripple sets ranging from 0.5-20cm, rare climbing ripples	Abundant preserved organics (leaves, sticks)	Channel, splay, and blowout wing. Represents ripple migration in low flow regime.
S	Massive sandstone (Sm)	Very fine to coarse-grained quartzose sandstone, white (fresh) to dark tan / yellow (weathered)	Lack of sedimentary structures, Thickness ranges 0.1-2m	Preserved whole trees, directly associated gravity-driven collapse structures	High volume sand movement of channel sands
M	Slumped sandstone (Sss)	Silty sandstone to medium-grained sandstone, ranges in color due to high argillaceous content	Dewatering structures common, some preservation of primary sedimentary structures but typically destroyed	None observed	Represent gravity-driven flows, bank collapse, slump structures, liquefaction

M	Faintly-laminated sandstone (Sfl)	Very fine to medium-grained quartzose sandstone, ranges in color (white-yellow-red) due to high argillaceous content	Contains faint low-angle laminations, one of the most common lithofacies	Common preserved organics (roots, leafs, sticks)	Formed during brief deceleration of high volume sand flow or Sm
M	Heterolithic Sandstone, Siltstone, Mudstone (H)	Lithology ranges from muddy siltstone to medium-grained sand, occurs in alternating bedding	planar-laminated, ripple-laminated, or faintly-laminated, Thickness ranges from 0.05-4m	Commonly rooting near top of H, but generally lacks bioturbation, some well-preserved organics in between laminations	Splay delta, waning flows, and abandoned channel fills
F	Laminated Mudstone (Flm)	Clay particles, slightly silty mudstone to pure mudstone, light to dark gray	Planar-laminations	Minor preserved organics (sticks, leafs), iron staining and nodules, some pyrite, very minor rooting	Floodplain lakes, with minor rooting and iron staining indicating temporary exposure
F	Paleosol (Fp)	Occurs in mud and siltstone to very fine-grained quartzose sandstone	Most characterized by rooting, primary bedding typically destroyed. Commonly,gleyed, mottled, containing slickenlines	Dominated by moderate to abundant rooting,	Moderately to very poorly drained, poorly developed simple soils. Slickenlines indicate vertisols, mottled and broken up / green paleosols indicate gleysol
F / O	Carbonaceous Mudstone (Fcm)	Dark gray to very black. Often shiny. Very fissile.	Often preserved, coalified organics. Abundant organics differentiate this lithofacies from laminated mudstone. Range in thickness from 0.02-1.5m	Sticks, roots, leafs, generally have been coalified	Basically coaly mudstones, and serve as a transitionary period between when floodplain lakes are not coal-producing.
O	Coal (C)	Black, shiny, high volatile bituminous a coal.	Well-developed cleats. Range in thickness from 0.03-2.5m	Shiny, black	Period during which floodplain lakes undergo period of peat-preservation

*Table 6 Table of lithofacies identified in core and outcrop, with information on lithology, major characteristics, fossils and special features, and interpretations of each. For Grain size, **Cg** = conglomerate, **S** = sand, **M** = mixed, **F** = fines, and **O** = organics.*

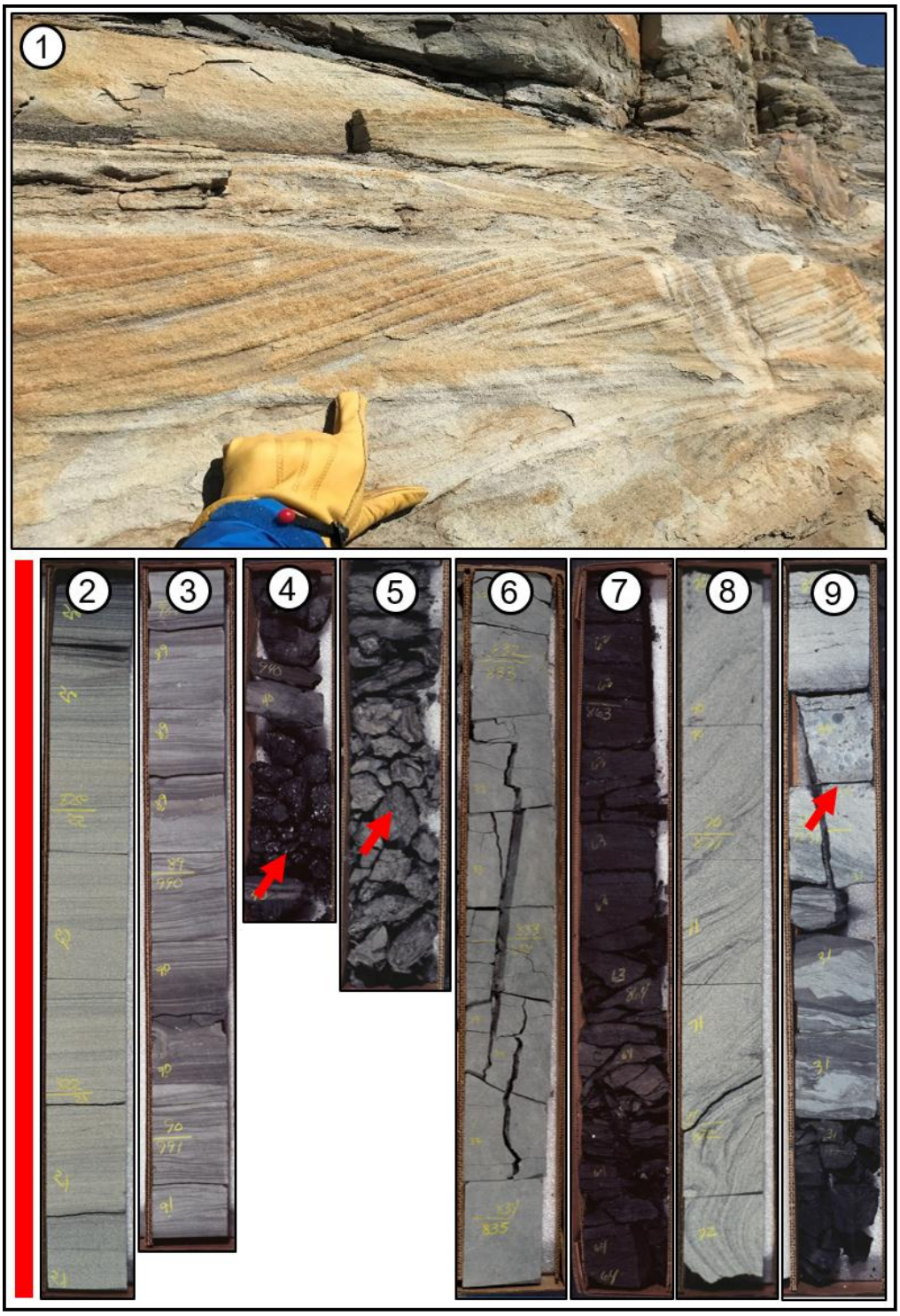

Figure 23 Lithofacies examples in outcrop and core. Scale for [1] is hand. Scale for [2-9] indicated by red line on left, which is 1m. [1] Planar cross-laminated sandstone (Spx) at base of a channel-belt assemblage (from TLSP). [2] Planar laminated sandstone (Sp) from Dover 21-1TR. [3] Heterolithic sandstone, siltstone, mudstone (H) from Dover 21-1TR. [4] Coal (C) indicated by red arrow, from State of Colorado 21-36R. [5] Poorly drained gleyed paleosol (Fp) from State of Colorado as 21-36R. [6] Moderately drained rooted floodplain (Fp) from Maverick. [7] Carbonaceous mudstone (Fcm) from Maverick 12-29 TR. [8] Slumped sandstone (Sss) from Maverick 12-29 TR. [9] Raton conglomerate (Cg) and contact of Raton Formation and Vermejo Formation, indicated by red arrow, from Maverick 12-29 TR.

Lithofacies Assemblage

Lithofacies in the core and outcrop of the Upper and Lower Coal Zone of the Raton Formation are grouped into three genetically related lithofacies assemblages. These associations are: channel-belt, floodplain, and lacustrine assemblages. In addition to these assemblages, the outcrops contained one superassemblage formed of a combination of assemblages: valley-fill. In general, channels cutting through floodplains and lakes deposit the channel-belt assemblage, floodplains deposit the floodplain assemblage, and lakes in floodplains deposit the lacustrine assemblage, which includes major coals.

Channel-Belt Assemblage

The channel-belt assemblage contains Cg, St, Spx, Sp, Sr, Sm, Sss, Sfl, and Fp lithofacies, is poorly to well-sorted, and ranges from pebbly conglomeratic to very fine-grained quartzose sandstone. The channel-belt assemblage is divided into three elements: bars, channel fills, and wings. Clustered or amalgamated channel-belts are common and occur in all three outcrops studied (**Figures 29-31**). However, the King Coal outcrop contains the only example of a confined amalgamation of several channel-belt assemblages, which together forms a valley-fill superassemblage (**Figure 30**). Valley-fill superassemblages, channel-belt assemblages, and their associated elements, are commonly encased in floodplain and lacustrine assemblages (**Figures 29-31**). Within the channel-belt assemblage, the channel-fill element is the most abundant, followed by the bar, and blowout wing elements.

Bar Element

Bars are characterized by lithofacies St, Sxp, Sp, and Sr and typically dominate channel belts. Bars have an erosive basal contact and can partially cannibalize one another. They typically have a sheet-like or lensoid geometry, and can locally stack, representing amalgamated channel-belts (**Figures 24, 30**). Bars are defined by their internal fining upward trends, internal accretion sets, and geometry (Miall, 1996; Sharma, 2013). Bars are bound by basal scours and capped by floodplain deposits.

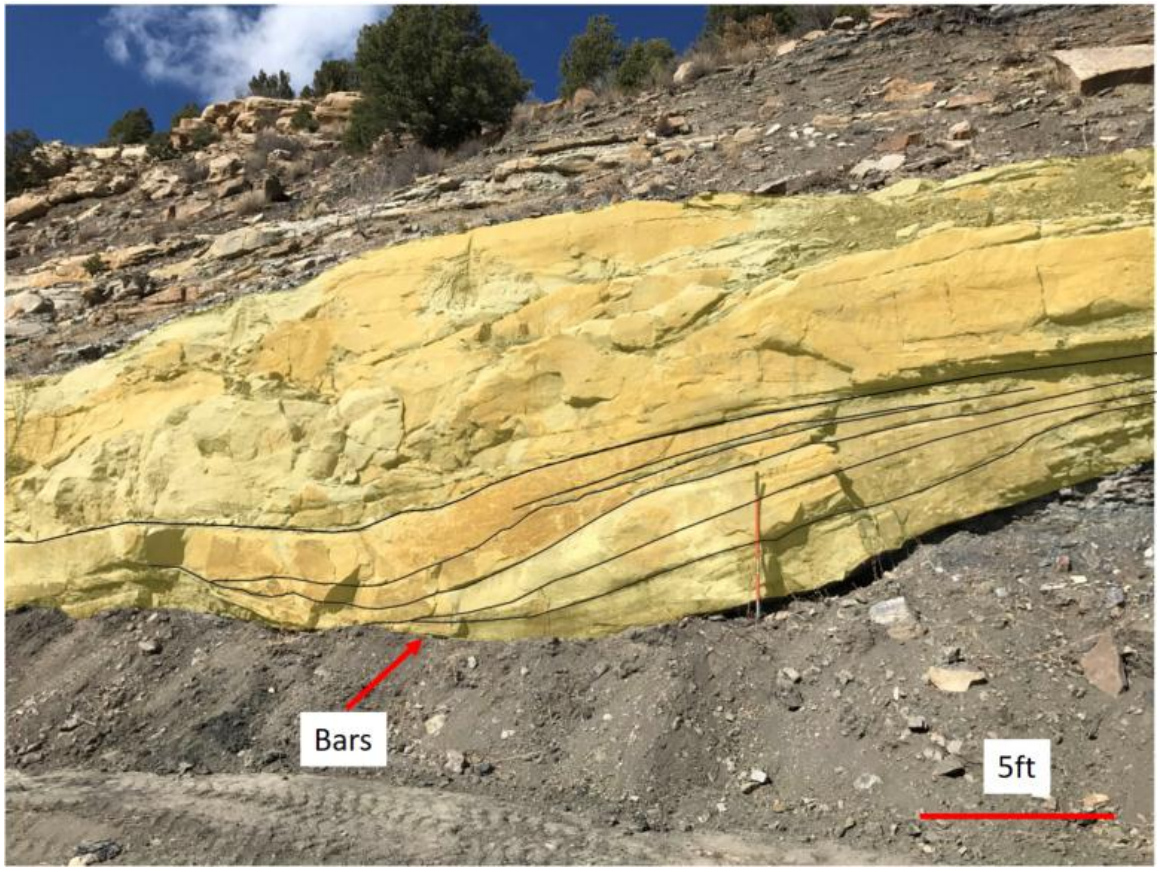

Figure 24 Set of bars representing amalgamating channel-belts, from King Coal outcrop.

Channel Fill Element

Channel fill elements are characterized by Cg, St, Spx, Sp, Sr, Sm, Sss, and Sfl lithofacies. Channel fill elements typically have a basal scour and their geometries are concave up, lensoid, and sometimes sheet-like, which likely represents adjacent channel fills. Channel fill elements in this study typically fine up, range in thickness from 5 to 24

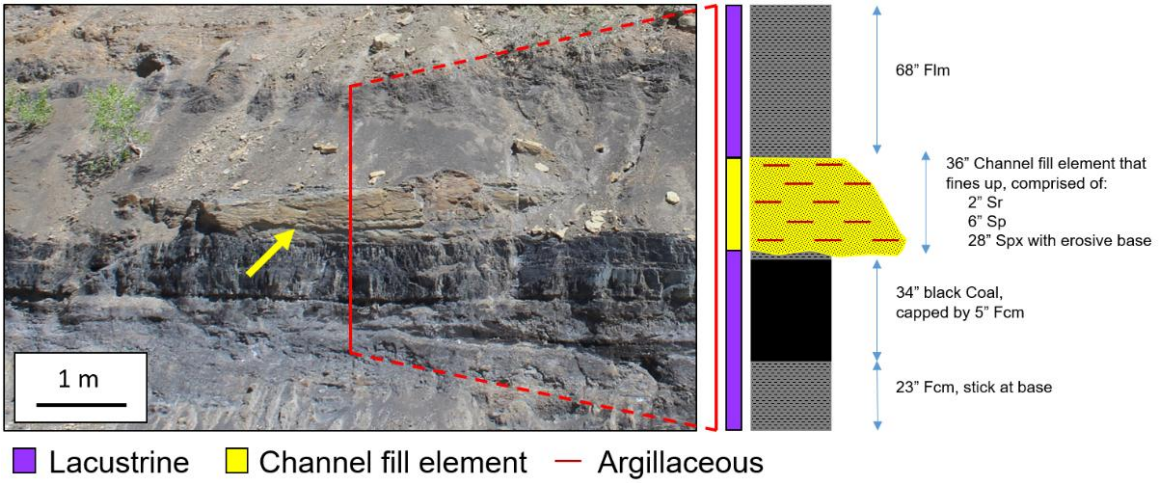

Figure 25 Channel-fill element with measured section. Yellow arrow indicates a channel-fill element, encased in lacustrine assemblage. Measured section (from Appendix Item 12). From TLSP Outcrop.

feet (1.5 to 8 m), and can extend laterally from 4 to 125 m. Similar to channel-belt assemblages, channel fill elements can also be encased in floodplain or lacustrine assemblages. A generalized single channel fill would have an erosive basal scour, fine upward, and then gradationally transition into an abandoned channel fill stage / lacustrine assemblage. A similar example occurs in TLSP outcrop (**Figure 25**).

Channel fill elements often contain preserved vegetative organics at their base, including roots, sticks, root balls (large siderite nodules formed around the base of trees and root systems), and even whole trees (**Figure 26**). Vegetation-induced sedimentary structures (VISS) are primary sedimentary structures formed by the presence of *in situ* plants and their syndepositional interaction with sediment (Noffke et al., 2001; Rygel et

al., 2004). VISS were well-documented in the Raton Formation Horner (2016), but their presence is mainly associated with splay assemblages.

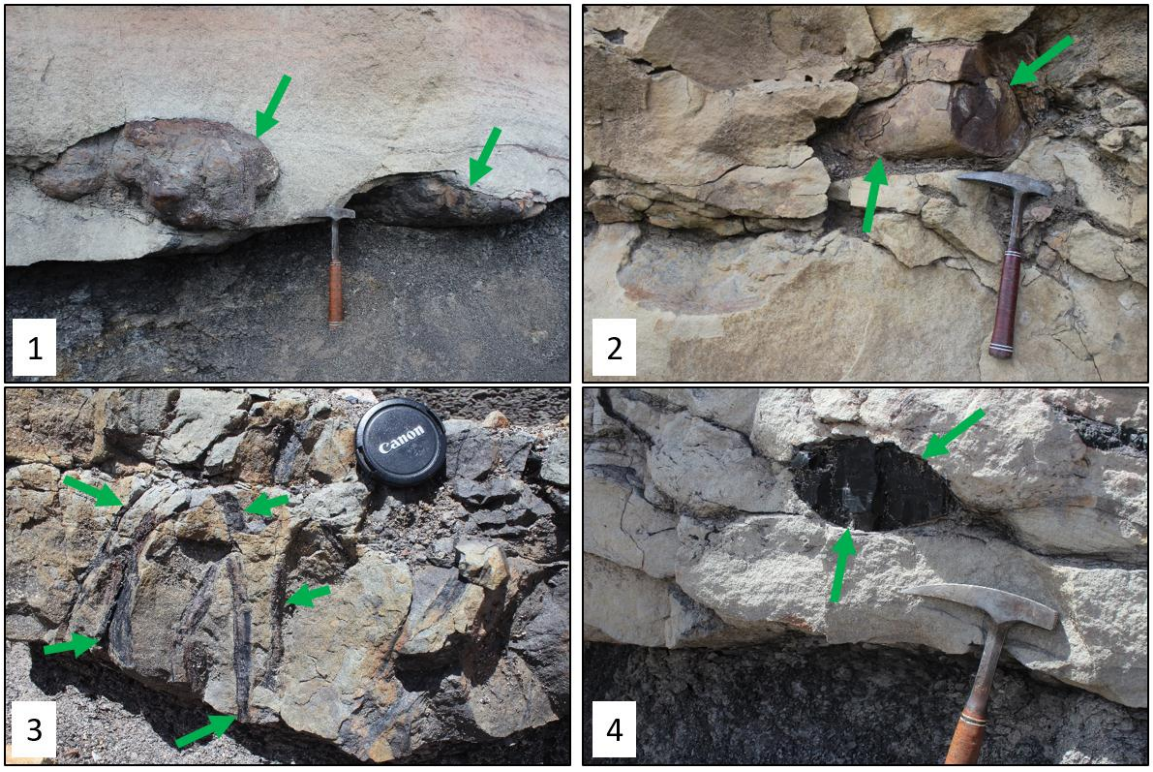

Figure 26 Four examples of preserved vegetation. All are located near the base of channel fill elements. Scale is provided by hammer except in [3], which is provided by camera lens. ***[1]*** *Root balls highlighted in green, from King Coal outcrop.* ***[2]*** *Preserved fallen tree, from King Coal outcrop.* ***[3]*** *Preserved stick impressions, from King Coal Outcrop.* ***[4]*** *Preserved, coalified stick or tree, from Trinidad Lake State Park outcrop.*

Blowout Wing Elements

Blowout wing elements are characterized by Sp, Sr, Sm, and Sfl lithofacies. Wings typically occur at the top of channel fill elements, and extend laterally from these elements as thin, tabular, and laterally extensive sheets on both sides of the channel.

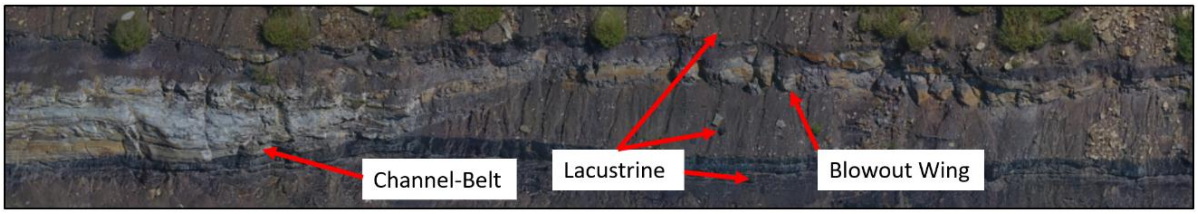

Figure 27 Annotated blowout wing. Shows a blowout wing, surrounded by lacustrine assemblage deposits,

Cross-laminated sandstone at the top of a channel-fill transitions upwards into ripple-laminated to faintly-laminated sandstone, which extends and tapers laterally as blow-out wings, often interfingering and clustering with other blowout wings (**Figure 27**). Thickness of wings range from 0.25 to 1m thick with lateral extent up to 300m. Blowout wings were first identified by Tomanka (2013), and are sand sheets perpendicular to channels that are propagating out into floodplain lakes or lacustrine environments. They form as subaqueous density flows over the sides of channel levees (Tomanka, 2013; Huling, 2014; Howe, 2017).

Scale of Channel-Belt Assemblage

The four cores and three outcrops in this study contained 28 single channel stories. In core, single channel stories were identified based on an erosional scour or lag at the base, a fining upwards sequence beginning with trough and planar-cross laminated sandstone and capped by fine-grain floodplain or lacustrine assemblage deposits. A similar identification scheme was used in outcrop, but the majority of channel thicknesses in outcrop were measured based on the concave-up geometry of channel deposits, as these could not be reached in-person, and likely contain a minimum of ~10% error. Channel story thicknesses from this collection ranged from 2 – 21.5 feet (0.75 – 7m), with an average thickness of 13.4 feet (4.08 m).

Table 7 Channel story thickness. Contains average measured thickness for single story channels measured in core and outcrop. Actual channel measurements follow the given average, in ordering of descending thickness. Specific tops and bottoms are on the core description and outcrop maps.

Location (Core, Outcrop)	Average Channel Thickness (ft)	No. Channels Measured
ZAMORA 22-14V	19 (21.5,19.75,18.5,16.25)	5
DOVER 24-1TR	10.2 (14,12.5,4)	3
MAVERICK 12-29 TR	12.4 (21.5, 19.5, 16, 8, 7.5, 2)	6
STATE OF COLORADO AS 21-36 TR	14.4 (17.5, 17, 13, 10)	4
TRINIDAD LAKE STATE PARK	10.1 (13.5, 13.5, 10.2, 3)	4
KING COAL	13.8 (15.5, 14.7, 14.4, 12.5, 12.1)	5
WILD BOAR	13.5 (13.5)	1

Floodplain Assemblage

The floodplain assemblage is characterized by Sp, Sr, Sfl, H, Flm, Fp, Fcm, and C lithofacies. The floodplain assemblage includes both poorly drained and moderately drained categories, but is dominated predominately by poorly drained. The UCZ and LCZ of the Raton Formation contain only simple paleosols, or immature underdeveloped paleosol profiles (Kraus and Aslan, 1993). Carbonaceous mudstone and coal are only present as very thin beds, within poorly drained floodplain deposits, and are not laterally extensive (termination of coals is observable at outcrop-scale). Moderately drained is defined as possessing more subaerial lithologies (i.e., heavily rooted Fp, Sfl, and H) than subaqueous (i.e., H, Sfl). Conversely, the poorly drained floodplain assembleage contains water-logged or hydromorphic floodplain deposits (i.e., H, Flm, Fp, Fcm, Fp (gleyed paleosol, vertisols containing iron-oxide nodules)) as the dominate assemblage (Krauss and Aslan, 1993; Aslan and Autin, 1999; Krauss and Hasiotis, 2006). While moderately drained

floodplain deposits are especially characterized by heavy rooting, poorly drained floodplain deposits also contain rooting, as even inundated floodplains may become emergent during the dry season. Well-drained and poorly-drained floodplains commonly alternate in core, though this is less easy to discern in outcrop, due to heavy weathering. Floodplain assemblages range in thickness from 0.25 - 7m, and, if not scoured or truncated by channel assemblage, can be very laterally extensive, and extend the entire length of outcrops (**Figure 31**). Floodplain assemblages lack distinct external geometric features other than being extensive and serving as a large-scale matrix assemblage in outcrop (**Figure 31**). The major discerning features between the floodplain and lacustrine assemblage is the presence of moderate-heavy rooting, simple paleosols, and lack of the relatively thick and extensive coals that are found in the lacustrine assemblage (**Figure 31**). Floodplain assemblages also can gradationally transition into lacustrine assemblages, and vice-versa (**Figure 30, 31**).

Splay / Sand Sheet Element

The splay / sand sheet element of the floodplain assemblage is characterized by Spx, Sr, Sp, Sm, and Sfl lithofacies, though this element is dominated by faintly-laminated to ripple-laminated very fine-grained sandstone, especially as asymmetrical ripples and climbing ripples. Crevasse splays and terminal splays are described in detail in the Raton Formation by Horner (2016) and McGregor (2017), who described and mapped a modern terminal splay in a DFS system in the Parana River system of Argentina. Geometrically, splay / sand sheets are tabular and, inherently, sheet-like. Terminal splays are well-studied in arid environments, and are described as lobular sediment bodies at the terminus of a

river or delta, deposited as subaerial sheet-floods (Lang et al., 2004; Fisher et al., 2006; Nichols and Fisher, 2007; Fisher et al., 2008). Crevasse, or overbank, splays occur when amplified discharge from a flood breaches the confining levee of a river, depositing coarser sediments in a sheet-like geometry on top of adjacent floodplain deposits (Coleman, 1988; Mjos et al., 1993; Cahoon et al., 2011). While terminal and crevasse splays are extremely abundant in the barren series of the Raton Formation (Horner, 2016; McGregor, 2017), they are less common in the UCZ and LCZ. Thicknesses range from 0.5 to 2 m, and typically extend and thin laterally up to 200 + m (**Figure 30**). Splays are interpreted as being deposited subaerially, often as sheetfloods, starting with the terminus of distributary channels, and out into the floodplain with a decreasing flow velocity (Lang et al., 2004; Fisher at al., 2007; North and Davidson, 2012; Horner, 2016; McGregor, 2017).

Lacustrine Assemblage

The lacustrine assemblage is characterized by Sp, Sr, Sfl, H, Fp, Flm, Fcm, and C lithofacies. The lacustrine assemblage is similar to the floodplain assemblege, but with a much higher percentage content of laminated mudstone, carbonaceous mudstone, and coal, with minor amounts of rooted floodplain. There is far less rooting than in the floodplain assemblage, and coal deposits are significantly thicker, and more extensive. Several coal seams, in outcrop, can be sandwiched between lacustrine mudstones (**Figures 29-31**). Individual coal beds have been mapped over distances greater than ten miles (Personal Comm. 2018, Sean Horne; Personal Comm. 2018, Roy Pillmore). The lacustrine assemblage varies in thickness from 0.5 to 8 m, and can be very laterally extensive when not truncated by channel fill assemblages. The lacustrine assemblage commonly extends

the entire length of outcrops (**Figure 29, 30**). Lacustrine deposits have been previously identified in the Raton Formation (Horner, 2016; Al-Refaei, 2016; McGregor, 2017). Similar to floodplain assemblages, lacustrine assemblages are broad "sheets" and typically serve as a matrix that channel and splay / sand sheet assemblages scour into (Huling, 2014; Horner, 2016) (**Figures 29, 30**). Lacustrine assemblages are most strongly characterized by laminated mudstone that has little bioturbation, carbonaceous mudstone, and coal.

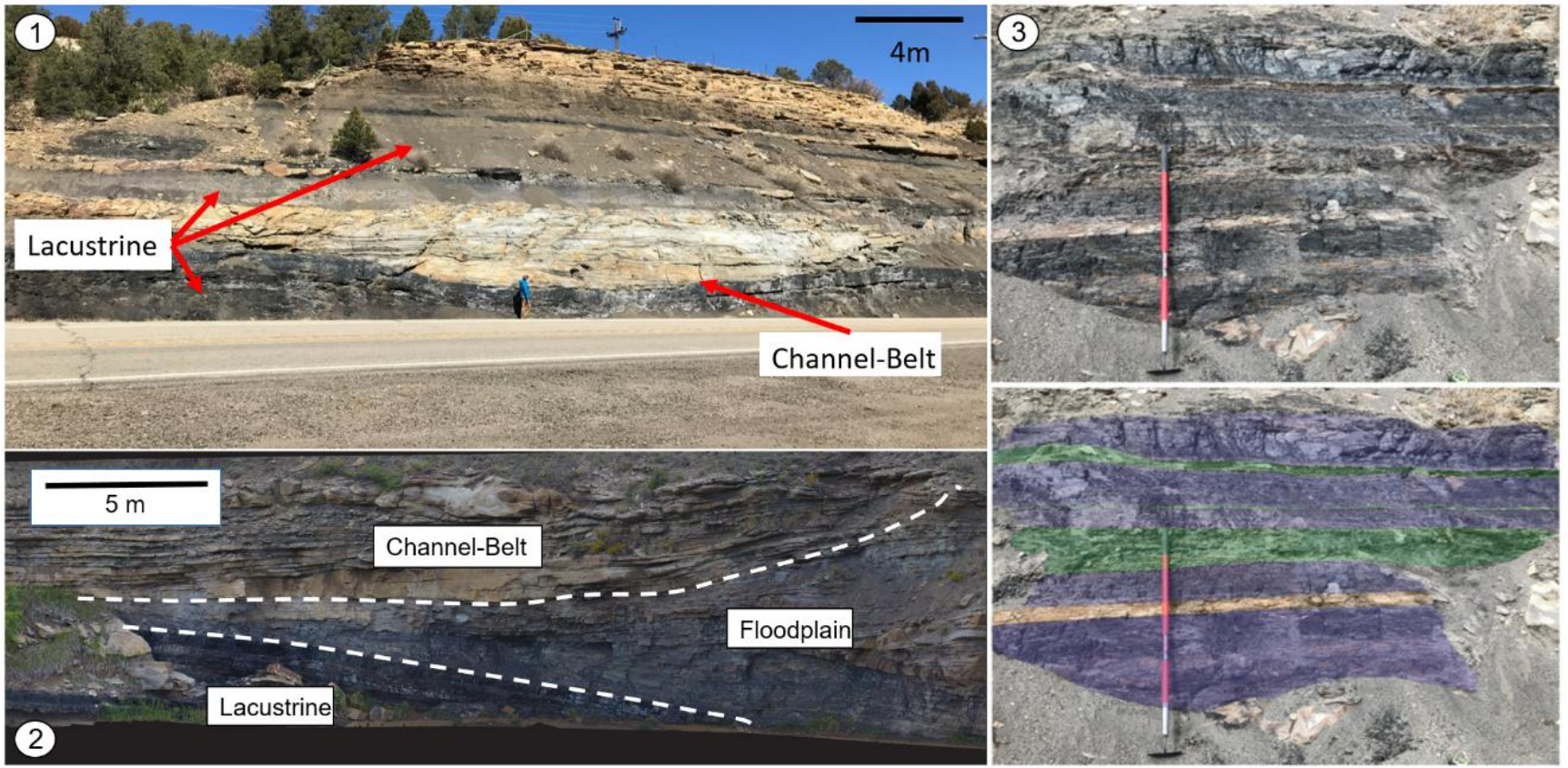

Figure 28 Examples of Lithofacies assemblages. ***[1]*** *Shows channel-belt assemblage encased in lacustrine assemblage (from Trinidad Lake State Park)).* ***[2]*** *Shows channel-belt, lacustrine, and floodplain assemblage (from Wild Boar).* ***[3]*** *Shows a typical lacustrine assemblage with coal (purple), carbonaceous mudstone (green), and a ripple-lamianted sandstone (Sr) (from King Coal).*

Lithofacies Assemblage	Lithofacies Included	Architectural Elements (Lithofacies Included)	Geometry
Channel-Belt	Cg, St, Spx, Sp, Sr, Sm, Sss, Sfl, Fp	Bar (St, Sxp, Sp, Sr) Channel Fill (All) Blowout Wings (Sp, Sr, Sm, Sfl)	Lensoid, tabular, concave up, basal scour
Floodplain	Spx, Sr, Sp, Sm, Sfl, H, Flm, Fp, Fcm, C	Floodplain (Sp, Sr, Sfl, H, Flm, Fp, Fcm, C) Splay / Sand Sheet (Spx, Sr, Sp, Sm, Sfl, H)	Tabular, Lacking
Lacustrine	Sp, Sr, Sfl, H, Fp, Flm, Fcm, C	N/A	Tabular, Lacking

Table 8 Summary of lithofacies assemblages.

Digital Outcrop Models (DOMs)

Trinidad Lake State Park DOM

Trinidad Lake State Park outcrop comprises predominately lacustrine assemblage strata, with multiple channel-belts encased in lacustrine deposits, and is stratigraphically located in the Lower Coal Zone of the Raton Fm. Discounting cover, TLSP is dominated by significant lacustrine assemblage deposits, followed second by channel fill assemblage. A representative example of the channel-belt assemblage is located in the lower-left portion of the outcrop (**Figure 29**), with wings extending out into lacustrine assemblage deposits from the top of the channel to the right. The top third of the outcrop contains several channel-belt assemblages with wings extending far out into the lacustrine assemblage, with a mud-filled channel infill deposit in the middle of the outcrop.

The TLSP outcrop shows the presence of coals within the lacustrine assemblage, general dominance in the Upper and Lower Coal Zone of lacustrine assemblage, and channel-belt and blowout wings that extend out into lacustrine assemblage deposits. A coal extends for the entirety of this outcrop (200+ meters) and is in the middle of a lacustrine lithofacies assemblage. Smaller coals also exist in the lacustrine assemblage but are truncated by channel-belt assemblage deposits.

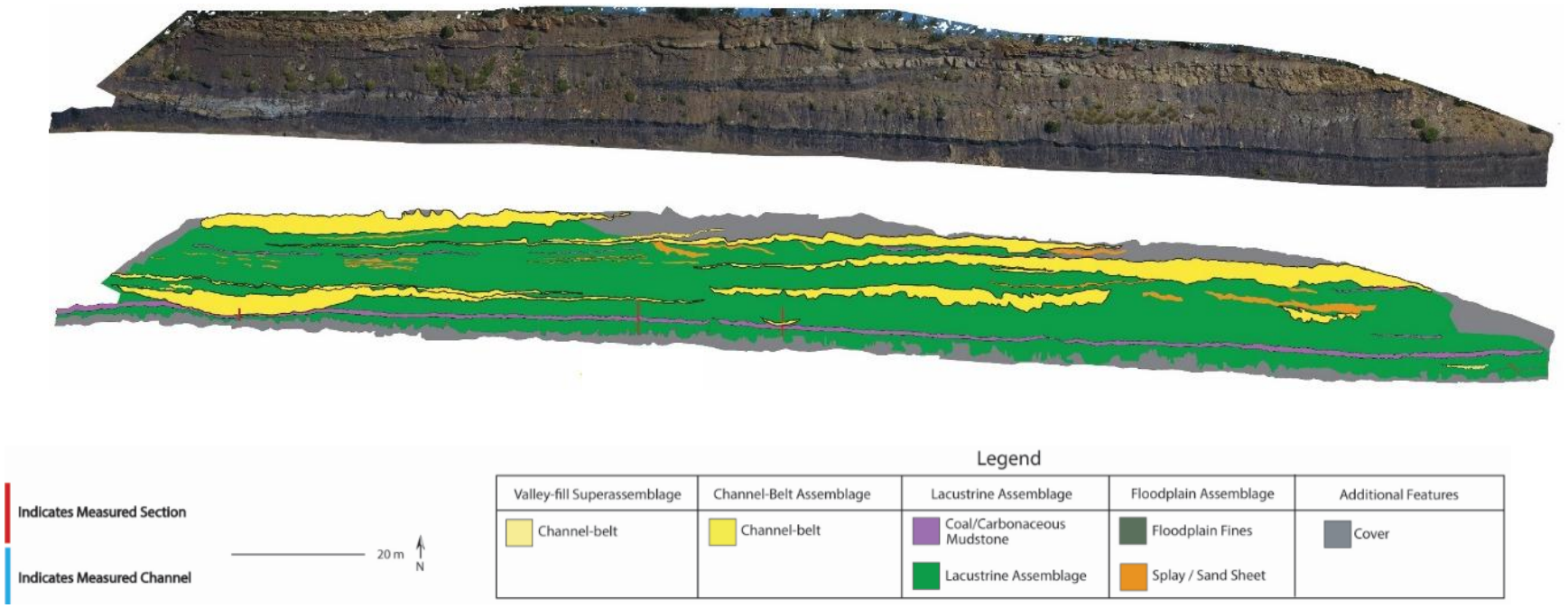

Figure 29 Unannotated and annotated DOM of Trinidad Lake State Park Outcrop. Scale Indicated. See Appendix Item 3.

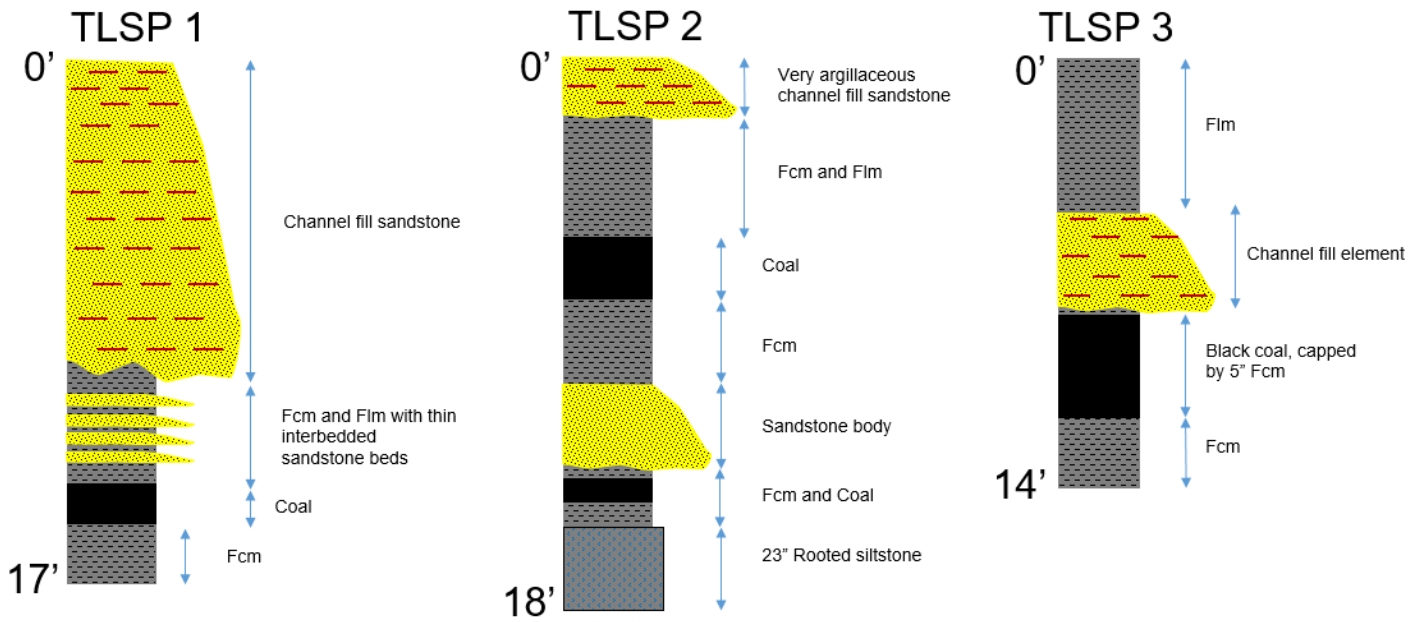

Figure 30 Generalized measured sections from Trinidad Lake State Park outcrop. Detailed measured sections located in Appendix.

King Coal DOM

Discounting cover, King Coal outcrop is dominated by channel assemblage (including the only confined valley-fill superassemblage sandstone in the lower right quadrant of the plate), lacustrine, and lastly floodplain assemblages. The bottom right of the outcrop contains a thick lacustrine assemblage (**Figure 28.3, 31**) with significant, separate coal seams encased in carbonaceous and laminated mudstone.

King Coal is a prime example of how amalgamated channels and valley-fill deposits cut into both floodplain and lacustrine assemblages, and that thick coal seams are most commonly contained within the lacustrine assemblage. King Coal also contains a transition, from lacustrine to floodplain to lacustrine assemblages, through which channel-belt assemblages and the valley-fill superassemblage incised.

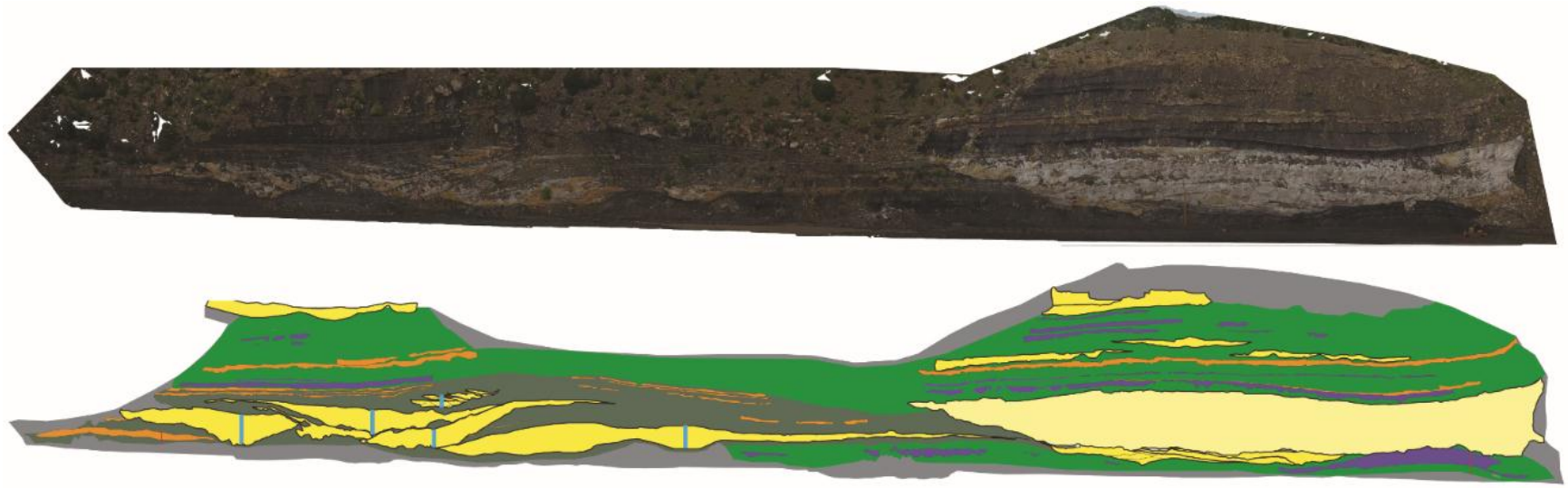

Indicates Measured Section

20 m

N

Legend

Valley-fill Superassemblage	Channel-Belt Assemblage	Lacustrine Assemblage	Floodplain Assemblage	Additional Features
Channel-belt	Channel-belt	Coal/Carbonaceous Mudstone	Floodplain Fines	Cover
		Lacustrine Assemblage	Splay / Sand Sheet	

Figure 31 Unannotated and annotated DOM of King Coal Outcrop. Scale indicated. See Appendix Item 4. Blue bars indicate location of measured channel.

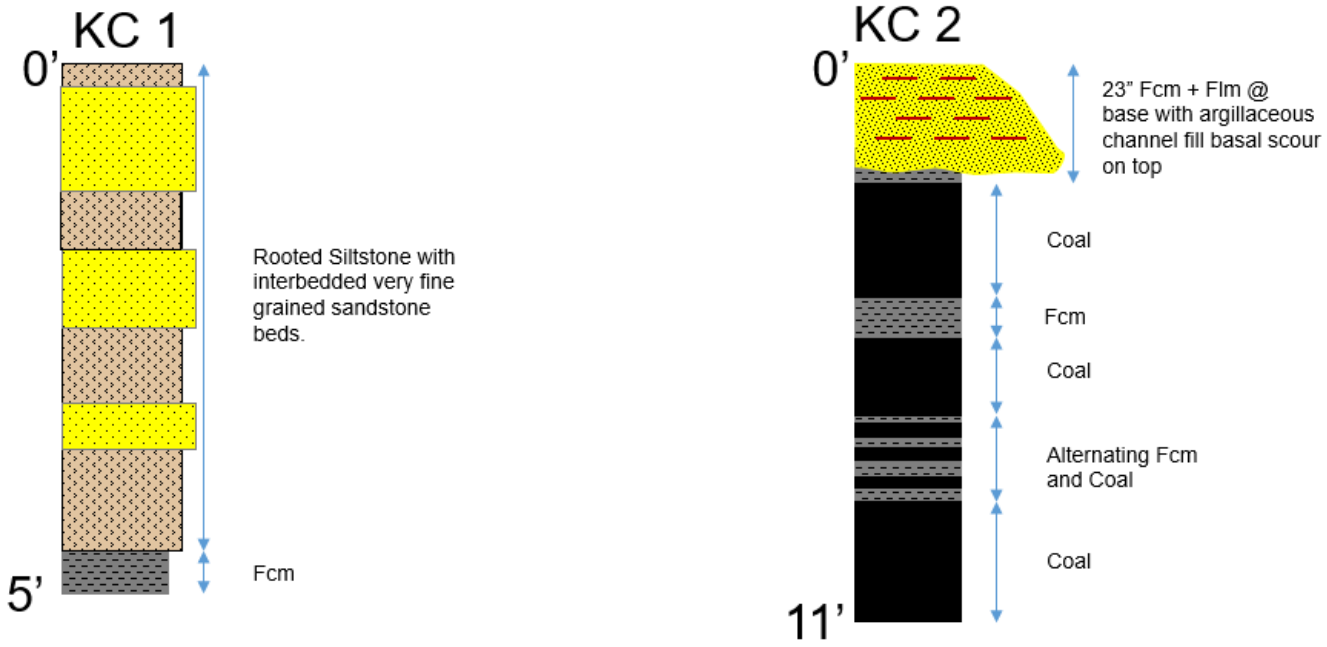

Figure 32 Generalized measured sections from King Coal outcrop. Detailed measured sections located in Appendix.

Wild Boar DOM

Discounting cover, Wild Boar is dominated by channel-belt assemblage (abandoned channel infill above), floodplain assemblage deposits, and lastly lacustrine assemblage with significant coal deposits. The Wild Boar outcrop provides another good example showing how thick coals are contained within lacustrine assemblage mudrocks, a transition from lacustrine to floodplain assemblage, and channel-belt assemblage incising floodplain assemblage deposits (**Figure 33**).

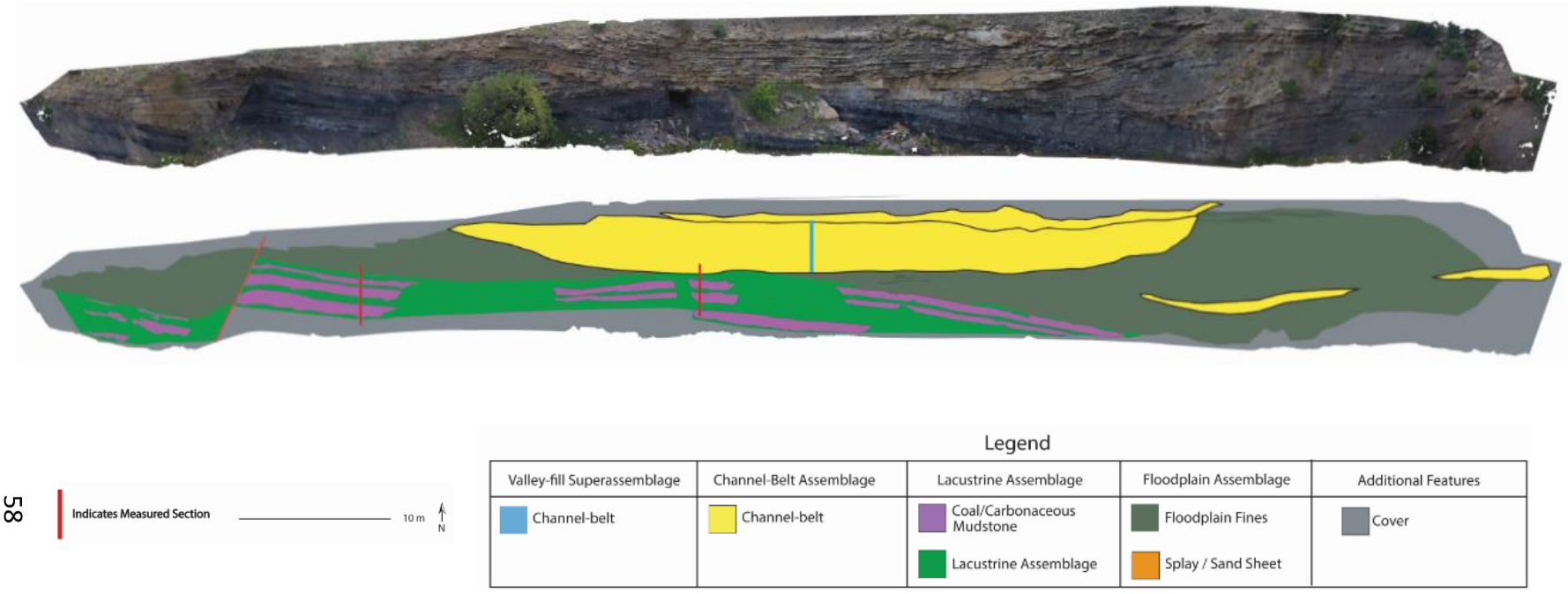

Figure 33 Unannotated and annotated DOM of Wild Boar Outcrop. Scale indicated. See Appendix Item 5. Blue bars indicate location of measured channel.

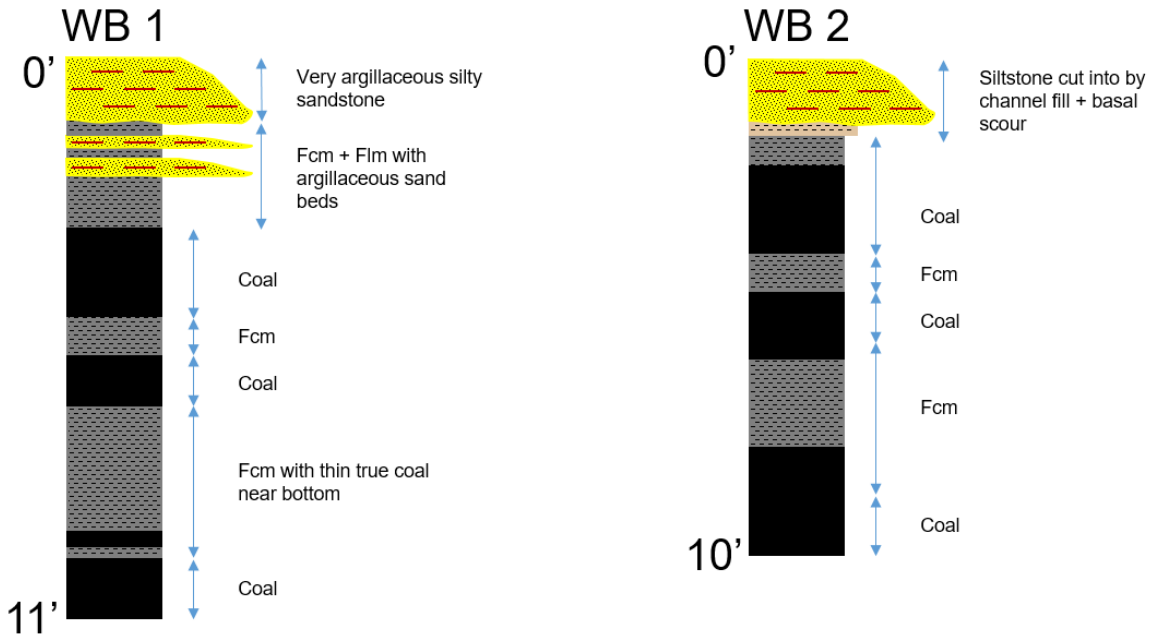

Figure 34 Generalized measured sections from Wild Boar outcrop. Detailed measured sections located in Appendix.

CHAPTER FOUR: Discussion

Peat Environment for Raton Coals

Raton Formation coals are vitrinite-rich (**Figures 16-18; Appendix 1**) suggesting that the primary component of the coals is woody material (58%). Though vitrinite dominates the coals (**Figure 32**), not all maceral components, and thus not all peat composition, is the same (**Figures 16, 18**). Raton coals also contain significant inertinite (**Figure 35**), with samples 3A WB and 4A TLSP containing the most (53% and 39% respectively). This suggests some form of degradation of plant materials prior to deposition, potentially by wildfires or preferred oxidation of vitrinite-materials during decomposition. This is consistent with some of these peats being mounded for some phases of deposition (Lamberson et al., 1996; Jasper et al., 2017; Personal Comm., Dr. Thomas Demchuk). The high mineral content in 1A BDO and 2C KC is attributed to sampling rocks more similar to carbonaceous shales than true coal, and is not interpreted as being represented of the other true coals. 1A BDO contains a relatively high proportion of liptinite (42%). The presence of liptinite is still indicative of a low-lying, inundated/flood-prone environment (Singh and Singh, 1991; Peterson et al., 1998).

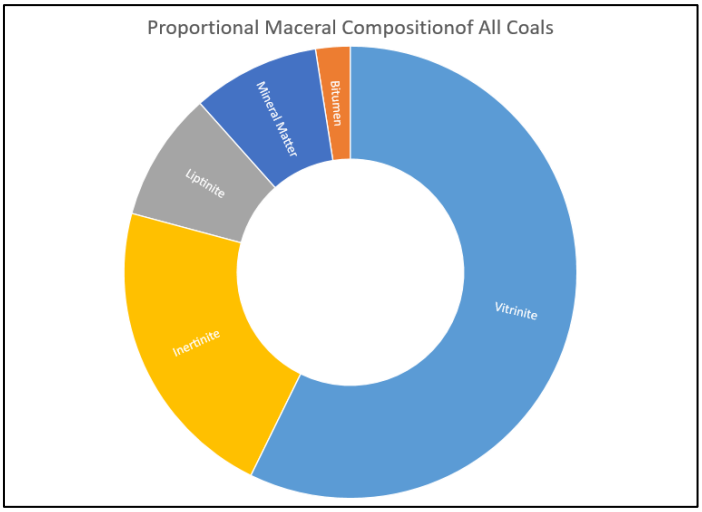

Figure 35 Proportional maceral composition of all coals.

The abundance of preserved vegetative material in all lithofacies assemblages, particularly sticks and ferns, provides further evidence for a woody environment for the

Raton Formation (**Figure 26**). This presence of woody materials is consistent with previous studies (Lee and Knowlton, 1917; Ash and Tidwell, 1976; Flores, Pillmore, and Mereweather, 1985; Wolfe and Upchurch, 1987; Johnson and Ellis, 2002; Horner, 2016). This abundance of woody materials in both maceral content in coals and as macrofossils in outcrop for most facies leads to the conclusion that the Raton landscape was largely forested across its many subenvironment.

The palynoflora suggest a generally wet environment for Raton coals and associated facies. The overall palynofloral assemblage was sparse, and represented only by the 1A BDO sample. This BDO sample was dominated by the fern spore *Laevigatosporites* sp., and other non-descript fern spores. *Laevigatosporites* sp., a tree fern associated with wet forests, and other non-descript fern spores, suggests a predominately wet paleoenvironment and possibly wet paleoclimate (Phillips et al., 1985; Liu et al., 2002; Jennerhjahn et al., 2004; Personal Comm. with Dr. Thomas Demchuk). The presence of lacustrine algae spores in the assemblage from this study further substantiate the evidence for a wet environment, and is used to identify lacustrine coals (Hagemann and Wolf, 1989).

The woody characteristics of the coal composition from maceral contents and preserved organics, coupled with the palynofloral assemblage from this study and Farley (1990), provides evidence that these coals formed in a very woody and wet paleoenvironment. Farley (1990) identified four major palynofloral assemblages (**Figure 36)**: *A, B, C, and D*. *Assemblage A* contains non-unique taxa that exist in a broad-ranging ecological tolerances throughout the late Cretaceous and early Paleocene, *Assemblage B* contains taxa that are found where ground is saturated at least for part of the year (seasonally) or near the edges of lakes, ponds, or ephemeral bodies of water as marshes.

Assemblage C contains freshwater green algae and planktonic species that are characteristic of freshwater lakes and ponds, and *Assemblage D* contained algae species which are common inhabitants of mires (Farley, 1990).

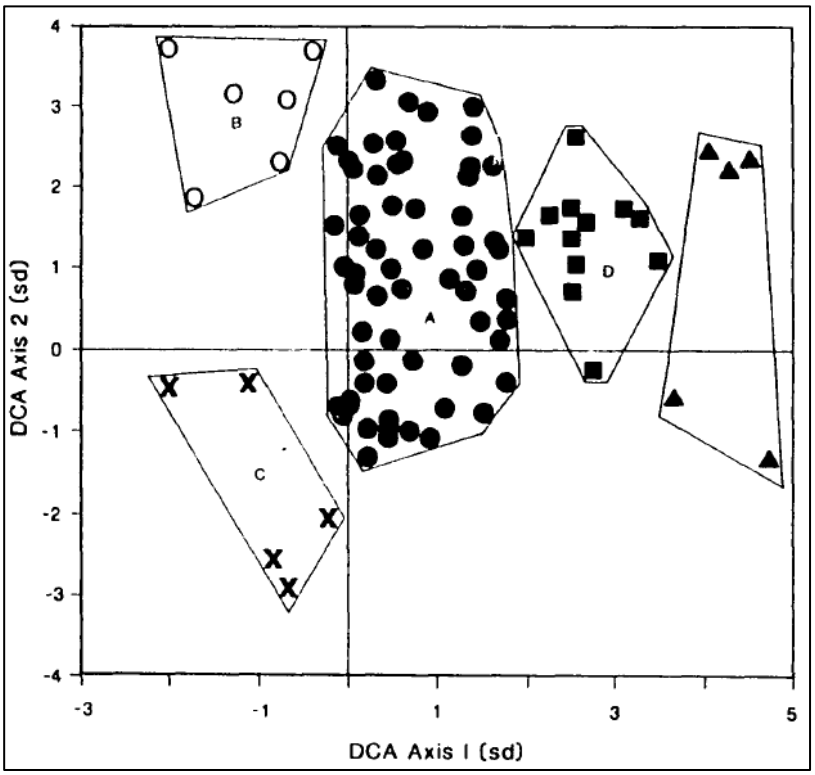

Figure 36 Palynofloral assemblages identified by Farley (1990), and displayed on a detrended correspondence analysis graph, using standard deviation as a unit. Assemblage A [non-unique K-Pg] is displayed as black dots, B [Marsh] is displayed as circles, C [freshwater lakes and ponds] is displayed as Xs, and D is displayed as squares.

Channel-Floodplain and Fluvio-Lacustrine Systems of UCZ and LCZ

The floodplain and lacustrine lithofacies assemblages are the primary deposits in the Upper and Lower Coal Zones of the Raton Formation, and serve as a type of large-scale matrix that encases the channel-belt assemblages and valley-fill assemblage. These rocks also contain coal deposits with distinctive characteristics (thickness and lateral continuity) that are representative of the processes that formed them.

Channel-Floodplain System

The floodplain assemblage deposits dominate the Channel-Floodplain System, and serves as a matrix within which channel-belt assemblage deposits are encased. The thinner coal seams deposited in the Upper and Lower Coal Zones of the Raton Formation are predominately located within the floodplain lithofacies assemblage. No outcrops from this study contained true coals deposited in the floodplain assemblage, but all cores contained thin (less than two feet) coals stratigraphically positioned in-between floodplain assemblage deposits. In addition to the thin coals, very thin (1-6 inches) layers of carbonaceous mudstone are commonly contained within floodplain assemblage deposits. Wet, inundated, low-lying areas of isolated floodplain are the likely depositional environment for these thinner coals. In addition to generally low-lying areas adjacent to fluvial channels, seasonal and smaller floodplain lakes also account for the thinner coals.

The Grijalva river system in the Tabasco region of Mexico serves as a modern analog for the channel-floodplain system of the upper and lower coal zone of the Raton Formation. The Grijalva is a river system in a high-accommodation, poorly drained basin with a prominent wet floodplain containing floodplain lakes, floodplain mudflats, and propagating tie channels cutting through lakes (Hull, 2016). Based on the identification of lithofacies, lithofacies assemblage mapping, organic petrography, and palynological results of this study, these same features are represented in the Upper and Lower Coal Zone of the Raton Formation. The channel-floodplain system of the Raton Formation, and the floodplain lithofacies assemblage associated with it, contain rooted floodplain deposits with only simple immature soils and shallow floodplain lakes with minor rooting. In the Grijalva system, larger floodplain lakes typically remain rather constant, while smaller lakes can be ephemeral or even seasonal, producing simple rooted soils (Stoner, 2010). The water table in the Grijalva is highly variable, and large swathes of relatively dry floodplain or previously propagating channels are frequently flooded, as well as smaller floodplain lakes (**Figure 38**). While the Grijalva system relates well to the

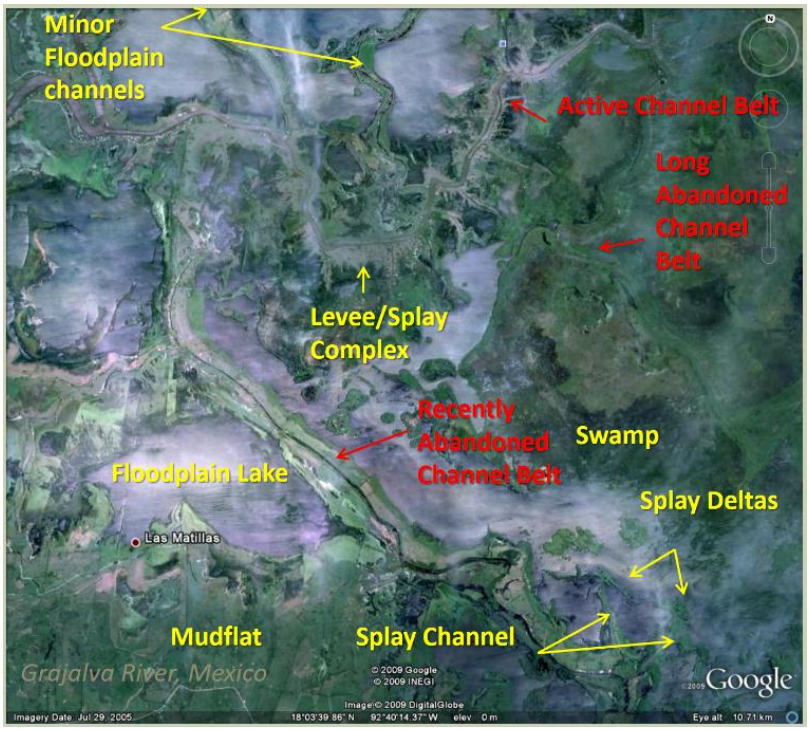

Figure 37 Geomorphological features of the Grijalva River and its poorly drained floodplain (from Hull, 2016). Geomorphological features of the Grijalva River and its poorly drained floodplain (from Hull, 2016).

channel-floodplain portion of the UCZ and LCZ of the Raton Fm., it does not explain everything, specifically the deposition of the thicker and very laterally extensive coals documented by Horne (unpublished), Pillmore (Personal Comm.), and Osterhout (2014).

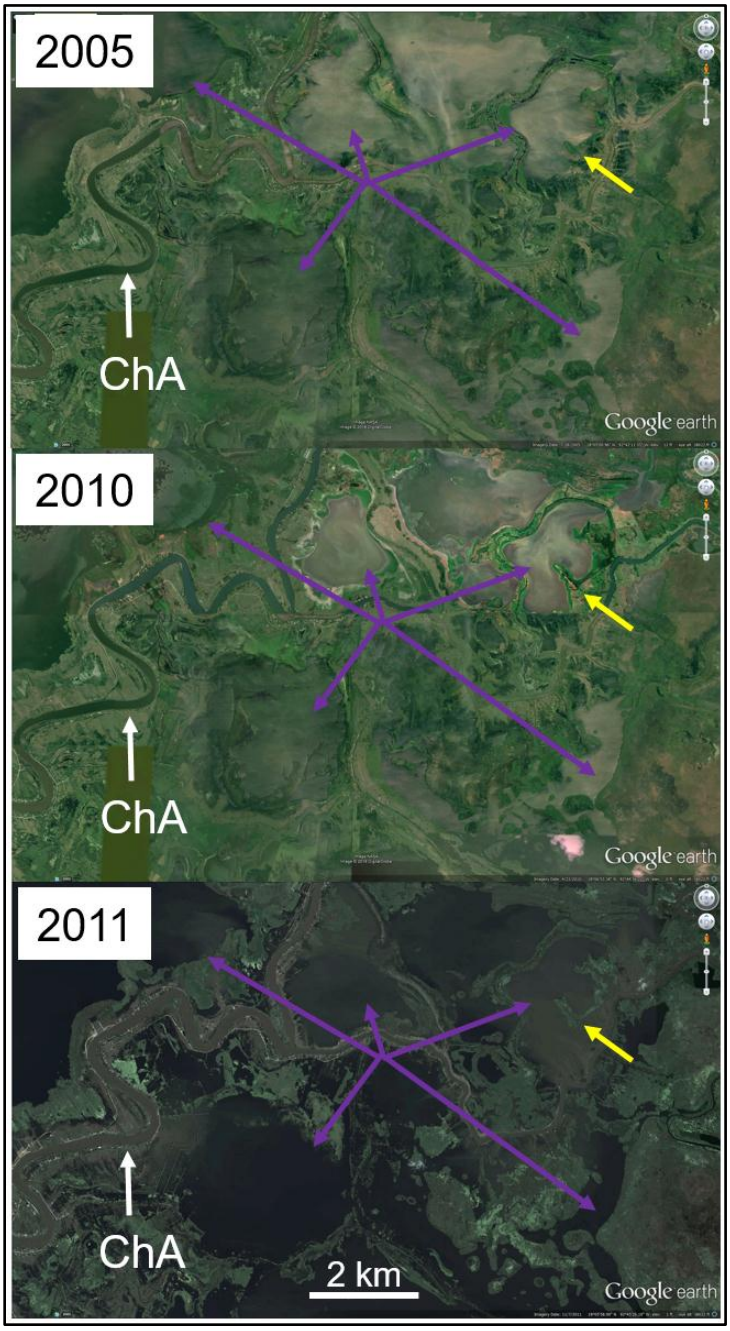

Figure 38 Time series of images from Google Earth of the Grijalva River and flood plain through time. The white arrow indicates the main trunk channel, the purple arrows indicate floodplain lakes, and the yellow arrow indicates a propagating tie channel through a floodplain lake that becomes submerged following a rise in water table. Scale is indicated in lowest image and pertains to all images.

Fluvio-Lacustrine System and Thick Coal Deposition

Prograding fluvial channels dominate the shallow expansive lakes in this system. Channel-belt sandstones are encased in lacustrine assemblage deposits (**Figures 29-31**). This asserts a non-marine fluvial system with channels that penetrate shallow standing bodies of water (**Figures 29, 31**). This aligns well with that of a fluvo-lacustrine system (Huling, 2014). Based on the average single story channel thickness of 13.4 feet, channel widths are likely near 990 feet (Figure 36; Holbrook and Wanas, 2014).

$$w_c = 8.8\ d_m^{1.82}$$

Figure 39 Channel width equation. Wc = channel width, dm = mean average channel depth.

Thick coals in the Raton Formation formed in association with large lakes. All the thick coals are encased in lacustrine sections, and represent peat-prone subenvironments within the lake assemblage. Coals in all outcrops and core were directly related to carbonaceous and laminated mudstones (Fcm and Flm), and were predominately located within lacustrine assemblages (**Figures 29-33**). All three thick (≥ 2 foot) coals in outcrop from this study (base King Coal, base Wild Boar), and eight of thirteen thick (≥ 2 foot) coals in core were located in lacustrine assemblages, and all in the middle of lacustrine muds. Palynofloral assemblage analysis of Raton Formation coals, with its prominent lacustrine algae and indication of the presence of standing water, is also consistent with lacustrine deposition.

Deposition of peats that make up the thick coals of the Upper and Lower Coal Zone of the Raton Formation occur as a mere phase of the lacustrine lifecycle when specific conditions meet those necessary for peat preservation. Peat preservation occurs when net

primary productivity (NPP) of peatland exceeds decomposition or destruction (Frolking et al., 2001). In a woody peatland, groundwater level must be high enough for the growth and preservation of organic material, commonly trees, yet not so high that the vegetation is drowned (Phillips et al., 1985; Cecil, 1990; Bohacs and Suter, 1997). Lastly, but of equal importance, these must be still waters lacking any influx of sediment that has the potential to destroy or inhibit preservation (Cecil, 1993; Bohacs and Suter, 1997). A peat-preserving environment records a delicate balance. Only when all of these stipulations are met is peat preserved.

Cyclical lithological change from laminated mudstone to carbonaceous mudstone to coal deposits in the Raton Formation represents a gradational change between periods in the lacustrine lifecycle that are preserving peat, and periods that are not. Coals represent only a portion of the entire preserved lacustrine lifecycle, approximately 10-20%. The presence of carbonaceous shales or mudstones represents this transitionary period (**Figure 28.3**). Variability in the organic composition, or maceral proportionality of the coal samples, indicates the presence of raised peat swamps along with the flooded woody swamps. Organic accumulation likely exceeded the water level and mounded at least temporarily during coal accumulation, though mostly coals appear to have formed in standing water. Such small-scale variability in coal type has been documented before (DiMichelle, 1989), and Phillips et al., (1985) proposed a model where topographically higher land, such as older levee deposits, experienced degradation of peat. This results in inertinite and general heterogeneity in coals, similar to the slight heterogeneity seen in the Raton Formation coal samples (**Figures 16-18**). Carbonaceous shales or mudstones represent the lacustrine lifecycle at a point when it is not fully preserving or depositing

peat, as likely not all criteria for peat preservation are met. The widespread deposition and preservation of peat, and the following transformation of peat into coal, is a product of very expansive lacustrine systems in the Upper and Lower Coal Zones of the Raton Formation.

While the Grijalva river system fits the channel-floodplain part of the depositional model of the upper and lower coal zone, it does not replicate the lacustrine assemblege. Two possible modern analogs for the fluvio-lacustrine system of the UCZ and LCZ of the Raton Formation are the Hay-Zama Lake system of Alberta, Canada, and Okefenokee Swamp system of northern Georgia. Hay-Zama is a group of multiple shallow fresh-water lakes in far northwestern Alberta situated on a gentle slope. The Hay-Zama system contains lakes with varying water depths. During the wet season,

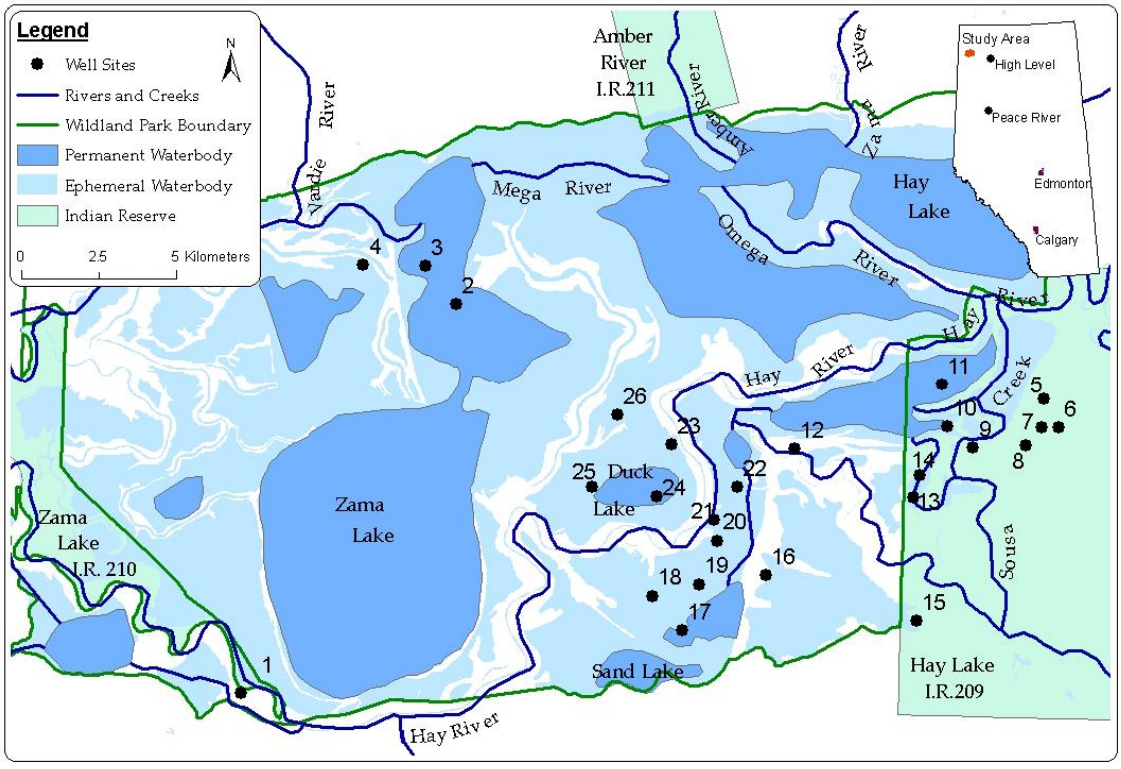

Figure 40 Hay-Zama Lake System. Dark blue represents active channels, regular blue represents lakes, and light blue represents ephemeral lakes. White areas represent levees and channel deposits (Wright, 2005).

these lakes are considerably more expansive, and several lakes will often merge to form one larger lake (**Figure 40**) (Wright, 2005; Huling, 2014). This mechanism, of protracted

standing shallow water with disceting channels is similar to the fluvio-lacustrine environment of the Raton Formation. The Okefenokee Swamp system of southeastern Georgia is a permanently inundated, peat-forming swampland. The swampland consists of standing water with floating marsh grass or "prairies," tree "houses" made of mostly cypress trees, and standing water (Cohen, 1974). Within this swampland are two main rivers with fluvial channels that cut through and drain the swamp proper (Cohen, 1974). The Okefenokee is approximately 412,000 acres in size, and actively produces peat, with its thickest recorded peat deposits being 15 feet thick (Cypert, 1961; Cohen, 1974). While the Okefenokee swamp is a fluvio-lacustrine system that produces peat, it differs from the Raton in that its peat has a higher sulfur content (Casagrande et al., 1977), which is likely due to a small marine influence on the system (Cohen, 1974). The Okefenokee undergoes fires during dry seasons, with major fires that burned three quarters of the entire swamp in 1954 and 1955 (Cypert, 1961). The occurrence of fires will lead to production of inertinite macerals in the coals formed from this modern coal-forming environment (Suarez-Ruiz, 2008). Both modern analogs fit certain aspects of the fluvio-lacustrine system of the UCZ and LCZ of the Raton Formation, but neither are truly ideal examples.

Channel-Floodplain and Fluvio-Lacustrine Mechanics

In order to change from a channel-floodplain system to a fluvio-lacustrine system, a change in groundwater level must occur. Stage one (**Figure 41 A & B**) would be characterized by a trunk channel with adjacent floodplain deposits (rooted floodplain fines and paleosols). Splay events and splay channels are common during the subaerial stage one, depositing the splay / sand sheet elements of the floodplain assemblage. Following an

increase in the groundwater table, previous floodplain area are inundated with water (**Figure 41 C & D**). Inundation causes lithofacies associated with the lacustrine assemblage, such as laminated mudstone (Flm) and carbonaceous mudstones (Fcm). Where conditions favored no sediment influx and preservation of organics peat deposited. If the lake experienced sediment influx, peat preservation did not occur. Prograding channels advancing out into lakes could be an example of this, ending peat deposition and instead depositing channel-belt assemblages within lacustrine assemblages, complete with blowout wings. If the water table continued to rise, outpacing deposition of sediments, or sediment supply was cut off, a sustained groundwater table would allow the lacustrine assemblage to completely encase any channel-belt assemblage (**Figure 41 E & F)**.

While this change in groundwater table vs the land surface must have occurred for the preservation of peat, the mechanism by which this occurs is up for debate. A decrease in sediment supply from the source, whether isolated to a smaller lacustrine system or basin-wide, would favor peat formation. Conversely any significant influx of sediment would kill this peat preservation. Subsidence as a result of tectonics or sediment loading is one possibility for the increase in accommodation and rise in groundwater level (DeCelles and Giles, 1996). Another possibility, initially proposed by Flores, theorizes that ground-water may have been forced out of pores by depositional loading from the depositional center of the basin, increasing the groundwater level (Kreitler, 1979; Flores, 1985). Further, fixed channels building alluvial ridges with minimal overbank deposition could aggrade and pull the water table above the surrounding floodbasin land surface. This would trigger widespread floodplain inundation and lacustrine environments.

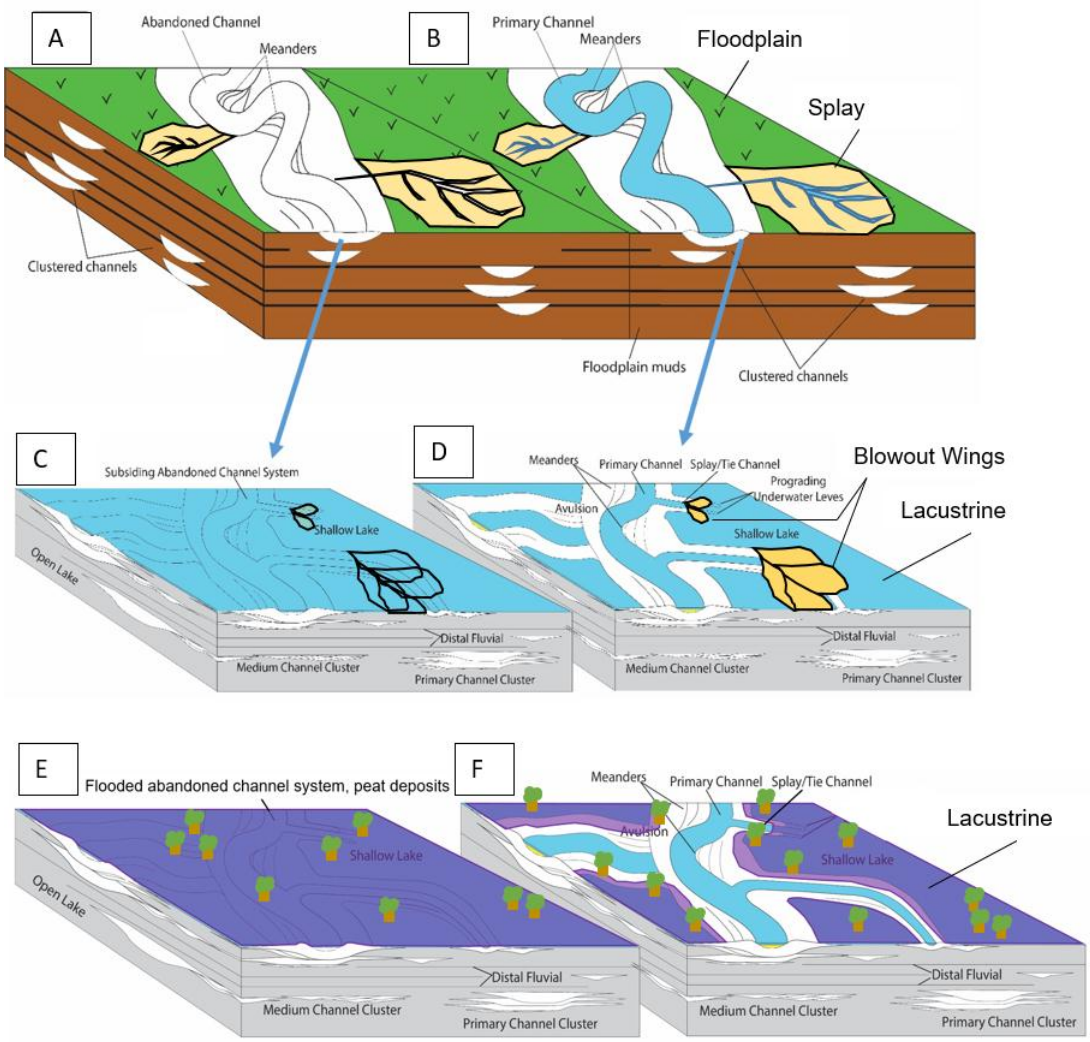

Figure 41 Depositional model for Upper and Lower Coal Zone of Raton Fm. via progressive time series of 3-D models (modified from Huling & Holbrook, 2016). ***[A]*** *and* ***[B]*** *depict abandoned and active channel belts, respectively, with typical subaerial floodplain deposits. The brown depicts floodplain deposits which encase channel belt deposits.* ***[C]*** *and* ***[D]*** *depict a flooded abandoned channel and active channel, respectively. Lake deposits encase channel deposits.* ***[E]*** *and* ***[F]*** *depict a further flooded abandoned and active channel that is receiving no sediment input, with peat deposition occurring in a lacustrine environment.*

Barren Series and DFS

Deposits of the barren series, or rocks lacking in coal deposits (Pillmore and Flores, 1984), significantly differ from those of the upper and lower coal zones of the Raton Formation. Most distinctly, the barren series outcrops contain an abundant terminal splay assemblage that does not occur in the upper and lower coal zones (Horner, 2016; McGregor, 2017). Deposits of the barren series are much coarser, with large channel-belt and valley-fil assemblages, abundant terminal splays, and very little true coal. These deposits have been proposed as signature medial and distal portions of a distributive fluvial system (DFS) (Horner, 2016) resulting from a temporary increased sediment influx compared to accommodation. The peat-preserving depositional systems of the UCZ and LCZ, while different from the distributive system of the barren, still likely functions as a DFS, yet wetter and more fine-grained. Much like a typical DFS, the UCZ and LCZ system would consist of a radial network of both active and inactive channels that work their way through an inundated floodplain that undergoes periods of episodic prolonged flooding, eventually terminating in floodplains or lakes. This aligns with the DFS geomorphic model (Hartley et al., 2010). It differs however in that the system is inundated from the apex and lacks the transition from a subaerial megafan to a wet system past a spring line down dip from the initial distributive node.

Industry Application

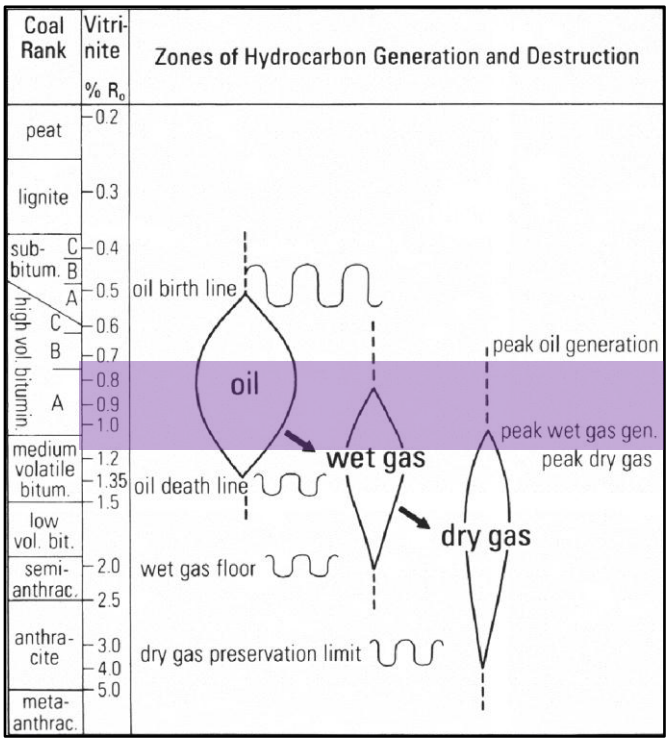

Figure 42 Oil and gas windows relative to vitrinite reflectance. The purple box indicates the range that coals from this study fall into. (Modified from Suarez-Ruiz, 2012).

Source, Migration, and Connectivity

The Raton Formation coals are coal bed methane source rocks, and their depositional environment / style affects potential migration and connectivity. Vitrinite reflectance values (mean range of 0.73 – 0.99) place these coals in the oil and gas windows (**Table 5, Figure 42**). Presence of solid bitumen in coals (**Figures 16-18, 21, Appendix Item 1**) indicate the coals sampled should be viewed as a speculative source rock (Magoon, 1988). Hydrocarbon production of oil (Personal Comm., Roy Pillmore) and gas (Carlton, 2006; Osterhout, 2014) from the Raton Formation confirms the Raton Formation coals as a *known* source rock (Magoon, 1988). These source rocks have been found to exist as thick and extensive coals, representative of large extensive lacustrine systems and general widespread flooding of the Raton Basin.

The stratigraphic position of coal (source rocks) in the lacustrine lithofacies assemblage has implications for hydrocarbon migration, or flow out of the source rocks. Because coals are commonly located within "tight" or low porosity / permeability carbonaceous and laminated mudstones, migration of hydrocarbons out of the coal may be inhibited. Conversely, if coals are juxtaposed directly against relatively higher porosity and

permeability reservoir rocks, such as the valley-fills, channel-belts, terminal splays, and blowout wings, hydrocarbons may flow out of the coal and into these rocks more readily. This study finds that coals most commonly occur in the middle of lacustrine muds, and juxtaposition with reservoir rocks would likely require faulting or incision by fluvial sandstones. If migration did occur, laminated mudstones in the lacustrine assemblage may also serve as a stratigraphic seal for hydrocarbons stored in the channel-belt sandstone reservoir rocks.

Blowout wings and terminal splays have the potential to increase connectivity in high-accommodation fluvio-lacustrine systems (Huling, 2014; Hull, 2016; Huling & Holbrook, 2016; Howe, 2017). Thin (0.5 – 2 m) laterally extensive (>300m in Raton Fm., observed 4-6x channel width in modern analogs (Howe, 2017)) blow out sand sheets may connect to thicker reservoir rocks, and serve as a migration conduit for oil and gas. The same possibilities are proposed for the terminal splays in the splay-rich Barren zone of the Raton Formation, with terminals splays acting as the fluid conduit (Horner, 2016; McGregor, 2017). Thinner sandstones, when identified using geophysical logs, would likely be ignored as a reservoir. Instead perforation of these sandstones, could potentially positively affect reserves, via connectivity to larger channel-belt sandstone bodies, and influence exploration and production.

General Implications

Understanding the lacustrine depositional environment of coals has general implications regarding hydrocarbon exploration and production. The sensitive nature of the peat-preserving environment described above means that small changes in the system, such as brief return of the influx of sediment, could shut down the peat factory, changing deposited lithology to mudstones or shales. This lake system could just as easily go back to preserving peat, and is why an increase in groundwater level has the capability of vastly increasing lateral continuity of peat deposition and preservation. The delicate nature of the peat-preserving environment, and thus the possibility of frequently fluctuating lithology, could also cause splitting of coal seams, which has been previously documented in the Raton coals (Pillmore, 1969; Flores, 1993; Flores and Bader, 1999). Splitting could also be a product of splays, as they are common causes for coal seam splitting (Horne et al., 1978).

The chemical content of these coals, being low in Sulphur (**Table 4**), is also preferable for gas production, as Sulphur-rich, or "sour," gas increases cost of production and transportation (Schmidtt, 1991). Raton Formation coals being derived from and deposited in predominately freshwater lakes, as evidenced by all organic composition data and lithofacies mapping, is the dominant factor for this low-Sulphur chemical composition. The lacustrine environment of the Raton Formation coals has direct implications for hydrocarbon source, migration, connectivity, reservoir, and seal properties, and thus affects exploration and production. These effects may be analogous to similarly deposited coals.

CHAPTER FIVE: Conclusions

1) Organic petrography results from coal and carbonaceous mudstone samples in this study reveal a vitrinite-dominated (woody) coal composition.
2) Sparse palynology results included a dominance of tree fern spores, which suggests a wet paleoenvironment. Qualitative analysis also reveals a relatively high abundance of non-descript lacustrine algae, which suggests standing water was present at time of deposition, potentially only seasonally. Marshes, lakes, and peat mires were the dominant palynofloral assemblages. This further corroborates evidence that the coal in the Upper and Lower Coal Zone of the Raton Formation was deposited in a mostly submerged environment.
3) The depositional system for the Upper and Lower Coal Zones of the Raton Formation is interpreted to contain both a channel-floodplain and a fluvio-lacustrine system. Both have fine-grained deposits dissected by a sandy channel-belt assemblage. Thick extensive coals are deposited within the fluvio-lacustrine system, allowing for widespread lakes to deposit and preserve peat.
4) Core and outcrop analysis reveal that coals were not deposited in discrete and ephemeral swamps, but were instead deposited in short-lived peat-friendly phases of more lasting and extensive lake systems of the fluvio-lacustrine system..
5) A possible modern analog for the channel-floodplain system is the Grijalva river and floodplain lake system in the state of Tabasco, Mexico. A possible modern analog for the fluvio-lacustrine system is the Hay-Zama Lake System of Alberta, or the Okefenokee Swamp system of southern Georgia, USA.

6) The freshwater lacustrine environment of the Raton Formation coals has implications for hydrocarbon exploration and production. This includes a presence of a low-sulphur laterally continuous source, migration, reservoir presence in the form of fluvio-lacustrine channel sands, associated reservoir connectivity of these rocks, and seal properties due to direct lateral and vertical relation of continuous carbonaceous and laminated mudstone with source coals.

References

Alrefaei, Y. Y. (2017). Implications of Lithofacies Association and Architecture for Low and High-accommodation System Tracts from the Sandstone Dominated Zone (the Barren Series) of the Cretaceous-Paleocene Raton Formation, Trinidad, Colorado (Doctoral dissertation).

Ash, S. R., & Tidwell, W. D. (1976). Upper Cretaceous and Paleocene floras of the Raton basin. In Colorado and New Mexico: New Mexico Geological Society, Guidebook 27th field conference (pp. 197-203).

Ashley, G. M. (1990). Classification of large-scale subaqueous bedforms: a new look at an old problem-SEPM bedforms and bedding structures. Journal of Sedimentary Research, 60(1).

Aslan, A., & Autin, W. J. (1999). Evolution of the Holocene Mississippi River floodplain, Ferriday, Louisiana: insights on the origin of fine-grained floodplains. Journal of Sedimentary Research, 69(4).

Baltz, E. H. (1965). Stratigraphy and history of Raton Basin and notes on San Luis Basin, Colorado-New Mexico. *Bulletin of the American Association of Petroleum Geologists, 49*(11), 2041-2075. doi:http://dx.doi.org/10.1306/A6633882-16C0-11D7-8645000102C1865D

Bohacs, K. and Suter, J. (1997). Sequence stratigraphic distribution of coaly rocks: fundamental controls and paralic examples. *AAPG bulletin*, *81*(10), pp.1612-1639.

Bridge, J. S., & Mackey, S. D. (1992). A theoretical study of fluvial sandstone body dimensions. The geological modelling of hydrocarbon reservoirs and outcrop analogues, 213-236.

Bush, M. A., Horton, B. K., Murphy, M. A., & Stockli, D. F. (2016). Detrital record of initial basement exhumation along the Laramide deformation front, southern Rocky Mountains. *Tectonics, 35*(9), 2117-2130.

Cahoon, D. R., White, D. A., & Lynch, J. C. (2011). Sediment infilling and wetland formation dynamics in an active crevasse splay of the Mississippi River delta. Geomorphology, 131(3-4), 57-68.

Cant, D. J., & Walker, R. G. (1976). Development of a braided-fluvial facies model for the Devonian Battery Point Sandstone, Quebec. Canadian Journal of Earth Sciences, 13(1), 102-119.

Carlton, D. R. (2006). Discovery and development of a giant coalbed methane resource, Raton Basin, Las Animas County, southeast Colorado.

Carter, D.A. (1956). Coal deposits of the Raton Basin, *in* McGinnis, C.J., ed., Geology of the Raton Basin, Colorado: Rocky Mountain Association of Geologists Guidebook, p. 89–92.

Casagrande, D. J., Siefert, K., Berschinski, C., & Sutton, N. (1977). Sulfur in peat-forming systems of the Okefenokee Swamp and Florida Everglades: origins of sulfur in coal. Geochimica et Cosmochimica Acta, 41(1), 161-167.

Catuneanu, O. (2006). *Principles of sequence stratigraphy*. Amsterdam, Netherlands (NLD): Elsevier, Amsterdam.

Cecil, C. B. (1990). Paleoclimate controls on stratigraphic repetition of chemical and siliciclastic rocks. Geology, 18(6), 533-536.

Cecil, C. B., Dulong, F. T., Cobb, J. C., & Supardi, X. X. (1993). Allogenic and autogenic controls on sedimentation in the Central Sumatra Basin as an analogue for Pennsylvanian coal-bearing strata in the Appalachian Basin. SPECIAL PAPERS-GEOLOGICAL SOCIETY OF AMERICA, 3-3.

Clarke, P. R., Cornelius, C., & Turner, P. (2002). Alluvial Processes and Sansbody Architecture in the Raton Basin. Paper presented at the AAPG Rocky Mountain Section, Laramie, Wyoming.

Clarke, P., Cornelius, C., & Turner, P. (2004). A Refined Lithostratigraphy for the Raton Formation: Implications for Alluvial Heterogeneity, Coal-Forming Environments and Coal Bed Distribution-Raton Basin. Paper presented at the 2004 Denver Annual Meeting.

Cohen, A. D. (1974). Petrography and paleoecology of Holocene peats from the Okefenokee swamp-marsh complex of Georgia. Journal of Sedimentary Research, 44(3).

Coleman, J.M. (1988) Dynamic changes and processes in the Mississippi River delta. *Geological Society of America Bulletin*, 100(7), 999-1015.

Cooper, J. R. (2006). *Igneous intrusions and thermal evolution in the Raton Basin, CO-NM: contact metamorphism and coal-bed methane generation.* University of Missouri--Columbia.

Cypert, E. (1961). The effects of fires in the Okefenokee Swamp in 1954 and 1955. American Midland Naturalist, 485-503.

DeCelles, P. G., & Giles, K. A. (1996). Foreland basin systems. Basin research, 8(2), 105-123.

Diessel, C.F.K. (1992). Coal-Bearing Depositional Systems. SpringerVerlag, Berlin. 721 pp.

Dimichele, W. A., & Nelson, W. J. (1989). Small-scale spatial heterogeneity in Pennsylvanian-age vegetation from the roof shale of the Springfield Coal (Illinois Basin). Palaios, 276-280.

Fielding, C. R. (2006). Upper flow regime sheets, lenses and scour fills: extending the range of architectural elements for fluvial sediment bodies. Sedimentary Geology, 190(1), 227-240.

Fisher, J., Nichols, G., & Waltham, D. (2007). Unconfined flow deposits in distal sectors of fluvial distributary systems: Examples from the Miocene Luna and Huesca Systems, northern Spain. Sedimentary Geology, 195(1), 55-73.

Fleming, R. F. (1989). Fossil Scenedesmus (Chlorococcales) from the Raton Formation, Colorado and New Mexico, USA. Review of palaeobotany and palynology, 59(1-4), 1-6.

Fleming, R. F., & Nichols, D. J. (1990). The fern-spore abundance anomaly at the Cretaceous-Tertiary boundary: a regional bioevent in western North America. In Extinction events in Earth history (pp. 347-349). Springer, Berlin, Heidelberg.

Flores, R. M. (1984). Comparative analysis of coal accumulation in Cretaceous alluvial deposits, southern United States Rocky Mountain basins. Memoir - Canadian Society of Petroleum Geologists, 9, 373-385.

Flores, R. M. (1985). Coal Deposits in Cretaceous and Tertiary Fluvial Systems of the Rocky Mountain Region.

Flores, R., Pillmore, C., & Merewether, E. (1985). Overview of Depositional Systems and Energy Potential of Raton Basin, Colorado and New Mexico.

Flores, R. M., & Pillmore, C. L. (1987). Tectonic control on alluvial paleoarchitecture of the Cretaceous and Tertiary Raton Basin, Colorado and New Mexico. Special Publication - Society of Economic Paleontologists and Mineralogists, 39, 311-320.

Flores, R. M. (1993). Geologic and geomorphic controls of coal development in some Tertiary Rocky Mountain basins, USA. International journal of coal geology, 23(1-4), 43-73.

Flores, R. M., & Bader, L. R. (1999). A summary of Tertiary coal resources of the Raton Basin, Colorado and New Mexico. USGS Professional Paper.

Frolking, S., Roulet, N. T., Moore, T. R., Richard, P. J., Lavoie, M., & Muller, S. D. (2001). Modeling northern peatland decomposition and peat accumulation. Ecosystems, 4(5), 479-498.

Ghazi, S., & Mountney, N. P. (2009). Facies and architectural element analysis of a meandering fluvial succession: The Permian Warchha Sandstone, Salt Range, Pakistan. Sedimentary Geology, 221(1-4), 99-126.

Gibling, M. R. (2006). Width and thickness of fluvial channel bodies and valley fills in the geological record: a literature compilation and classification. Journal of sedimentary Research, 76(5), 731-770.

Graham, J. R., Collinson, J. D., & Lewin, J. (1983). Modern and ancient fluvial systems. SPEC PUBL INT ASSOC SEDIMENTOL, 6, 473.

Hackley, P. C., & Cardott, B. J. (2016). Application of organic petrography in North American shale petroleum systems: A review. International Journal of Coal Geology, 163, 8-51.

Hagemann, H. W., & Wolf, M. (1989). Paleoenvironments of lacustrine coals-the occurrence of algae in humic coals. International journal of coal geology, 12(1-4), 511-522.

Harbour, R. L., & Dixon, G. H. (1959). *Coal resources of Trinidad-Aguilar area, Las Animas and Huerfano Counties, Colorado*.

Hartley AJ, Weissmann GS, Nichols GJ, Warwick GL. (2010). Large distributive fluvial systems: characteristics, distribution, and controls on development. Journal of Sedimentary Research 80:167–183.

Haszeldine, R. S. (1984). Muddy deltas in freshwater lakes, and tectonism in the Upper Carboniferous coalfield of NE England. Sedimentology, 31(6), 811-822.

Hills, R.C. (1888) The recently discovered Tertiary beds of the Huerfano River Basin, Colorado: Colorado Scientific Society, Proceedings, v. 3, p. 148–164.

Holbrook, J. (2001). Origin, genetic interrelationships, and stratigraphy over the continuum of fluvial channel-form bounding surfaces: an illustration from middle Cretaceous strata, southeastern Colorado. Sedimentary Geology, 144(3-4), 179-222.

Holbrook, J., & Wanas, H. (2014). A fulcrum approach to assessing source-to-sink mass balance using channel paleohydrologic paramaters derivable from common fluvial data sets with an example from the Cretaceous of Egypt. Journal of Sedimentary Research, 84(5), 349-372.

Horne, J. C., Ferm, J. C., Caruccio, F. T., & Baganz, B. P. (1978). Depositional models in coal exploration and mine planning in Appalachian region. AAPG bulletin, 62(12), 2379-2411.

Horner, R. J. (2016). Facies characterization and architectural context of terminal splay sandstone beds in the cretaceous-paleocene raton formation, colorado (Order No. 10250078). Available from Dissertations & Theses @ Texas Christian University; ProQuest Dissertations & Theses Global.

Horner, R.J., McGregor, G.E., and Holbrook, J.M. (2017). Vegetation induced sedimentary structures and fossilized trees in terminal splay sandstone beds of the Cretaceous – Paleocene Raton Formation, Colorado. Geological Society of America Abstracts with Programs. Vol. 49, No. 2

Howe, T. (2017). The Evolution and Stratigraphic Architecture of Fluvio-Lacustrine Deltas: Reservoir Characteristics from the Red River Delta, Lake Texoma and the Denton Creek Delta, Grapevine Lake, TX (MS Thesis, Texas Christian University).

Huerta, P., Armenteros, I., & Silva, P. G. (2011). Large-scale architecture in non-marine basins: the response to the interplay between accommodation space and sediment supply. *Sedimentology, 58*(7), 1716-1736. doi:10.1111/j.1365-3091.2011.01231.

Huling, G. A. (2014). Evidence for clustering of delta-lobe reservoirs within fluvio-lacustrine systems, Jurassic Kayenta Formation, Utah [electronic resource]. UMI thesis.

Huling, G., & Holbrook, J. (2016). Clustering of elongate muddy delta lobes within fluviolacustrine systems, Jurassic Kayenta Formation, Utah. Autogenic Dynamics and Self-Organization in Sedimentary Systems: SEPM Special Publication, 106.

Hull, M. (2016), A modern reservoir analogue for a poorly drained "high accommodation" fluvial system: Sedimentary processes, architecture, and reservoir connectivity of the Grijalva system, Tabasco State, Mexico, Ph.D. thesis, 139 pp., The University of Texas at Arlington, Arlington, Texas.

Jasper, A., Agnihotri, D., Tewari, R., Spiekermann, R., Pires, E. F., Da Rosa, Á. A. S., & Uhl, D. (2017). Fires in the mire: Repeated fire events in Early Permian 'peat forming'vegetation of India. Geological Journal, 52(6), 955-969.

Jennerjahn, T. C., Ittekkot, V., Arz, H. W., Behling, H., Pätzold, J., & Wefer, G. (2004). Asynchronous terrestrial and marine signals of climate change during Heinrich events. Science, 306(5705), 2236-2239.

Jervey, M. T. (1988). Quantitative geological modeling of siliciclastic rock sequences and their seismic expression. *Special Publication - Society of Economic Paleontologists and Mineralogists, 42*, 47-69.

Johnson, R. B., Dixon, G. H., & Wanek, A. A. (1956). *Late Cretaceous and Tertiary stratigraphy of the Raton Basin of New Mexico and Colorado*. Socorro, New Mexico, United States (USA): N. M. Geol. Soc., Socorro, New Mexico.

Johnson, R. C., & Finn, T. M. (2001). Potential for a basin-centered gas accumulation in the Raton Basin, Colorado and New Mexico. U. S. Geological Survey Bulletin.

Johnson, R. B., & Wood Jr, G. H. (1956). Stratigraphy of Upper Cretaceous and Tertiary Rocks of Raton Basin, Colorado and New Mexico. *AAPG Bulletin, 40*(4), 707-721.

Johnson, K. R., & Ellis, B. (2002). A tropical rainforest in Colorado 1.4 million years after the Cretaceous-Tertiary boundary. Science, 296(5577), 2379-2383.

Jones, B. G., & Rust, B. R. (1983). Massive sandstone facies in the Hawkesbury Sandstone, a Triassic fluvial deposit near Sydney, Australia. Journal of Sedimentary Research, 53(4).

Jurich, D., & Adams, M. A. (1984). Geologic Overview, Coal, and Coalbed Methane Resources of Raton Mesa Region--Colorado and New Mexico.

Krauss, M. J., & Aslan, A. (1993). Eocene hydromorphic paleosols: significance for interpreting ancient floodplain processes. Journal of Sedimentary Research, 63(3).

Krauss, M. J., & Hasiotis, S. T. (2006). Significance of Different Modes of Rhizolith Preservation to Interpreting Paleoenvironmental and Paleohydrologic Settings: Examples from Paleogene Paleosols, Bighorn Basin, Wyoming, U.S.A. Journal of Sedimentary Research, 76(4), 633-646. doi:10.2110/jsr.2006.052

Kreitler, C. W. (1979). Ground-water hydrology of depositional systems. In Galloway, WE, and others, Depositional and ground water flow systems in the exploration for uranium, a research colloquium: The University of Texas at Austin, Bureau of Economic Geology (pp. 118-176).

Lamberson, M. N., Bustin, R. M., Kalkreuth, W. D., & Pratt, K. C. (1996). The formation of inertinite-rich peats in the mid-Cretaceous Gates Formation: implications for the interpretation of mid-Albian history of paleowildfire. Palaeogeography, Palaeoclimatology, Palaeoecology, 120(3-4), 235-260.

Lang, S. C., Hicks, T. R., Benson, J., Reilly, M., Kassan, J., & Chidsey, T. C., Jr. (2004). Reservoir analogues for ephemeral fluvial, lacustrine delta and terminal splay successions; examples from the Lake Eyre basin, central Australia. Annual Meeting Expanded Abstracts - American Association of Petroleum Geologists, 12, 98.

Lee, W. T., & Knowlton, F. H. (1917). Geology and paleontology of the Raton Mesa and other regions; Colorado and New Mexico U. S. Geological Survey Professional Paper. Reston, VA, United States (USA): U. S. Geological Survey, Reston, VA.

Liu, X., Shen, J., Wang, S., Yang, X., Tong, G., & Zhang, E. (2002). A 16000-year pollen record of Qinghai Lake and its paleo-climate and paleoenvironment. Chinese Science Bulletin, 47(22), 1931.

Magoon, L. B. (1988). The petroleum system—a classification scheme for research, exploration, and resource assessment. Petroleum systems of the United States: US Geological Survey Bulletin, 1870, 2-15.

Matuszczak, R. A. (1973). Wattenberg Field Denver Basin, Colorado. The Mountain Geologist.

McCabe, P. J., & Parrish, J. T. (1992). Tectonic and climatic controls on the distribution and quality of Cretaceous coals. *Geological Society of America Special Papers*, *267*, 1-16.

McGregor, G. E. (2017). Humid Terminal Splays as Sand-Sheet Reservoirs: A First Look at the Modern, Andean Foreland, and a New Look at the Ancient, Raton Basin (Doctoral dissertation, Texas Christian University).

Miall, A. D. (1985). Architectural-element analysis: A new method of facies analysis applied to fluvial deposits. *Earth-Science Reviews, 22*(4), 261-308. doi:http://dx.doi.org/10.1016/0012-8252(85)90001-7

Miall, A. D. (1988). Reservoir heterogeneities in fluvial sandstones; lessons from outcrop studies. *AAPG Bulletin, 72*(6), 682-697. doi:http://dx.doi.org/10.1306/703C8F01-1707-11D7-8645000102C1865D

Miall, A.D., 1996, The Geology of Fluvial Deposits: Sedimentary Facies, Basin Analysis, and Petroleum Geology. Springer, Berlin, 582 pp.

Miall, A. D. (2013). *The Geology of Fluvial Deposits: Sedimentary Facies, Basin Analysis, and Petroleum Geology*: Springer Berlin Heidelberg.

Mjos, R., Walderhaug, O., Prestholm, E., Marzo, M., & Puigdefabregas, C. (2009). Crevasse splay sandstone geometries in the Middle Jurassic Ravenscar Group of Yorkshire, UK. Alluvial Sedimentation: International Association of Sedimentologists, Special Publication, 17, 167-184.

Nichols, G., & Fisher, J. (2007). Processes, facies and architecture of fluvial distributary system deposits. Sedimentary Geology, 195(1), 75-90.

Noffke, N., Gerdes, G., Klenke, T., & Krumbein, W. E. (2001). Microbially induced sedimentary structures: a new category within the classification of primary sedimentary structures. Journal of Sedimentary Research, 71(5), 649-656.

North, C. P., & Davidson, S. K. (2012). Unconfined alluvial flow processes: recognition and interpretation of their deposits, and the significance for palaeogeographic reconstruction. Earth-Science Reviews, 111(1), 199-223.

Osterhout, S., Soetrisno, H., & Fitter, T. (2013). *Reservoir Characterization and Architecture of the Raton Basin Coal Bearing Sediments*. Pioneer Natural Resources.

Osterhout, S. L., Rothkopf, B. W., & Soetrisno, H. (2014). Raton Basin: Raton Basin Coal Bed Methane Gas Field, Colorado and New Mexico.

Orth, C. J., Gilmore, J. S., Knight, J. D., Pillmore, C. L., Tschudy, R. H., & Fassett, J. E. (1981). An iridium abundance anomaly at the palynological Cretaceous-Tertiary boundary in northern New Mexico. *Science, 214*(4527), 1341-1343.

Penn, B. S., & Lindsey, D. A. (1996). *Tertiary igneous rocks and Laramide structure and stratigraphy of the Spanish Peaks region, south-central Colorado: road log and descriptions from Walsenberg to La Veta (first day) and La Veta to Aguilar (second day)*: Colorado Geological Survey

Petersen, H. I., Bojesen-Koefoed, J. A., Nytoft, H. P., Surlyk, F., Therkelsen, J., & Vosgerau, H. (1998). Relative sea-level changes recorded by paralic liptinite-enriched coal facies cycles, Middle Jurassic Muslingebjerg Formation, Hochstetter Forland, Northeast Greenland. International Journal of Coal Geology, 36(1-2), 1-30

Phillips, T. L., Peppers, R. A., & Dimichele, W. A. (1985). Stratigraphic and interregional changes in Pennsylvanian coal-swamp vegetation: environmental inferences. International Journal of Coal Geology, 5(1-2), 43-109.

Pillmore, C. (1969). Geology and coal deposits of the Raton coal field. *Colfax County, New Mexico: Mountain Geologist, 6*(3), 125-142.

Pillmore, C. L. (1976). Commercial coal beds of the Raton coal field, Colfax County, New Mexico. *Guidebook - New Mexico Geological Society*(27), 227-247.

Pillmore, C., Nichols, D., & Fleming, R. (1999). Field guide to the continental Cretaceous–Tertiary boundary in the Raton Basin, Colorado and New Mexico. *Colorado and Adjacent Areas, 1*, 135-155.

Pillmore, C., & Flores, R. (1984). Field guide and discussions of coal deposits, depositional environments, and the Cretaceous-Tertiary boundary, southern Raton Basin. Paper presented at the Western Geological Excursions: Geological Society of America, Annual Meeting Guidebook,

Pillmore, C. L., & Flores, R. M. (1987). Stratigraphy and depositional environments of the Cretaceous-Tertiary boundary clay and associated rocks, Raton Basin, New Mexico and Colorado. *Geological Society of America Special Papers, 209*, 111-130.

Pillmore, C. L., Flores, R. M., & Bauer, P. W. (1990). Cretaceous and Paleocene rocks of the Raton Basin, New Mexico and Colorado; stratigraphic-environmental framework. Tectonic development of the southern Sangre de Cristo Mountains, New Mexico: New Mexico Geological Society Guidebook, 41, 333-336.

Rowland, J. C., Dietrich, W. E., Day, G., & Parker, G. (2009). Formation and maintenance of single-thread tie channels entering floodplain lakes: Observations from three diverse river systems. Journal of Geophysical Research: Earth Surface, 114(F2).

Rygel, M. C., Gibling, M. R., & Calder, J. H. (2004). Vegetation-induced sedimentary structures from fossil forests in the Pennsylvanian Joggins Formation, Nova Scotia. Sedimentology, 51(3), 531-552.

Rygel, M. C., & Gibling, M. R. (2006). Natural geomorphic variability recorded in a high-accommodation setting; fluvial architecture of the Pennsylvanian Joggins Formation of Atlantic Canada. Journal of Sedimentary Research, 76(11), 1230-1251. doi:http://dx.doi.org/10.2110/jsr.2006.100

Schmitt, G. (1991). Effect of elemental sulfur on corrosion in sour gas systems. Corrosion, 47(4), 285-308.

Shanley, K. W., & McCabe, P. J. (1994). Perspectives on the sequence stratigraphy of continental strata. *AAPG Bulletin, 78*(4), 544-568.

Sharma, R. J. (2013). Fluvial architecture and sequence stratigraphy of the Upper Williams Fork Formation, Plateau Creek Canyon, Piceance Basin, Colorado. UNIVERSITY OF COLORADO AT BOULDER.

Singh, M.P., Singh, P.K., 1996. Petrographic characterization and evolution of the Permian coal deposits of the Rajmahal basin, Bihar, India. Int. J. Coal Geol. 29, 93-l 18.

Stach, E. (1982). Stach's textbook of coal petrology.

Stevens, S., Lombardi, T., Kelso, B., & Coates, J. (1992). Geologic assessment of natural gas from coal seams in the raton and vermejo formations, raton basin. Topical report, January 1991-June 1992.

Stoner, S. B. (2010). Fluvial architecture and geometry of the Mungaroo Formation on the Rankin Trend of the Northwest Shelf of Australia. THE UNIVERSITY OF TEXAS AT ARLINGTON (Master's Thesis).

Stoner, S. B., & Holbrook, J. (2008). Geometric Trends for Floodplain Lakes in High Accommodation Floodplains (abs.). Paper presented at the AAPG Annual Convention and Exhibition, San Antonio, TX.

Strum, S. (1985). *Lithofacies and Depositional Environments of the Raton Formation (Upper Cretaceous--Paleocene) of Northeastern New Mexico*.

Stuart, J. Y., Mountney, N. P., McCaffrey, W. D., Lang, S. C., & Collinson, J. D. (2014). Prediction of channel connectivity and fluvial style in the flood-basin successions of the Upper Permian Rangal Coal Measures (Queensland). *AAPG Bulletin, 98*(2), 191-212. doi:http://dx.doi.org/10.1306/06171312088

Suárez-Ruiz, I., Flores, D., Mendonça Filho, J. G., & Hackley, P. C. (2012). Review and update of the applications of organic petrology: Part 1, geological applications. International Journal of Coal Geology, 99, 54-112.

Sýkorová, I., Pickel, W., Christanis, K., Wolf, M., Taylor, G. H., & Flores, D. (2005). Classification of huminite—ICCP System 1994. International Journal of Coal Geology, 62(1-2), 85-106.

Tavani, S., Granado, P., Corradetti, A., Girundo, M., Iannace, A., Arbués, P., ... & Mazzoli, S. (2014). Building a virtual outcrop, extracting geological information from it, and sharing the results in Google Earth via OpenPlot and Photoscan: An example from the Khaviz Anticline (Iran). Computers & Geosciences, 63, 44-53.

Taylor, G.H., Teichmuller, M., Davis, A., Diessel, C.F.K., Littke, R., Robert, P., (1998). Organic petrology. Gebrüder Borntraeger. Berlin. 704 pp.

Tomanka, G. D. (2013). Morphology, Mechanisms, and Processes for the formation of a non-bifurcating fluvial-deltaic channel prograding into Grapevine Reservoir, Texas. University of Texas at Arlington (Master's Thesis).

Topper, R., Scott, K., & Watterson, N. (2011). Geologic model of the Purgatoire River watershed within the Raton Basin, Colorado. *Colorado Geological Survey.*

Tissot, B.P., Welte, D.H., 1984. Petroleum Formation and Occurrence. 2nd Edition. Berlin, Springer-Verlag, 699 pp.

Wanek, A. A. (1963). Geology and fuel resources of the southwestern part of the Raton coal field, Colfax County, New Mexico. Reston, VA, United States (USA): U. S. Geological Survey, Reston, VA.

Weissmann GS, Hartley AJ, Nichols GJ, Scuderi LA, Olson ME, Buehler HA, Banteah R. (2010). Fluvial form in modern continental sedimentary basins: distributive fluvial systems. Geology 38:39–42.

Weissmann, G. S., Hartley, A. J., Scuderi, L. A., Nichols, G. J., Davidson, S. K., Owen, A., Ghosh, P. (2013). Prograding distributive fluvial systems: geomorphic models and ancient examples. *New Frontiers in Paleopedology and Terrestrial Paleoclimatology: SEPM, Special Publication, 104*, 131-147.

Wolfe, J.A., and Upchurch. (1987). Leaf assemblages across the Cretaceous-Tertiary Boundary in Raton Basin, NM and CO. *Geology, Vol. 84*, 5096-5100.

Wright, V. P., & Marriott, S. B. (1993). The sequence stratigraphy of fluvial depositional systems: the role of floodplain sediment storage. *Sedimentary Geology*, *86*(3-4), 203-210.

Wright K. 2005, Hay-Zama Lakes waterfowl staging and bald eagle nesting monitoring program, 2004. Data Report, D-2005-030, produced by Alberta Conservation Association, Peace River, Alberta, Canada. 21 pp + Ap

APPENDIX

1) Maceral Table

Breakdown of each individual coal sample count by maceral type, and further subdivided within each maceral type.

Available as supplemental file. Please refer to supplemental file 1.

2) Plate 1: TLSP

Unannotated and annotated digital outcrop model of Trinidad Lake State Park outcrop.

Available as supplemental file. Please refer to supplemental file 2.

3) Plate 2: KC

Unannotated and annotated digital outcrop model of King Coal outcrop.

Available as supplemental file. Please refer to supplemental file 3.

4) Plate 3: WB

Unannotated and annotated digital outcrop model of Wild Boar outcrop.

Available as supplemental file. Please refer to supplemental file 4.

5) Dover Core Description

Digitized core description of DOVER 21-1 TR, produced using Easy Core.

Available as supplemental file. Please refer to supplemental file 5.

6) Maverick Core Description

Digitized core description of MAVERICK 12-29 TR, produced using Easy Core.

Available as supplemental file. Please refer to supplemental file 6.

7) Zamora Core Description

Digitized core description of ZAMORA 22-14V, produced using Easy Core.

Available as supplemental file. Please refer to supplemental file 7.

8) State of CO Core Description

Digitized core description of STATE OF COLORADO AS 21-36 TR, produced using Easy Core.

Available as supplemental file. Please refer to supplemental file 8.

9) TLSP MS 1

Measured section collected at Trinidad Lake State Park outcrop, produced using Easy Core.

Available as supplemental file. Please refer to supplemental file 9.

10) TLSP MS 2

Displays a measured section collected at Trinidad Lake State Park outcrop, produced using Easy Core.

Available as supplemental file. Please refer to supplemental file 10.

11) TLSP MS 3

Displays a measured section collected at Trinidad Lake State Park outcrop, produced using Easy Core.

Available as supplemental file. Please refer to supplemental file 11.

12) KC MS 1

Displays a measured section collected at King Coal outcrop.

Available as supplemental file. Please refer to supplemental file 12.

13) KC MS 2

Displays a measured section collected at King Coal outcrop, produced using Easy Core.

Available as supplemental file. Please refer to supplemental file 13.

14) WB MS 1

Displays a measured section collected at Wild Boar outcrop, produced using Easy Core.

Available as supplemental file. Please refer to supplemental file 14.

15) WB MS 2

Displays a measured section collected at Wild Boar outcrop, produced using Easy Core.

Available as supplemental file. Please refer to supplemental file 15.

VITA

Ross Ingram Harrison was born March 30, 1989, in Shreveport, Louisiana. He is the son of Dr. George Kenneth Harrison and Deborah Jo Walters Harrison. He grew up in Shreveport, LA and graduated from C.E. Byrd High School in 2007.

Following high school, Ross enrolled in Texas Christian University, where he spent four years and completed a BA in English with a Business Minor in 2011. Following school, Ross worked for a year in the financial services industry. It was during this time that he decided to return to school and pursue a degree in geology.

In August of 2013, Ross returned to school at Louisiana State University in Baton Rouge, LA. During his time at LSU, Ross was an undergraduate researcher in the LSU Structure and Tectonics research group for one year, and a student worker in the LSU Coastal Studies Institute for a little over a year. He graduated in May of 2016 with a BS in Geology. It was at LSU that Ross truly developed his love for the study of the earth, as well as his technical foundation in geology. Immediately after graduating, Ross worked as a Teaching Assistant at LSU's Charles Barney Geology Field Camp, located outside of Colorado Springs, CO, a place which he loves.

In August of 2016, Ross enrolled in graduate school at Texas Christian University under Dr. John Holbrook. Following his first year of school, Ross was a geology intern at Occidental Petroleum, working in Permian EOR. Following completion of graduate school, Ross is set to begin work at OXY full-time in July 2018.

ABSTRACT

DEPOSITIONAL ENVIRONMENTS OF CRETACEOUS-PALEOGENE COAL BEDS AND SURROUNDING STRATA WITHIN THE RATON BASIN OF COLORADO AND NEW MEXICO, USA

by Ross Harrison, M.S. Candidate, 2018
Department of Geology
Texas Christian University

Dr. John Holbrook, Thesis Advisor, Professor of Geology

Dr. Richard Denne, Hunter Enis Chair of Petroleum Geology

Bo Henk, Adjunct Professor of Geology

The Raton Basin of Colorado and New Mexico is a Laramide foreland basin that has been important to coal geology since its first identification as a coal resource in 1821, and as a major Coal Bed Methane resource in the modern era. This study serves as an investigation into the depositional model of the Cretaceous-Paleocene Raton Formation's coal deposits and their surrounding fluvial deposits, specifically by: analyzing outcrops through facies mapping and architecture analysis, performing core descriptions and interpretations, and conducting organic petrography, palynology, chemical analysis and vitrinite analysis of coals. Results reveal that the relatively extensive and laterally continuous woody coals formed in a lacustrine depositional environment during periods of preferential peat preservation in the lacustrine lifecycle.